PREPARATION, CHARACTERIZATION AND PERFORMANCE STUDY OF NEW POLYSULFONE BASED NANOFILTRATION MEMBRANES FOR WATER FILTRATION

Thesis

Submitted in partial fulfillment of the requirements for the degree of

DOCTOR OF PHILOSOPHY

By

MAHESH S. PADAKI.
(REG. NO. 082003 CY08F05)

DEPARTMENT OF CHEMISTRY

NATIONAL INSTITUTE OF TECHNOLOGY KARNATAKA,

SURATHKAL, MANGALORE – 575025.

December, 2012

PREPARATION, CHARACTERIZATION AND PERFORMANCE STUDY OF NEW POLYSULFONE BASED NANOFILTRATION MEMBRANES FOR WATER FILTRATION
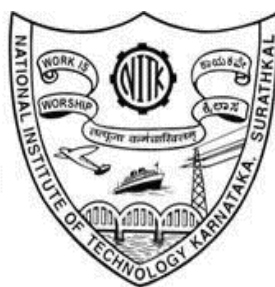
Thesis

Submitted in partial fulfillment of the requirements for the degree of

DOCTOR OF PHILOSOPHY

By

MAHESH S. PADAKI.
(REG. NO. 082003 CY08F05)

DEPARTMENT OF CHEMISTRY

NATIONAL INSTITUTE OF TECHNOLOGY KARNATAKA,

SURATHKAL, MANGALORE – 575025.

December, 2012

DECLARATION

I hereby *declare* that the thesis entitled **Preparation, characterization and performance study of new polysulfone based nanofiltration membrane for water filtration** which is being submitted to the **National Institute of Technology Karnataka, Surathkal** in partial fulfillment of the requirements for the award of the Degree of *Doctor of Philosophy* in *Chemistry* is a *bonafide report of the research work carried out by me.* The material contained in this thesis has not been submitted to any University or Institution for the award of any degree.

<div align="right">

Reg. No. CY08F05, Mahesh S. Padaki

Department of Chemistry

</div>

Place**:** NITK, SURATHKAL

Date:

CERTIFICATE

This is to *certify* that the thesis entitled **Preparation, characterization and performance study of new polysulfone based nanofiltration membrane for water filtration** submitted by **Mr. Mahesh S. Padaki.** (Register Number: CY08F05) as the record of the research work carried out by him is accepted as the thesis submission in partial fulfillment of the requirements for the award of degree of **Doctor of Philosophy.**

Dr. Arun M. Isloor
Research Guide

Chairman- DRPC

*Dedicated to
my beloved
Dada, Akka
and
brothers*

ACKNOWLEDGEMENTS

Water Water every where

not a drop to drink!!

ABSTRACT OF THE THESIS

Nanofiltration (NF) is a membrane based liquid separation technology which displays separation characteristics in the intermediate range between Reverse Osmosis (RO) and Ultrafiltratiom (UF). RO is capable of producing very clean water and high concentrate rejection. UF may be used for removal of suspended solids and large organic molecules. Most of the membranes were prepared from organic polymers. Inorganic polymers tend to be expensive. Cellulose derivatives, polysulfone, polyamides polyvinyldifloride are presently available polymers which are being extensively used for membrane preparation. For membranes to be competitive with conventional technology, a membrane process needs to operate with a high rate of flux, high degree of selectivity and high resistance to fouling. There are three main areas of interest when it comes to improving membrane performance: the synthesis process, post-synthesis modification and application process. These three processes were focused and discussed in present work.

Synthesis of polymers, chemical modification of polymers and surface modification of the membranes were performed and discussed in this thesis. Polysulfonylaminobenzamide (PSAB), methylated polysulfonylaminobenzamide (mPSAB), poly[(4-aminophenyl)sulfonyl]butanediamide (PASB) and methylated poly[(4-aminopheonyl)sulfonyl]butanediamide (mPASB) were synthesized. Chitosan (CS) was modified into N-Phthaloyl chitosan (NCS) and polysulfone (PSf) was modified into sulfonated polysulfone (sPSf). These polymers were blend with polysulfone for the preparation of NF membranes. Surface modification was mainly carried out by chemical modification, physical vapor deposition and beam irradiation.

The general properties of prepared membranes fall in UF and NF regime. The properties varied depending on the nature of the polymer, the functional group present in the polymer and manufacturing process. It was shown that the novel polymers and polymer modification enhanced the performance of the membrane.

Keywords: Nanofiltration, Polymer modification, Novel polymer, N-Phthaloyl chitosan and Physical vapor deposition.

TABLE OF CONTENTS

ABBREVIATIONS

Al-Aluminuim

ATR-IR-Attenuated Total Reflectance-Infrared Spectroscopy

AFM-Atomic Force Microscopy

CS-Chitosan

CA-Cellulose acetate

DSC-Differential Scanning Calorimetry

DIPS-Diffusion Induced Phase Separation

DMF-Dimethylformamide

ED-Electrodialysis

GPC-Gel Permeation Chromatography

IR-Infrared radiation

IEC-Ion Exchange Capacity

LiCl-Lithuim chloride

L_p-Hydraulic permeability coefficient

MF-Microfiltration

MWCO-Molecular Weight Cut-Off

mPASB-methylated Poly[(4-aminophenyl)sulfonyl]butanediamide

mPSAB-methylated Polysulfonylaminobenzamide

$MgSO_4$-Magnesuim sulphate

M_w-Average molecular weight

NF-Nanofiltration

NMR-Nuclear Magnetic Resonance

NMP-N-methyl-2-pyrolidone

NOCC- N,O-carboxymethyl chitosan

NaOH-Sodium hydroxide

NaCl-Sodium chloride

Na_2SO_4-Sodium sulphate

NCS- N-Phthaloyl chitosan

PEG-Polyethylene glycol

PASB-Poly[(4-aminophenyl)sulfonyl]butanediamide

PSAM-Poly styrene-alt-maleic anhydride

PIAM-Poly isobutylene-alt-maleic anhydride

PSf-Polysulfone

PA-Polyamide

PI-Polyimide

PES-Polyethersulfone

PAN-Polyacrylonitrile

PPA-Polypiperzineamide

PEI-Polyethyleneimine

PP-Polypiperzine

PMMA-Polymethylmethacrylate

PVD-Physical Vapor Deposition

PVDF-Polyvinylidenefluoride

PSAB-Polysulfonylaminobenzamide

RO-Reverse Osmosis

sPSf-Sulfonated polysulfone

SEM-Scanning Electron Microscopy

T_g-Glass transition temperature

TDI-Toluene diisocyanate

UF-Ultrafiltration

PV-Pervaporation

LIST OF FIGURES

LIST OF TABLES

CHAPTER 1

INTRODUCTION TO MEMBRANE TECHNOLOGY

CHAPTER 2

STATE OF ART AND OBJECTIVES OF THE WORK

CHAPTER 3

POLYSULFONE AND NOVEL POLYMERS BLEND MEMBRANES

CHAPTER 4

MODIFICATION OF CHITOSAN AND ITS BLEND MEMBRANE

CHAPTER 5

SURFACE MODIFICATION OF THE MEMBRANE

CHAPTER 6

CONCLUDED REMARKS AND SCOPE OF THE FUTURE WORK

Abstract: This is an introductory chapter, which deals with brief account of membrane technology. It includes definition of the membrane, membrane classification, applications of membranes, membrane preparation and characterization.

In 21st century, water purification and desalination are challenging aspects to all researchers. In water treatment, recycle – reuse, purification and pollution control are the main objectives. The major challenge is to provide safe drinking water to people at much cheaper rates in order to fulfill the basic needs for survival of life on earth.

With the key objective of accessibility and affordability, the task of providing fresh water has become a complex issue and there is a need for optimal utilization of natural water resources besides supplementary with the use of appropriate desalination and water purification technologies.

The total water market in India is estimated to be US$ 14 billion for municipal, industrial, residential and other requirements, out of which the industrial market alone enjoys about US$ 3.5 billion at present. Gross waste water generation is more than 30000 million liters per day (MLD) and it is estimated to touch 83000 MLD by 2050. Water recycling and reuse is already implemented in several industries which demonstrate its usefulness. Almost all the industries need to gear up for water recycling and zero discharge. Inspite of these efforts, water accessibility still continues to pose as a problem

Large scale desalination of sea water was first introduced in the 1950s by the Professor of Scottish University; he launched the multistage flash distillation concept. At that time, mild steel was a natural choice for the flash chambers, however, leakage in the flash chambers allowed oxygen to enter into the evaporators resulting in corrosion.

In 1970, some industries introduced stainless steel lining for flash chambers. Use of stainless steel made whole process costly for the production of relatively cheaper product like water, so small scale industries could not implement this process. Hence,

when compared to this type of process, membrane filtration is much more cost effective and very much suitable for water purification and desalination (InDA news 2009).

In olden days, membrane filtration was not considered to be a technically important separation process, but considering its myriad applications in different fields, it is gaining much more importance in recent years.

Membrane technology is an emerging technology and because of its multidisciplinary characteristics it can be used in large number of separation processes. The benefits and drawbacks of membrane technology can be summarized as follows,

- Separation can be carried out continuously.
- Energy consumption is generally low.
- Membrane process can easily be combined with other separation process.
- Separation can be carried out under mild conditions.
- Membrane properties are variable and can be adjusted.

The drawbacks of the membrane technology

- Concentration polarization/membrane fouling.
- Low membrane life time.
- Low selectivity or flux.

Membrane fouling and low flux are the major problems in membrane technology but in comparison with other techniques, it gives good results in the form of pure water at low cost (Mulder 1996).

Even though water purification is the major area of membrane application, there are many other fields wherein membrane technology is being effectively utilized, namely in agricultural sector for controlled delivery of fertilizer, landfill leachate, pharmaceutical industry (chiral separation), power generation (fuel cell), pulp and paper industry (water recycle), semiconductor, specialty chemicals (drug delivery), dairy industry (fat separation) and textile industry (dyes separation). The worldwide sales of synthetic membranes are estimated at over US$ 2 billion (in 2003). The annual growth rate for

most membrane products are more than 5 %, in some segments up to 12–15 %. For example, market of the by far largest commercial membrane process, the 'artificial kidney' (hemodialysis) has a turnover of US$ 1 billion and more than 230 Mio m^2 membrane area is produced annually for this application.

1.1 INTRODUCTION TO MEMBRANE TECHNOLOGY

A membrane is an interphase between two adjacent phases acting as a selective barrier, regulating the transport of substances between two compartments. The main advantage of membrane technology is its unique separation principle i.e., the transport selectivity of the membrane which distinguishes it from other unit operations in (bio) chemical engineering. Separation by the use of membranes does not require additives and can be performed isothermally at low temperatures and at low energy consumption in comparison with other thermal separation processes (Ulbricht 2006).

Membranes are part of our daily life; they exist as long as life exists. Membranes and membrane processes are not recent invention. The preliminary membrane experiments were conducted by *Grahm* in 1863. Sourirajan in 1963 prepared novel asymmetric polymer membrane for desalination. However, the preparation of synthetic membranes and their utilization on a large industrial scale are more recent development which has rapidly gained substantial importance due to the large number of practical applications. The heart of every membrane process is membrane itself, which can be considered as a perm selective barrier or interface between two homogeneous phases. Separation is achieved because the membrane transports one component more readily than others due to differences in physical and/or chemical properties between the membrane and the permeating components (Mulder 1996).

There are two factors that determine the effectiveness of a membrane filtration process; selectivity and productivity. Selectivity is expressed by parameter called rejection or separation factor (expressed by percent rejection). Productivity is expressed in terms of flux (expressed by unit L/m^{2}h). Selectivity and productivity both are membrane-dependent properties.

Synthetic membranes for water purification can be classified according to their selectivity, their structure, morphology and the membrane material. The nature of the selective barrier i.e., porous, nonporous, charged or with special chemical affinity, dictates the mechanism of permeation and separation in combination with applied driving force for transport through the membrane.
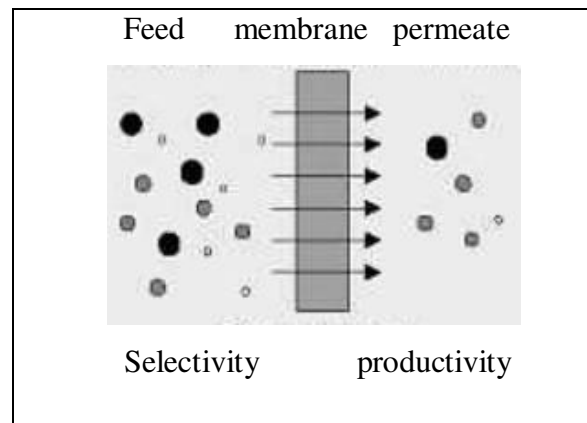
Figure 1.1 Schematic representation of membrane filtration

(Source: Mulder 1996)

Transport through porous membranes is possible by viscous flow or diffusion flow; and the selectivity is based on size exclusion (sieving mechanism) and charge exclusion. This means permeability and selectivity are mainly influenced by membrane pore size as well as size and charge of the feed component. Molecules with larger size than the largest membrane pore will be completely rejected and molecules with smaller size can pass through the barrier (MeCoy 1995).

Transport through nonporous membranes is based on solution-diffusion mechanism (George and Thomas 2001, Wijamans and Baker 1995). Therefore, interactions between permeate and the membrane material dominate the mass transport and selectivity. Solubility and chemical affinity on one hand and influence of polymer structure on mobility on the other hand serve as selection criteria. However, the barrier structure may also change by uptake of certain substances from the feed and in those cases real selectivity can be much lower than ideal ones obtained from experiments using only one component in the feed or at low feed activities.

4

Separation using charged membranes, either nonporous (swollen gel) or porous (fixed charged groups on the pore wall), is based on charge exclusion (Donnan effect; ions or molecules having the same charge as the fixed ions in the membrane will be rejected, whereas species with opposite charge will be taken up and transported through the membrane) (Mulder 1996). Therefore, the type of charge and charge density are the most important characteristics of these membranes. Finally, molecules or moieties with special affinity for substances in the feed are the basis for carrier-mediated transport through the membrane with which very high selectivity can be achieved; the diffusive fluxes are higher for (immobilized) liquid membranes than for polymer-based fixed-carrier membranes. Concentration polarization can dominate the trans-membrane flux in ultrafiltration (UF), which is described by boundary-layer models. Polarization effects are more important in reverse osmosis (RO), nanofiltration (NF), pervaporation (PV), electrodialysis (ED) or carrier-mediated separation (Ulbricht 2006).

Water purification membranes are porous membranes, classified into four different types depending on their pore size.

1. **Microfiltration (MF):** The average pore size ranges from 0.1 to 10 μm and low pressures (0.1–2 bar) are sufficient to obtain high permeability (50 $Lm^{-2}h^{-1}$ bar^{-1}). Microfiltration is frequently used as a pre-treatment step for NF and RO. They retain particles by means of sieving.

2. **Ultrafiltration (UF):** Retains both particles and macromolecules by the same sieving mechanism as MF. UF membranes are characterized by their molecular weight cut-off, which is the molecular mass of a solute with 90 % rejection. Components with molecular mass above the cut-off have high rejection, whereas components with molecular mass below the cut-off are retained only partially. The cut-off for UF lies typically between a few 1,000 and 100,000 Da, which corresponds with pore sizes between a few nanometers to 0.1μm. Permeability between 10 and 50 $Lm^{-2}h^{-1}bar^{-1}$ are obtained with pressures between 1 to 5 bar.

3. **Reverse Osmosis (RO):** It is possible to retain small organic molecules and ions from a solution. These membranes are particularly used for desalination application. As this process uses dense membranes which have high hydrodynamic resistance, low permeability (0.05–1.4 $Lm^{-2}h^{-1}bar^{-1}$) are realized only with high-pressure gradients (10–70 bar). Instead of sieving, separation is obtained due to sorption and diffusion through the membrane.

4. **Nanofiltration (NF):** The properties of NF lie between UF and RO. These membranes found their origin in the 1970s as modified RO membranes having high water fluxes. NF membranes require much lower pressure (2-20 bar) than RO, leading to significant energy savings. Moreover, NF combines high permeability (1.5-15 $Lm^{-2}h^{-1}bar^{-1}$) with a high retention of dissolved organic molecules with a molecular mass above 200 Da. The cut-off of NF is positioned between 150 to 1,000 Da. Due to charge interactions with the membrane multivalent ions are well retained (Mulder 1996).
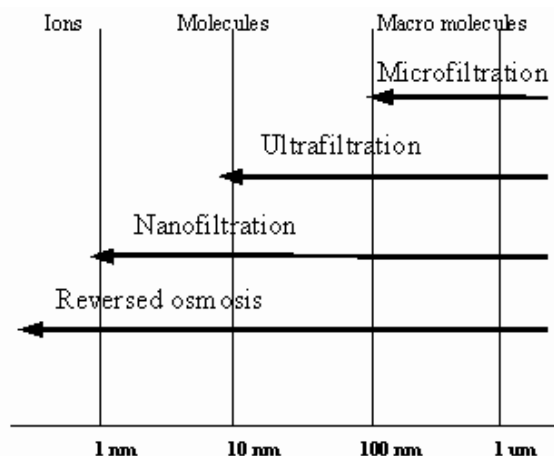
Figure 1.2 Classification of membrane process on the basis of pore size

(Source: Mulder 1996)

Several polymeric NF membranes made of cellulose acetate (CA), polyamide (PA), polypiperazineamide (PPA), polyimide (PI) or polyethersulfone (PES) are commercially available. Membrane materials, particularly polymeric membranes are still

dominating a very broad range of industrial applications. This is due to their following advantages,

1. Many different types of polymeric materials are commercially available.

2. A large variety of different selective barriers i.e., porous, nonporous, charged membranes can be prepared by versatile and robust methods.

3. Production of large membrane area with consistent quality is possible on a technical scale at reasonable cost based on reliable manufacturing processes.

4. Various membrane shapes (flat sheet, hollow-fiber, capillary, tubular, capsule; and formats including membrane modules with high packing density can be produced.

However, membrane polymers also have some limitations.

1. A very well-defined regular pore structure is difficult to achieve,

2. Mechanical strength,

3. Thermal stability and

4. Chemical resistance (e.g., at extreme pH values or in organic solvents)

1.2 MATERIAL FOR MEMBRANE

The selection of polymer for a porous membrane is based on the requirements of the manufacturing process and performance under application conditions. The following material properties are important to be considered:

1. Film-forming properties indicate the ability of a polymer to form a cohesive film. The macromolecular structure, especially molar mass and attractive interactions between chain segments are crucial in this regard.

2. Mechanical properties involve film strength, film flexibility and compaction stability (especially of a porous structure). The latter is most important for high-pressure processes (e.g., for the porous substructure of an integrally anisotropic RO membrane). Many commercial flat-sheet membranes are prepared on a nonwoven support material for this reason. Since hollow fiber membranes are self-supporting, their mechanical stability is especially relevant.

3. Thermal stability requirements depend very much on the application. In order to ensure the integrity of pore structure in the nanometer dimension, T_g of the polymer should be higher than the process temperature.

4. Chemical stability requirements include resistance of polymer at extreme pH values and other chemical conditions. It must be resistant towards cleaning agents such as strong acids, bases and/or oxidation agents which are usually used to clean the fouled membrane. The stability in special solvents is also important in selected cases, especially when processes with non-aqueous mixtures are considered.

5. The hydrophilicity–hydrophobicity balance correlates with wettability of the material. Surface wettability is also critical for fouling; cellulose is an excellent example of hydrophilic polymer known for its low fouling charecreristic. Certain hydrophobic polymers, for instance Polyvinylidenefluoride (PVDF) or Polyethersulfone (PES) show better chemical and thermal stability.

Considering all the above criteria, PSf, PES, PAN, PVDF and cellulose-based polymers like cellulose acetates (CA) and regenerated cellulose are mostly used for commercial UF membranes (Drioli and Giorno 2009). It is difficult to observe all the above mentioned characteristics in one single polymer. This difficulty can be overcome by mixing of two polymers as polymer composite and polymer blend.

Polymer composites are physical mixtures of a polymer (the matrix) and a reinforcing filler (the dispersed phase) that serves to improve some desired properties such as modulus, abrasion resistance, wettability, surface roughness and surface charge. Filler may be inorganic such as calcium carbonate or organic for example graphite fiber. Practically any material can be used as composite matrix, including ceramic, carbon and polymers.

Polymer blends are physical mixtures of two or more structurally different homo and/or copolymers. Blending is another classical technique for membrane modification.

Compared to composite methods, blending would result in alteration of membrane properties. The original blending method is to directly mix hydrophilic macromolecules with membrane matrix (Amiji 1995). Subsequently, amphiphilic copolymers have received much attention in membrane hydrophilicity modification because hydrophilic segments can be 'anchored' onto the hydrophobic membrane matrix in order to keep the hydrophilic segments stable (Hester et al. 1999, Wang et al. 2006 and Raana et al. 2005). Moreover, it has been reported that hydrophilic segments always aggregate onto the surface of membrane and pore channels which provide better anti-fouling property to membranes.

1.3 TECHNIQUES FOR MEMBRANE PREPARATION

1.3.1 Composite membranes

1.3.1.1 Plasma polymerization

Plasma polymerization involves buildup of a dense layer from the deposition of monomers produced in plasma. Plasma is an ionized gas produced by electric discharge. It is composed of electrons, ions, gas atoms and various molecules in ground and excited states. The monomers are converted into reactive forms and hence induce polymerization. As a result, hydrophobic surface can become hydrophilic (Yamaguchi et al. 1991) and vice versa. The different but active monomers polymerize at any surface including the surfaces of microporous support membranes. Under proper conditions, plasma films can become strongly bonded and highly cross-linked (Gong et al. 2000).

Plasma treatment can be used for several purposes: polymerization on surface layer (Friedrich et al. 2004), pore size reduction (Xle et al. 2005) or enlargement (Bryjak et al. 2004) and grafting of functional groups (Bryjak et al. 2002). Plasma polymer layers are generally defect free. The structures are generally complex, unlike homopolymers, and the structures depend on plasma conditions.

1.3.1.2 Interfacial Polymerization

The basic interfacial polymerization technique on the surface of porous support is known (Morgon et al. 1965) to have a number of features which includes strict

requirements of monomer purity and reagent stoichiometry. Cadotte (1977) has applied this concept to the preparation of commercially successful FT-30 desalination membrane. A polysulfone support is coated with an aqueous solution containing at least 0.01% of p-phenyl diamine after which it is brought into contact with a hexane solution containing 1,2,4-trimesoyl chloride (Figure 1.3).
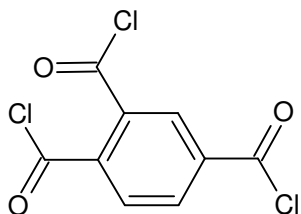
Figure 1.3 1,2,4-trimesoyl chloride
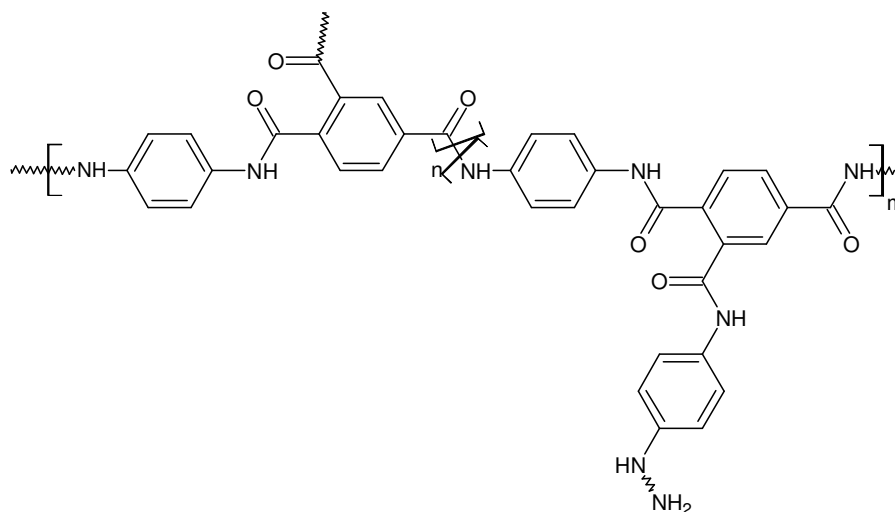
Figure 1.4 Cross-linked polyamide polymer

Reaction is swift and is terminated when the completed interfacial thin film inhibits further reaction. Only slightly more than two of every three carboxylic acid chloride groups condense, so that the lightly cross-linked final membrane polymer closely resembles the structure (Figure 1.4).

1.3.1.3 Dip-coating

Dip-coating method includes application of either a polymer or a pre-polymer solution directly onto the porous support where it is subsequently dried or cured. The advantage of this procedure is that it eliminates the difficulty of handling thin films. It has the disadvantage that only those solutions which do not interact with the porous support may be utilized in the application of barrier layer. This of course is not a disadvantage if,the coating is applied from an aqueous solution. This approach was first utilized by Cadotte in the application of an aqueous solution of polyethyleneimine (PEI) and the subsequent reaction with tolyene diisocyanate (TDI) in hexane to yield cross-linked polyurea which constituted the NS-100 membrane.

1.3.2 Blend membranes

Blend membranes are mostly fabricated by a process called phase inversion, which can be achieved through three principal methods: immersion precipitation (wet-casting) (Van de Witte et al. 1996), dry-casting (Pinnau and Koros 1991) and thermally-induced phase separation (Lyold et al. 1990). In all these techniques, an initially homogeneous polymer solution thermodynamically becomes unstable due to different external effects and phase separates into polymer lean and polymer rich phases. Membrane formation occurs by egress of solvent and ingress of non-solvent into the cast solution, leaving a two phase system. The polymer-rich phase forms the matrix of the membrane while the polymer-lean phase which is rich in solvent and non-solvent fills the pores. Solvent-non-solvent exchange occurs most rapidly at the interface. Polymer precipitates much faster at the top surface than in the underlying substrate. This produces an asymmetric membrane having a dense surface layer on top of a microporous support. Dense layer thickness and sub-layer morphology is dependent on many variables, especially on the rate of solvent-non-solvent exchange. Most commercial membranes are fabricated by process which include an immersion precipitation step (Reuvers and Smloders 1987).

Membrane formation

Stirring for 24h   **Casting the solution**
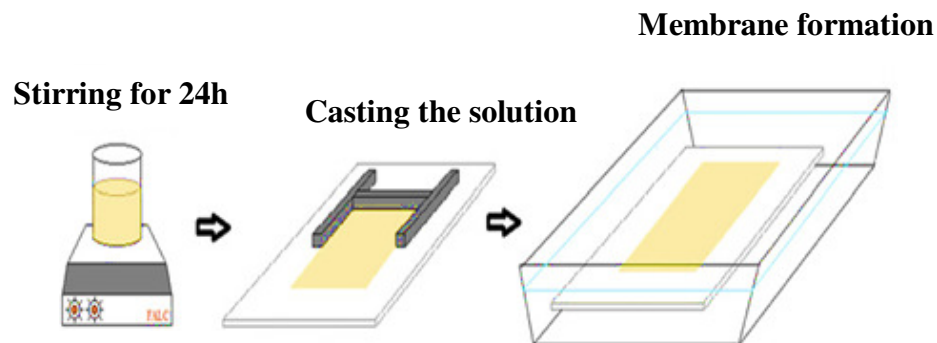
Figure 1.5 Schematic representation of membrane preparation process

1.3.2.1 Precipitation by solvent evaporation-dry process

The dry or complete evaporation process is the oldest and easiest to interpret the phase-inversion process. Casting solutions consist of three or more components: polymer, volatile solvent and pore forming non-solvent. The non-solvent should be substantially less volatile than the solvent (30-40° C minimum difference in boiling points between the two). Initially, the polymer solution is assumed to have a uniform composition. Although casting solution is homogeneous on the colloidal level, compatibility decreases as evaporation of solvent proceeds. Eventually, the solvent power of the remaining solvent system is insufficient to maintain one-phase solution and inversion into two-phase solution occurs. In the typical dry process, the fundamental reason for incompatibility which leads to phase inversion and gelation is the presence of non-solvent in the casting solution and strong polymer-polymer interaction forces (Jansen et al. 2005). As the solvent loss continues after phase inversion, the spherical micelles approach one another eventually making contact in the initial phase of gelation. As the gel network contracts, the micelles deform into polyhedral and the polymer molecules diffuse into the walls of neighbouring micelles causing an interaction of polymer molecules at the interface. Finally, the formation of numerous micelles with a large total surface area causes tearing of the walls which then retract and form the skeleton constituting the gel network.

1.3.2.2 Immersion precipitation-wet process

The wet or combined evaporation-diffusion technique is the variation of the phase-inversion process. Viscous polymer solution is either allowed to partially evaporate after which it is immersed into a non-solvent coagulation bath where remaining solvent is exchanged for the non-solvent (Stropink and Kaiser 2002). The end product of the wet process is water-swollen membrane. Moreover, the water content of membrane is a prime determinant of its functional performance. A wet-process solution must be relatively viscous at the moment of immersion in the non-solvent so that it will retain its integrity throughout coagulation. Moreover, the presence of pore formers within the casting solution prior to its immersion into a non-solvent coagulation bath is not a requirement of every wet-process solution. This process is known as Diffusion Induced Phase Separation (DIPS) process. In present research work, DIPS method was used for membrane preparation.

1.3.2.3 Thermal precipitation

A significant recent development in the technology of phase-inversion membranes is the invention of thermal process by Castro (1981). The thermal process is applicable to a wide range of polymers, which because of their poor solubility are otherwise inaccessible to the phase-inversion approach. In essence, the thermal process utilizes a latent solvent i.e., a substance which is a solvent at elevated temperatures, a non-solvent at lower temperatures, thermal energy to produce a phase separation and on further cooling resulting into membrane. The reason for the incompatibility which evokes phase separation is loss of solvent power by the removal of heat. Cooling decreases the polymer solubility and results in phase inversion. Since the solvent is nonvolatile in nature, it can be removed from the final gel by extraction with a liquid which is a solvent for the nonvolatile solvent and a non-solvent for the polymer.

1.4 CHARACTERIZATION TECHNIQUES

1.4.1 Attenuated Total Reflectance-Infrared spectroscopy (ATR-IR)

IR spectrometers have been used to analyze solids, liquids and gases by means of transmitting the infrared radiation directly through the sample. The technique of

Attenuated Total Reflectance (ATR) has in recent years revolutionized solid and liquid sample analysis because it combats the most challenging aspects of infrared analysis, namely sample preparation and spectral reproducibility. An ATR accessory operates by measuring the changes that occur in a totally internally reflected infrared beam when it comes into contact with the sample (indicated in Figure 1.6). An infrared beam is directed onto an optically dense crystal with a high refractive index at a certain angle. This internal reflectance creates an evanescent wave that extends beyond the surface of the crystal into the sample held in contact with the crystal. It can be easier to think of this evanescent wave as a bubble of infrared that sits on the surface of the crystal. This wave protrudes only a few microns (0.5 μ - 5 μ) beyond the crystal surface and into the sample. Consequently, there must be good contact between the sample and the crystal surface. In regions of the infrared spectrum where the sample absorbs energy, the evanescent wave will be attenuated or altered. The attenuated energy from each wave is passed back to the IR beam, which then exits the opposite end of the crystal and is passed to the detector in the IR spectrometer. The system then generates an infrared spectrum. In this present study, ATR-IR spectra were recorded using Nicolet Avatar FT-IR instrument.
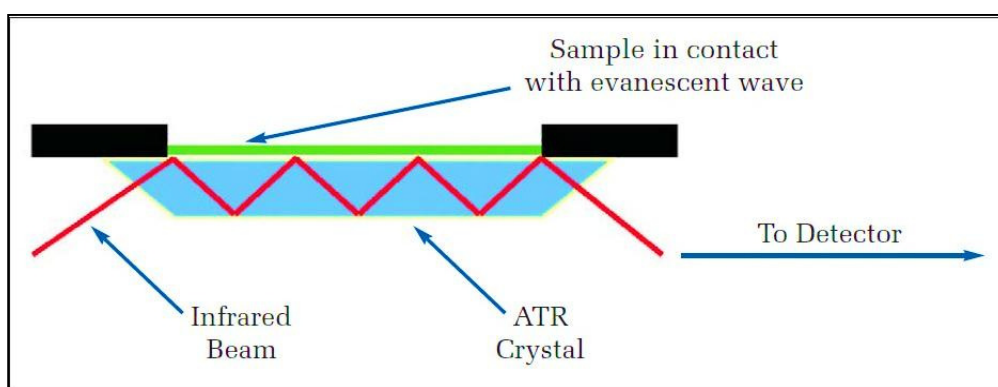
Figure 1.6 Pictorial representation of ATR-IR analysis

1.4.2 TGA analysis of polymers

Thermogravimetric Analysis (TGA) measures the amount and rate of change in the weight of a material as a function of temperature or time in a controlled atmosphere. Measurements are used primarily to determine the composition of materials and to

predict their thermal stability at temperatures up to 800°C. The technique can characterize materials that exhibit weight loss or gain due to decomposition, oxidation, or dehydration.

The dynamic thermogravimetric analysis of all the polymers have been carried out in nitrogen atmosphere with a heating rate 5ºC/min. in a platinum crucible. The thermogravmetric analyzer used was SII/EXSTAR6000/TG/DTA6300 in the temperature range 35-800ºC.

1.4.3 Differential scanning calorimetry (DSC)

Differential scanning calorimetry (DSC) is a thermo analytical technique in which the difference in the amount of heat required to increase the temperature of a sample and reference is measured as a function of temperature. Both the sample and reference are maintained at nearly the same temperature throughout the experiment. Generally, the temperature program for a DSC analysis is designed such that the sample holder temperature increases linearly as a function of time. The reference sample should have a well-defined heat capacity over the range of temperatures to be scanned.

The basic principle underlying this technique is that when the sample undergoes a physical transformation such as phase transitions, more or less heat will need to flow to it than the reference to maintain both at the same temperature. Whether less or more heat must flow to the sample depends on whether the process is exothermic or endothermic. For example, as a solid sample melts to a liquid, it will require more heat flowing to the sample to increase its temperature at the same rate as the reference. This is due to the absorption of heat by the sample as it undergoes the endothermic phase transition from solid to liquid. Likewise, as the sample undergoes exothermic processes (such as crystallization) less heat is required to raise the sample temperature. By observing the difference in heat flow between the sample and reference, differential scanning calorimeters are able to measure the amount of heat absorbed or released during such transitions. DSC may also be used to observe more subtle phase changes, such as glass transitions. It is widely used in industrial settings as a quality control instrument due to its

applicability in evaluating sample purity and for studying polymer curing. Schimadzu DSC 60 instrument, Japan, was used to study the T_g of the membranes.

1.4.4 Scanning Electron Microscopy (SEM)

A scanning electron microscope (SEM) is a type of electron microscope that images a sample by scanning it with a beam of electrons in a raster scan pattern. The electrons interact with the atoms that make up the sample producing signals which contain information about the sample's surface topography, composition and other properties such as electrical conductivity.

1.4.5 Contact angle

The contact angle is the angle at which a liquid/vapor interface meets a solid surface. The contact angle is specific for any given system and is determined by the interactions across the three interfaces. Most often the concept is illustrated with a small liquid droplet resting on a flat horizontal solid surface. The shape of the droplet is determined by Young-Laplace equation, with the contact angle playing the role of a boundary condition. Contact angle is measured using a contact angle goniometer. The contact angle is not limited to a liquid/vapor interface; it is equally applicable to the interface of two liquids.

The sessile drop method is measured by a contact angle goniometer using an optical subsystem to capture the profile of a pure liquid on a solid substrate. The angle formed between the liquid/solid interface and the liquid/liquid interface is recorded.

In present investigation the contact angle of the membrane was determined to understand the surface wetting characteristic of the membrane. Hydrophilic solids have a contact angle upto 90°. On highly hydrophilic surfaces, water droplets exhibit contact angles of 0° to 30°. If the solid surface is hydrophobic, the contact angle is larger than 90°. Highly hydrophobic surfaces have water contact angle as high as ~120°. Contact angle were measured by the sessile drop method, using a contact angle goniometer (OCA 15 EC, Germany).

1.4.6 Water uptake study of membranes

Water uptake study includes immersion of the membrane samples in deionized water at room temperature for 24 hrs, followed by blot drying the wet membranes to remove surface adhering water droplets which is then quickly weighed. Finally these membranes are vacuum dried at 80 °C-100 °C and weighed again. The water uptake of the membranes can be calculated by the weight gain of the swollen membrane with reference to the dry membrane and reported as weight percent water absorption. The water uptake can be calculated as follows, (Wittmann et al. 1998)

$$wateruptake(\%) = \left(\frac{W_w - W_d}{W_d} \right) \times 100$$

Where, W_w is the weight of wet membrane and W_d is the weight of dry membrane.

1.4.7 Surface charge of membranes

1.4.7.1 Ion exchange capacity (IEC)

IEC indicates the number of milimoles of ions exchangeable functional groups present on 1g of the dry membrane. The IEC of the membrane was measured by a conventional titration method. The membrane in H^+ form was immersed in a 2M NaCl solution for 24 hrs for the complete replacement of H^+ with Na^+. The immeresed solution after the removal of membrane was then titrated with 0.01M of NaOH using phenolphthalein indicator. The IEC value was calculated by following equation

$$IEC(mmol/g) = \left(\frac{0.01 \times 1000 \times V}{W_d} \right)$$

where V (L) is the volume of NaOH solution consumed by the titration and W_d (g) is the weight of the dry membrane sample. The titration was carried out with an accuracy of 0.001mM/g (Yan et al 2006).

1.4.7.2 Diffusion potential

Membrane potential ($\Delta\Psi$) of the charged membrane was measured in a two compartment cell, chamber I and chamber II as shown in Figure-1.7, both the chambers being separated by a vertical membrane of 2.0 cm^2 effective area.
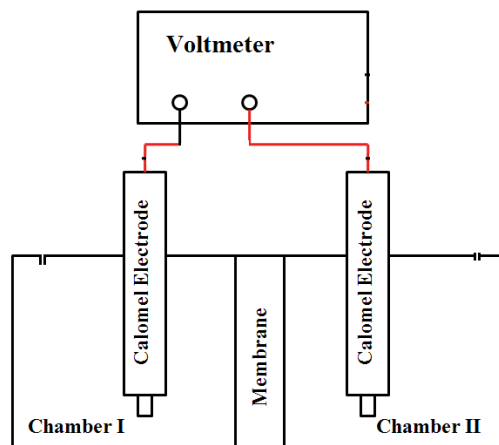
Figure 1.7 Diffusion potential cell

Chamber I contained 100 mM and chamber II contained different concentration electrolytic solution less than 100 mM. Diffusion potential difference across the membrane was measured using a voltmeter which was connected to a calomel electrode (Wanichapichart and Yu 2007).

1.4.8 Performance study of membranes

All the performance studies were done by using self-constructed filtration unit (Figure 1.8). All the permeation experiments were performed at room temperature. A circular membrane sample with diameter of 60 mm was placed in the test cell with the active surface facing towards the incoming feed. Effective membrane diameter was 50 mm. In order to minimize experimental error an average of three values reported.

1.4.8.1 Pure water flux

Water flux is important parameter in membrane performance study. The water flux was measured by direct measurement of permeate flow in terms of liter per meter square per hour (L/m^{2}h) at varied pressure. Hydraulic permeability coefficient of the membrane (L_p) was estimated from the slope of water flux and applied pressure.

$$L_P = slope \times 2.77 \times 10^{-10}$$

1.4.8.2 Molecular weight cut-off (MWCO)

Molecular weight cut-off is the characteristic property of a membrane which gives an idea about the pore size of the membrane and is related to rejection of a solute of given molecular weight. The molecular weight cut-off has linear relationship with the pore size of the membrane (Mahendran et al. 2004). In general, the molecular weight cut-off of the membrane is determined by identifying an inert solute of lowest molecular weight that has a solute rejection of 90 % in steady state filtration experiments (Jai and Tain 2009). The permeation cell was filled with Polyethylene glycol (PEG) solution and pressurized at a constant pressure of 200 kPa.

To Nitrogen cylinder

1. Feed solution
2. Reservoir
3. Pressure release ball valve
4. O-ring
5. Membrane
6. Stainless steel porous disc
7. Permeate
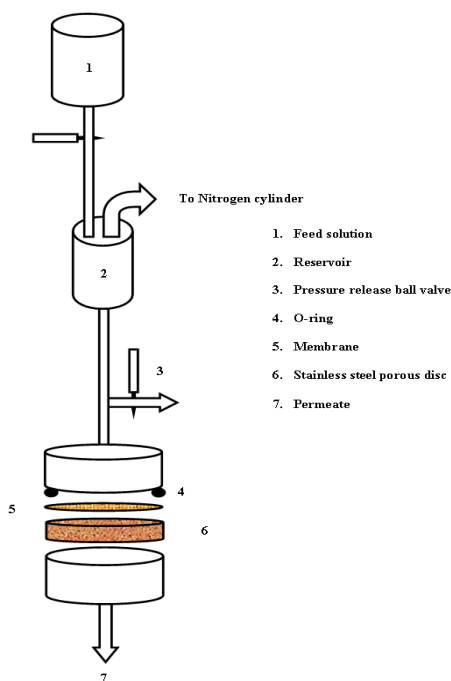
Figure 1.8 Self constructed filtration unit

During filtration, the permeate solutions of corresponding membranes were collected over a period of time in a graduated tube and were analysed for the concentration of PEG by UV–vis spectrophotometer (Shimadzu, Model UV-160A) (Mahendran et al. 2004). From the feed and permeate concentrations, the percentage rejection was calculated using the following equation.

$$\%R = \left(1 - \frac{C_p}{C_f}\right) \times 100$$

where C_p and C_f are the concentrations of the permeate and feed respectively.

Membrane showing less than 100 Da MWCO is categorized as RO membrane, 100 Da to 1000 Da as NF membrane, 1000 Da to 100000 Da as UF membrane and above 100000 Da as MF membrane.

1.4.8.3 Rejection study

Concentration of the salt solution was determined by conductivity experiment. It is usually expressed as parts per million (ppm). Cations found in water usually include calcium, magnesium, potassium and sodium whereas, anions include bicarbonate, carbonate, chloride, nitrate and sulfate. Conductivity is a good indicator of the measure of salinity in water. It is well-known that, the conductivity of any solution is directly proportional to the concentration of its ions. In general, the conductivity of salt solutions increase as the amount of dissolved salt increases. The exact increase in conductivity, is however, complicated by the relationship between the concentration of the salt and the mobility of its charged particles. The percent salt rejections were determined by comparing the conductivity difference of feed and permeate solutions. The percent rejection was calculated using the same equation used for MWCO study.
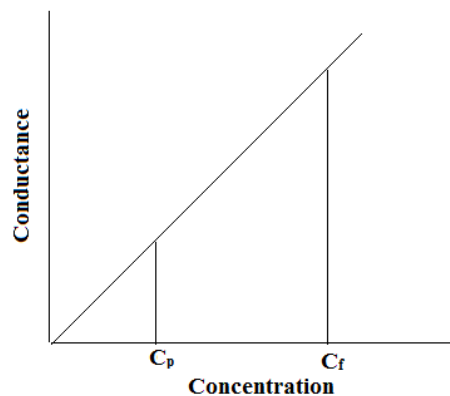
Figure 1.9 Typical plot of conductance v/s concentration

Abstract: This chapter includes literature review of the membrane research, objectives and scope of present research.

2.1 STATE OF ART

Polymeric membranes require high performance and durability. NF and RO as novel and powerful pressure-driven separation technology are widely used to separate or concentrate aqueous solutions containing organics and salts. In recent years, the application of membranes has increased rapidly in chemical, petrochemical, biological and desalination industries, since NF technology overcomes the operational problems that were previously associated with the conventional techniques. In the past few decade, great efforts have been put to develop new polymeric membranes.

In 1960, Sourirajan carried out desalination experiment using asymmetric membranes. However, the field remained relatively dormant with no much development till 1990. After 1990, research in this field started gaining momentum due to its application in different fields. Active research is in progress with the objective of advancement of membrane technology and many reports have been published in recent years.

Guan et al. (2005) reported sulfonation of polyethersulfone by chlorosulfonic acid and its membrane characteristics. The prepared membrane showed decrease in tensile strength with increase in degree of sulfonation. It was also observed that the hydrophilicity and water uptake of the membrane increased with an increase in the degree of sulfonation. This study proved to be very useful for specific application like proton exchange membranes for fuel cells.
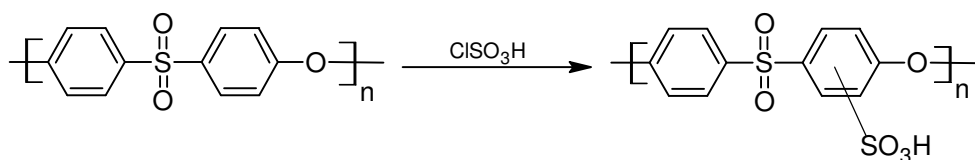
Figure 2.1 Sulfonation of polyethersulfone

Boussu et al. (2006) studied and compared the performance of commercial nanofiltration membranes with self-made polyethersulfone membranes. It has been shown that polyamide membranes showed lowest MWCO in addition to rough and hydrophilic membrane surface.

Young-nam et al. (2006) studied hypochlorite degradation of cross-linked polyamide membranes and observed changes in chemical/morphological properties. The objective of this work was to symmetrically investigate the effect of hypochlorite on chemical and morphological properties of a cross-linked polyamide membrane. It was observed that, the use of chlorine brings chemical changes and causes variation in the surface properties of cross-linked polyamide membrane.

Figure 2.2 Cross-linked polyamide

Florian et al. (2007) showed the preparation and characterization of novel solvent resistant nanofiltration composite membranes based on cross-linked polyurethanes. Through this work it has been demonstrated that, it is possible to produce polyurethane (PU) -based composite membranes as an alternative to establish poly(dimethylsiloxane) (PDMS) based membranes for the nanofiltration (NF) of non-aqueous solutions with promising characteristics for industrial applications.

Qin et al. (2007) reported nanofiltration for recovering waste water from a specific dyeing facility. This study indicated that, it would be feasible to recover the waste water up to 70 % from the dyeing facility using NF membrane process.

Sebastian et al. (2007) studied permeability of low molecular weight organics through nanofiltration membranes. Two NF membranes and one high flux RO membrane have been investigated to determine whether NF effectively removes assimilable organic carbon (AOC) and thus produce microbiologically stable water.

Yan et al. (2007) prepared and characterized Chloromethylated/Quaternized poly(phthlazinone ether sulfone ketone) (CMPPESK/QAPPESK) positively charged nanofiltration membranes. CMPPESK/QAPPESK was synthesized in laboratory and their filtration and thermal property were studied. The QAPPESK NF membranes showed higher rejection for high valance cations as well as anions.
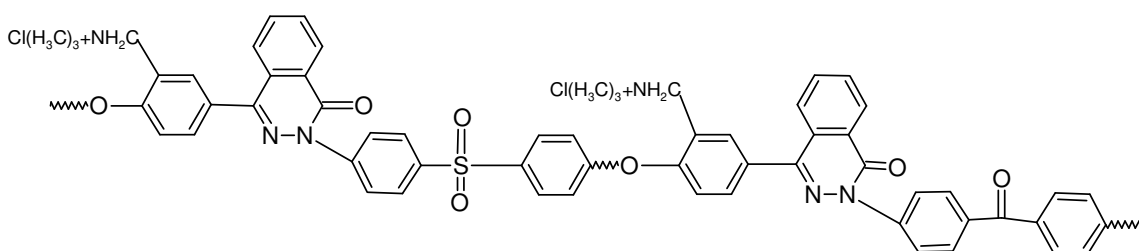
Figure 2.3 Chloromethylated/Quaternized poly(phthlazinone ether sulfone ketone)

Fan et al. (2008) studied preparation and characterization of polyaniline/ polysulfone nanocomposite ultrafiltration membrane. They showed that oxygen atom in the ether bond and sulfone group of polysulfone interacted with amine and protonated imine group of polyaniline by H-bonding causing the combination of polyaniline nanofibre and polysulfone substrate membrane thereby increasing the hydrophilicity and permeability.

Meihong et al. (2008) reported a study on preparation and performance of the thin-film composite nanofiltration membrane for the removal of sulfate from concentrated aqueous salt solution. Thin film composite nanofiltration membrane was prepared by interfacial polymerisation method between trimesoyl chloride and piperzine.
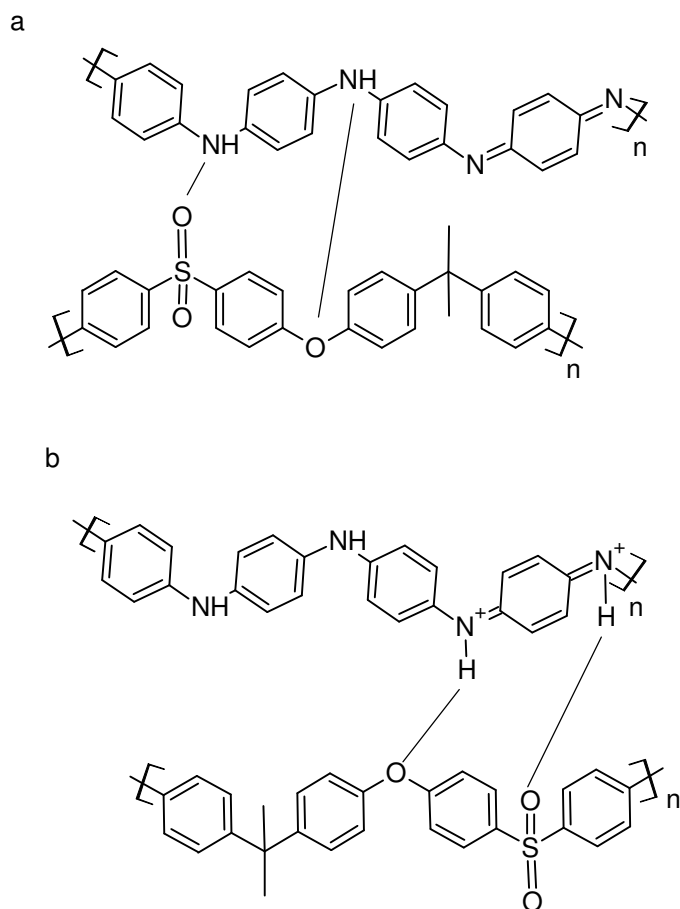
Figure 2.4 Hydrogen bonding between polysulfone and polyaniline

They used polysulfone porous membranes as supporting membrane. The membrane showed 75 L/m^{2}h of permeation flux with rejection 65 % for 2000 mg/L NaCl solution and rejection of 98 % for 2000 mg/L MgSO$_4$ solution at 1 MPa. They concluded that increasing the concentration of feed decreased the rejection and permeation of permeate.

Nilsson et al. (2008) studied the influence of pH, salt and temperature on nanofiltration membranes. The combined effect of pH, temperature and KCl had a considerable influence on membrane performance: KCl increased membrane swelling, which also increased with pH. The retention decreased with increasing temperature. The retention of KCl was less influenced by temperature than the retention of glucose. This work highlights the importance of temperature, pH, salt and ionic strength on the performance of NF membranes.

Li et al. (2008) studied Polysulfone/sulfonated Poly(ether ether ketone) blend membranes: morphology and their application in the filtration of alcohol based feeds. SPEEK lead to more open membrane structures and induced strong interaction between the membranes and polar solvents such as water and alcohols, thus leading to high flux.
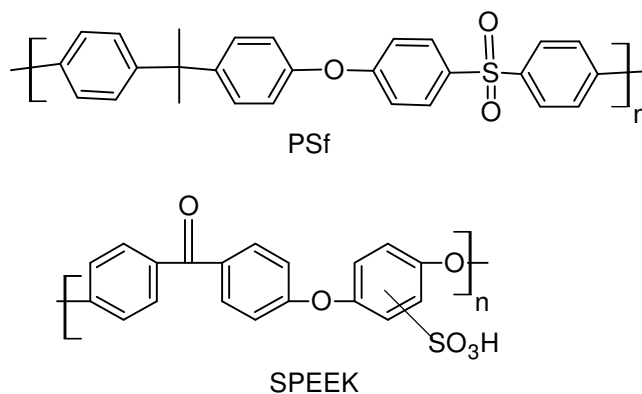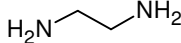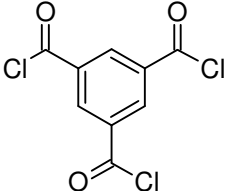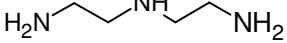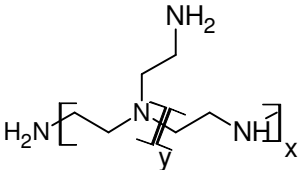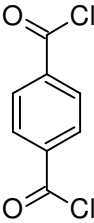
Figure 2.5 Polysulfone/sulfonated poly(ether ether ketone)

Jeon et al. (2008) reported performance of negatively charged nanofiltration membranes prepared from mixture of various dimethacrylates and methyl acrylic acid. The active layer of the composite membranes having desired salt rejection and water permeability characteristics for nanofiltration were fabricated from monomer mixture of various dimethacrylate and methyl acrylic acid (MAA).

Bratels et al. (2008) studied new generation of low fouling nanofiltration membranes. The performance of this plant has not equaled the stable results of the one that does add acid and antiscalent however the performance was quite reasonable and could be further optimized to find the lowest cost operating point.

Chaing et al. (2009) studied NF membranes synthesized from hyper branched polyethleneimine (PEI). They investigated the pore size effect by comparing two similar membranes of different pore sizes. The two membranes were synthesized by interfacially polymerizing trimesoyl chloride (TMC) with ethylenediamine (EDA), diethylenetriamine (DETA) and triphenyl chloride (TPC) with EDA and DETA.

Table 2.1 Diamines, polyamines and acid chlorides used for interfacial polymerization

Diamine and polyamine	Carbonyl chloride
EDA	TMC
DETA	
PEI	TPC

Hu et al. (2009) reported synthesis and characterization of sulfonated polyimides derived from 2,2-bis(4-sulfonyl)-4,4-oxydianiline as polymer electrolyte membranes for fuel cell applications. They prepared two types of sulfonated diamines, namely side chain type and main chain type. Side chain diamines showed higher water uptake than the main chain diamines.
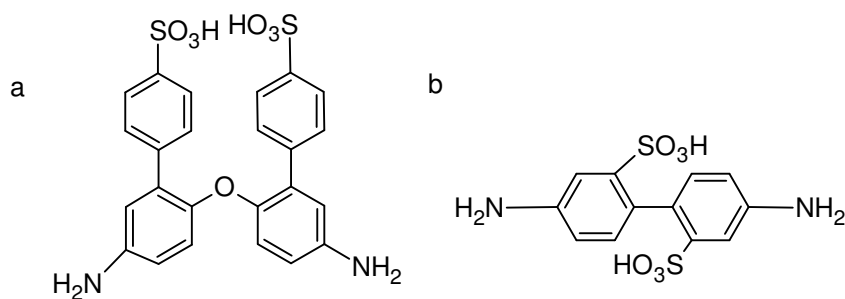
Figure 2.6 a) Side chain sulfonated diamine b) Main chain sulfonated daimine
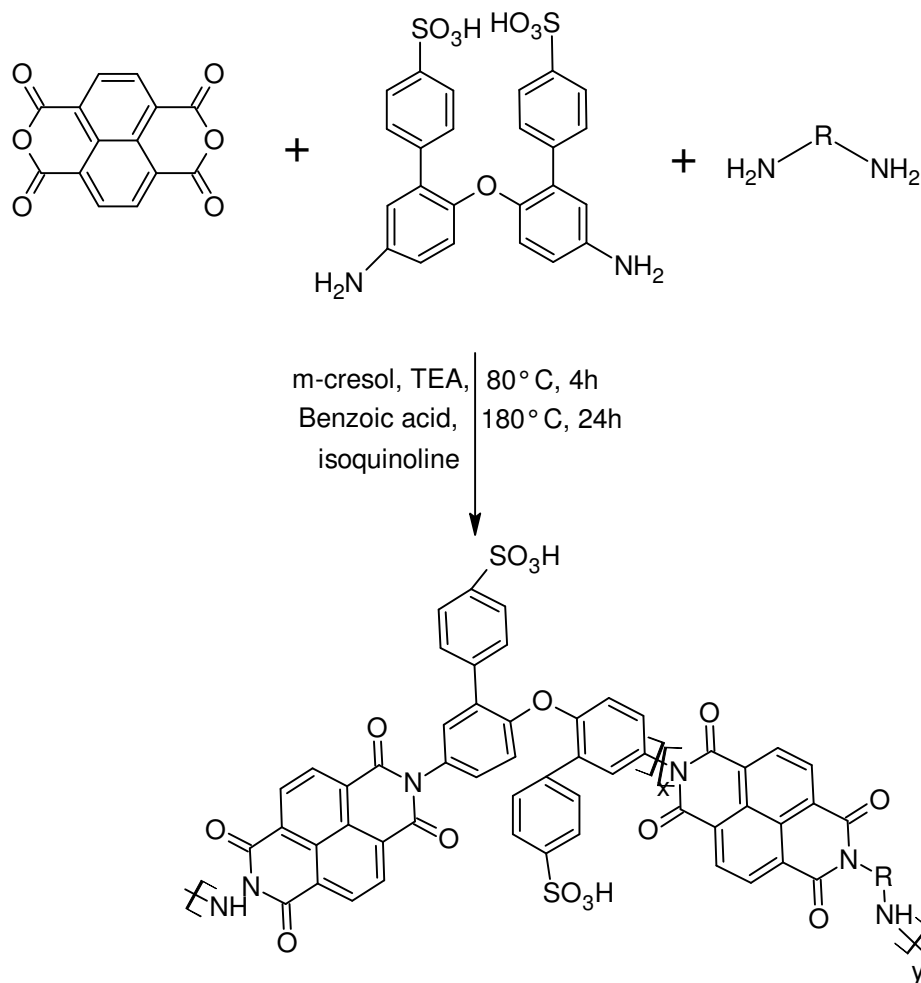
Figure 2.7 Synthesis of polymers using sulfonated diamines

Hegde et al. (2010) reported synthesis and desalination performance of Ar^{+} and N[+] irradiated polysulfone based new NF membrane. Polysulfone and poly(1,4- phenyl-ether-ether sulfone) blend membrane surface was irradiated by cold plasma and their properties were studied. N[+] irradiated membranes showed better performance than Ar^{+} irradiated membrane because, they showed relatively larger dielectric properties indicating greater void volume.

Arthanareeswaran and Starov (2011) performed experiments on the effect of solvents on performance of polyethersulfone UF membranes and their application for metal ion separations. The new polyethersulfone (PES) based UF membranes were

formed using a two stage process of dry and wet phase inversion in non-solvent coagulation bath. The effects of three different solvents such as, N,N-dimethylformamide (DMF), N-methyl-2-pyrrolidone (NMP) and Dimethyl sulphoxide (DMSO) of 82.5 % and 85 % concentrations on the performance of final membranes were extensively investigated. Separation of metal ions from aqueous solutions were studied for Ni (II), Cu (II) and Cr (III) using two complexing polymer ligands namely polyvinyl alcohol (PVA) and poly(diallyldimethylammonium chloride) (PDDA). The order of the pure water flux of PES membranes with different solvents was in the following order DMSO>NMP>DMF. PDDA and PVA showed a high rejection for tri-valent cations Cr (III) and lower rejection of divalent cations Ni (II) and Cu (II).

Basri et al. (2011) prepared polyethersulfone (PES)–silver composite UF membrane and studied effect of silver loading and PVP molecular weight on membrane morphology and antibacterial activity. Polyethersulfone–silver composite membranes were fabricated via a simple phase inversion method by using silver nitrate ($AgNO_3$) as an antibacterial agent and polyvinylpyrolidone (PVP) of molecular weight 10,000, 40,000 and 360,000 Da as dispersant in the dope formulation. From XPS and EDX examinations, it was observed that the resulting membrane prepared from 2 wt % $AgNO_3$ and PVP of 360,000 Da exhibited high concentration of Ag mainly due to high Ag-particle entrapment in the membrane structure. The uniform distribution of Ag particles has contributed significantly to 100 % inhibition against *Escherichia coli (E. coli)* growth within 24 h incubation. In addition, the results of pure water filtration test showed minimum silver loss during operation indicated better stability of membrane produced in terms of Ag-entrapment in membrane structure. Based on the findings, they have concluded that PES–silver composite membrane with PVP of 360,000 Da offers huge potential membrane for bacteria removal and disinfection.
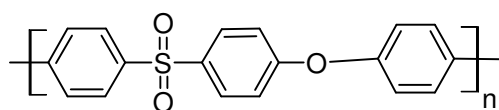
Figure 2.8 Structure of PES

Song et al. (2011) worked on improving performance of polysulfone UF membrane using PANiEB as both pore forming agent and hydrophilic modifier. Emeraldine base polyaniline (PANiEB), which is mostly soluble in N-methyl-2-pyrrolidone (NMP) and slightly soluble in water, was used as additive to prepare (PSf)/PANiEB membrane via immersion precipitation process. All the PSf/PANiEB membranes had higher porosity, larger surface pore size, more vertically interconnected finger-like pores and less macrovoids than PSf membrane. Pure water fluxes of PSf/PANiEB membranes were 1.7-2.8 times that of PSf membrane while rejection property including bovine serum albumin, egg albumin and trypsin rejections changed slightly. BSA UF experiment showed that PSf/PANiEB membranes had higher flux and better antifouling property than PSf membrane.
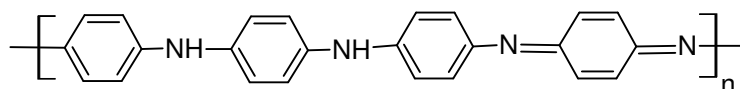
Figure 2.9 Structure of Polyaniline

Jin et al. (2012) prepared novel nanofiltration membrane containing SiO_2 nanoparticles with poly(amidoamine) (PAMAM) dendrimer and trimesoyl chloride (TMC) by interfacial polymerization on polysulfone (PSf) ultrafiltration membrane. The addition of nano-SiO_2 in the skin layer improved thermal stability, hydrophilicity and enhanced the membrane permeation properties without loss of rejection rate. The order of salt rejection rate is $Na_2SO_4 > MgSO_4 > MgCl_2 > NaCl$, which indicated that the PA-SiO_2 membrane was negatively charged. The zeta potentials for PA-SiO_2 membranes were more negative than that of PA membrane for nano-SiO_2 surface with more negatively charged hydroxyl groups. The nano-composite NF membrane is particularly suitable for treating acidic feeds and separating salt solution containing bivalent anions. The anti-fouling abilities were enhanced for PA-SiO_2 membrane while raw surface water treatment.
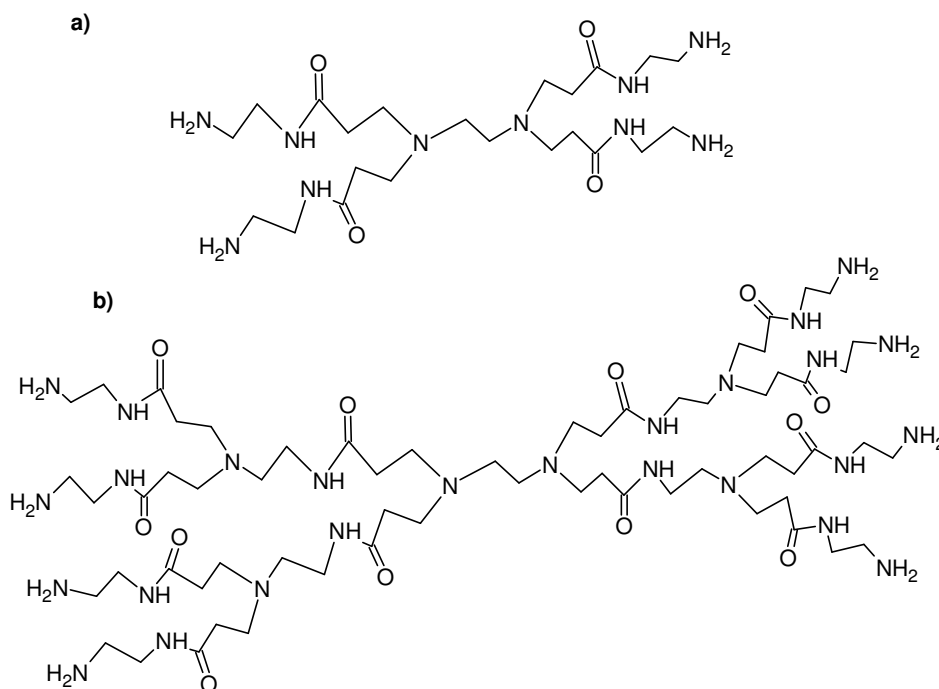
Figure 2.10 Chemical structure of PAMAM dendrimer (a) Generation 0 (b) Generation 1.

Zhang et al. (2012) Five different ratios of SiO_2-PAMPS nanoparticles were prepared and these nanoparticles were then blended with polysulfone (PSf)/N, N-Dimethylacetamide (DMAC)/Ethanol solution to fabricate hybrid ultrafiltration membranes via wet phase-inversion process. These experimental results suggested that the higher concentration of nanoparticles in casting solution induced a macrovoid enlargement of membrane cross section. Furthermore, the higher monomer mole ratio ($MSiO_2$/MAMPS) of the hybrid nanoparticles in casting solution resulted in a sharp increase of water flux of the ultrafiltration membrane. The hybrid ultrafiltration membrane (SiO_2-PAMPS 4-0.3 wt %) had water fluxes of 190 L/m^2h and 687 L/m^2h at 0.1 MPa and 0.5 MPa respectively. The SiO_2-PAMPS nanoparticles rather than SiO_2 nanoparticles showed excellent stability on membrane surface even after continuously shaking for 15 days.
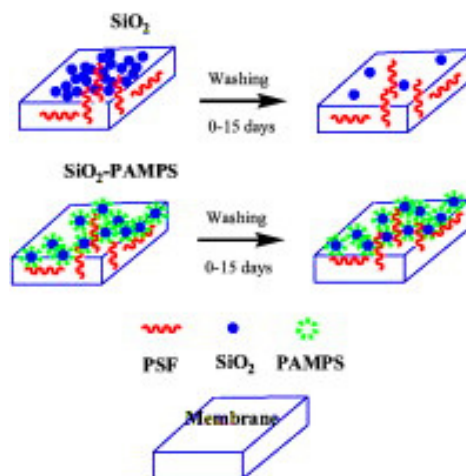
Figure 2.11 Schematic representation of membrane preparation
(Source: Zhang et al. 2012)

From this outlook it is clear that NF membranes have wide number of applications in separation technique. But it can be seen from the literature review that in order to fulfill the requirements of the process, there is a need of new polymer membranes which can exhibit symmetric nano pore size and uniform pore distribution. Also, membrane fouling is major drawback to membrane process, which needs to be overcome in order to increase membrane performance. There is also wide scope to improve chemical stability, mechanical strength and hydrophilicity of membranes. Presently very few polymers are known to show all the above characteristics, so preparation of novel polymer membrane with above mentioned characteristics is the greatest challenge. Keeping these challenges in view, present research work is proposed for the preparation of high flux and least fouling novel polymeric membranes.

2.2 PROPOSED WORK

In industrially established applications, some of the survey of the synthetic membranes has better overall performance. The very high salt rejection and water fluxes through the reverse osmosis membranes obtained using trans-membrane pressure of upto 100 bars may serve as an example for the adaptation of the membrane concept to technical requirement. However, relatively few of many possible separation principles

and processes have been fully explored yet. Consequently, a strong motivation for modifing established membrane materials and process is the current research in the field. So it is necessary to develop and technically implement novel membrane materials and processes.

Objectives

- Synthesis of amphiphilic polymers which can induce enhanced hydrophilicity
- Chemical modification of polymers to increase the hydrophilicity
- Characterization of polymers by NMR, IR and GPC studies of the above synthesized polymers
- Preparation of nanofiltration composite membranes with polysulfone
- Preparation of nanofiltration composite membranes with sulfonated polysulfone
- Surface modification of some composite membranes by physical and chemical methods
- Membrane characterization by ATR-FTIR, DSC, contact angle measurement and SEM
- Determination of membrane surface charge by measurement of ion exchange capacity (IEC) and diffusion potential
- Performance of the membrane in terms of flux, molecular weight cut-off (MWCO) and % rejection of salt solution

Abstract: This chapter deals with the synthesis of novel polymers. Polysulfonylaminobenzamide (PSAB), methylated polysulfonylaminobenzamide (mPSAB), poly[(4-aminophenyl)sulfonyl]butanediamide (PASB) and methylated poly[(4-aminophenyl)sulfonyl]butanediamide (mPASB) were prepared using sulfonamide derivatives and different acid chlorides. The polymer structures were confirmed by spectral studies. These polymers were blend with polysulfone (PSf) to obtain the membranes. The membrane characterization, performance studies and results were discussed in this chapter.

3.1 POLYSULFONE AND POLYSULFONYLAMINOBENZAMIDE BLEND MEMBRANES

PSf is a hydrophobic material which can provide mechanical strength to the membranes. PSf as a supporting membrane material has gained considerable amount of interest and has gathered much attention from researchers in recent years. Miao et al. (2006) prepared and characterized N,O-carboxymethyl chitosan (NOCC)/PSf composite NF membranes. They used PSf membrane as a support and NOCC as a top layer. Zhang et al. (2006) reported investigation on the structures and performances of a Polypiperazine amide PPA/PSf composite membrane. In this work Polypiperazine (PP) was cross-linked to the PSf membrane having 6000 Da MWCO.

Recently, many literatures have reported PSf and modified PSf as the material for the NF membrane (Ghosh et al. 2000, Amini et al. 2009). In NF membranes, the main challenge is to increase the flux and salt rejection while minimizing the operating pressure. However membrane process suffers from fouling, a phenomenon in which its pores get blocked and filtration efficiency drastically decreases (Nataly et al. 2008). Baruah et al. (2012) prepared PSf and a-Cyclodextrin membranes by the phase inversion method using different solvents. Effect of solvent on phase inversion process was studied.

Han et al. (2012) prepared composite membrane, composed of hyperbranched poly(amidoamine) (HYPAM) and polysulfone (PSf) which successfully enabled the removal of heavy metal ions from contaminated aqueous media. The dendritic chelating

agent HYPAM (Figure 3.1) was incorporated into PSf via a phase inversion process to produce a HYPAM/PSf membrane. The efficiency of Cd (II) removal was 51 % and resulted from metal ion complexation by a tertiary amine of HYPAM and primary amine and amide groups grafted onto the PSf membrane surface. Moreover, the water permeability and bovine serum albumin (BSA) retention of the HYPAM/PSf composite membrane were as high as 18 L m^{-2} h^{-1} at 1 bar and 85 % respectively.
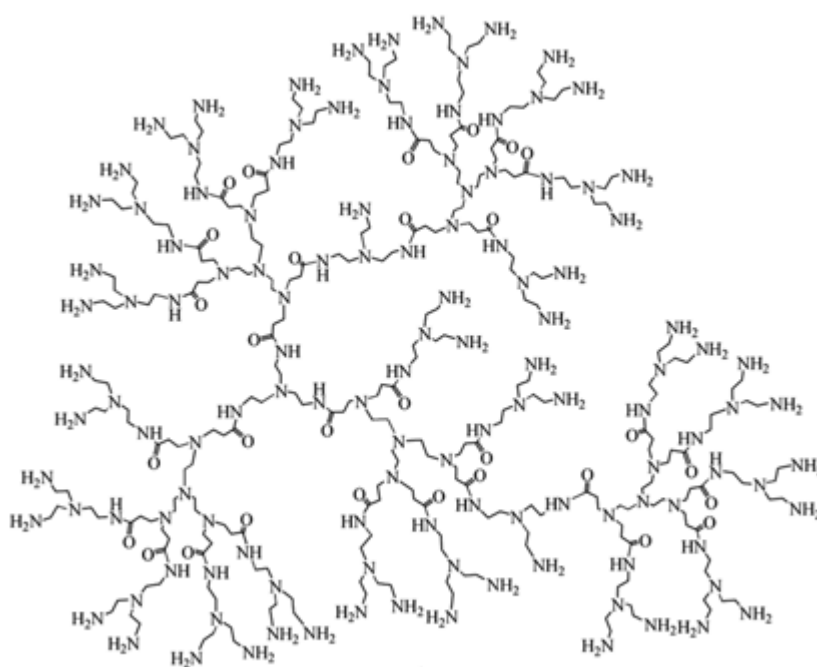
Figure 3.1 Structure of hyperbranched poly(amidoamine) (HYPAM)

(Source: Han et al. 2012)

Nowak (1989) reported, the transport and separation properties of PSf membrane depends on the substrate which is used for composition. He prepared PSf and PMMA blend membrane for rejection of dye particles from industrial waste.

Keeping these challenges in mind and with the aim of improving the productivity of the NF membrane, we have designed NF blend membranes made of different weight proportion of novel polymers and PSf by Diffusion induced phase separation (DIPS) method.

3.1.1 Experimental

3.1.1.1 Synthesis of polymers

Polymers were synthesized from sulfonamide and acid chlorides. 2 g (0.00985 mol) of freshly prepared terephthalic acid chloride was dissolved in 30 mL of NMP. To this solution, 2 g (0.0116 moles) of substituted 4-amino-1-benzensulphonamide, 3.1 g (0.0232 moles) of LiCl and 2-3 drops of Pyridine were added and then the reaction mixture was heated at 100°C for 20 hrs. After cooling the reaction mass to room temperature, it was poured into ice cold water. The solid mass was separated by filtration, washed with water and finally purified by ethyl acetate washing. The product was dried in vacuum oven at 50 °C for 15 hrs. The dried solid product was used for further characterization. Schematic representation of the reaction is shown in Figure 3.2.
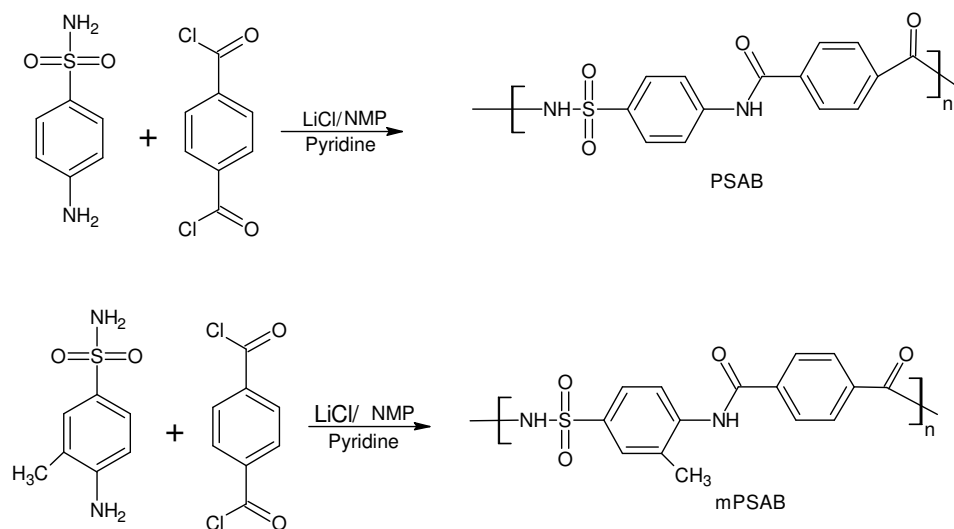
Figure 3.2 Synthetic route for the polymers

3.1.1.2 Preparation of membrane

The membrane was prepared by DIPS method. Udel PSf was used having molecular weight of 35,000 Da. PSAB and mPSAB were synthesized in the laboratory and reagent grade NMP was obtained from Merck-India and was used without any further purification. Both PSf and novel polymers in required amount were dried in

vacuum oven for 10 hrs. Different compositions of polymers were taken into a beaker and specified amount of NMP was added. Table 3.1 represents different concentration of polymers used for membrane preparation. The mixture was stirred for 24 hrs at 60 °C to get viscous solution and then degassed by allowing it to stand for one hr. The solution was filtered using G4 sand filters. Filtered polymer solution was cast on a glass plate using finely polished glass rod. The thickness of the membrane was maintained at 0.20 mm. Further it was allowed to stand at room temperature for 40 seconds for evaporation of solvents in the air. The membrane was then separated by immersing the glass plate in ice cold distilled water bath through phase separation process. Separated membrane was further washed with distilled water for several times and stored in distilled water for 24 hrs.

Table 3.1 Composition of polymers used for membrane preparation

Membrane	Polymer composition		
	PSf	PSAB	mPSAB
PSf:PSAB 70:30	70%	30%	-
PSf:PSAB 80:20	80%	20%	-
PSf:PSAB 90:10	90%	10%	-
PSf:mPSAB 60:40	60%	-	40%
PSf:mPSAB 70:30	70%	-	30%
PSf:mPSAB 70:30	80%	-	20%
PSf:mPSAB 70:30	90%	-	10%

3.1.2 Results and discussion

3.1.2.1 Characterization of polymer

ATR-IR spectra (Figure 3.3) showed peak at 3341 to 3350 cm^{-1} for NH stretching, 1661 cm^{-1} for the C=O, 1151 cm^{-1} due to O=S=O stretching and additional peak in mPSAB at 2943 cm^{-1} of CH$_3$ stretching. Figure 3.4 shows ^{1}H-NMR spectrum of PSAB. It is clearly observed that the peak at δ 10.73 corresponds to bridge amide NH whereas one more NH peak merged with the aromatic peak and peaks at δ, 7.3, 7.8, 7.9 and 8.1 (2H

each) correspond to eight aromatic protons, hence confirms the structure. Figure 3.5, ^{1}H NMR spectrum of mPSAB showed a multiplet at around δ 7.3 to 8.3 which included all aromatic protons as well as a NH proton in it. The bridged NH proton resonated at δ 10.7. The peak for methyl group protons attached to aromatic ring was observed at δ 2.3.

Molecular weight of the polymer was determined by gel permeation chromatography (GPC) using polystyrene as standard. PSAB and mPSAB showed M_w 3733 Da and 2084 Da with polydispersivity value of 3.4 and 2.1 respectively.
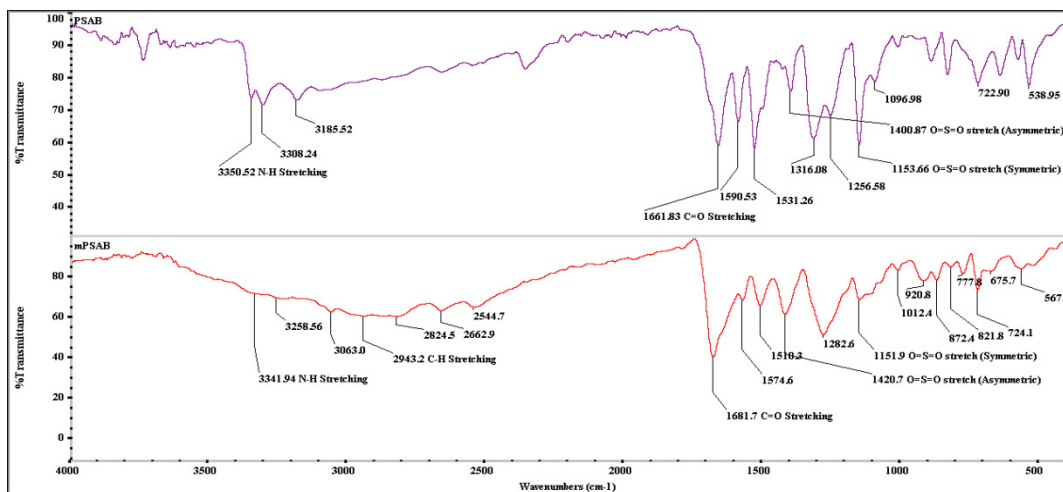
Figure 3.3 ATR-IR spectra of PSAB and mPSAB polymer
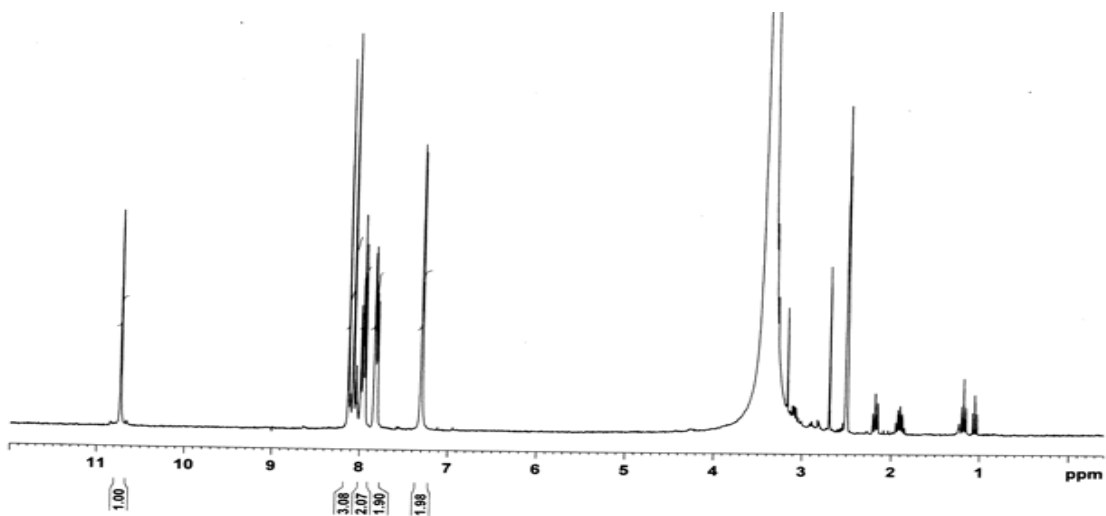
Figure 3.4 ^{1}H NMR spectrum of PSAB polymer
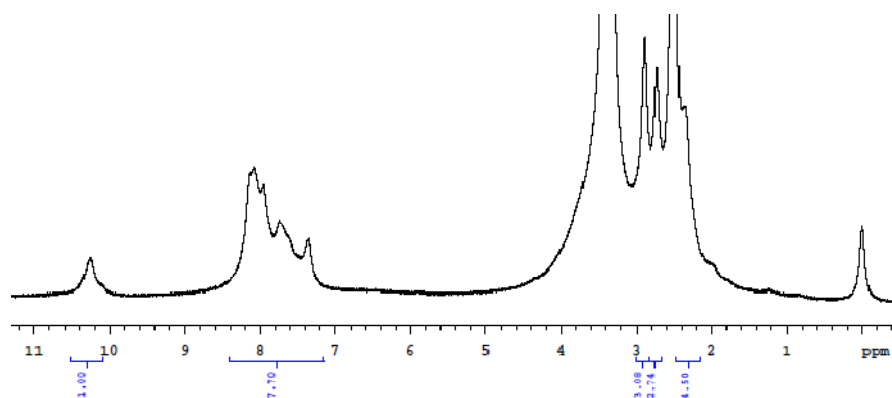
Figure 3.5 ^{1}H NMR spectrum of mPSAB polymer
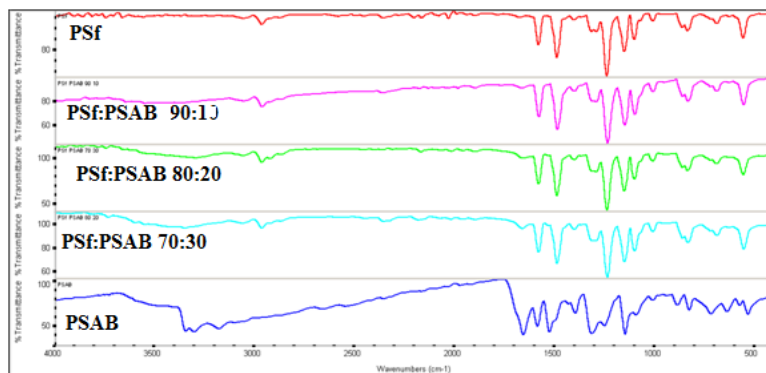
Figure 3.6 ATR-IR spectra of PSf:PSAB blend membranes

ATR-IR of the membranes was done for the confirmation of the composition of the polymers. The peaks present in the PSAB and mPSAB were also seen in the IR Spectra of the blend membranes. Figure 3.6 and 3.7 are ATR-IR spectra of PSf:PSAB and PSf:mPSAB blend membranes respectively.
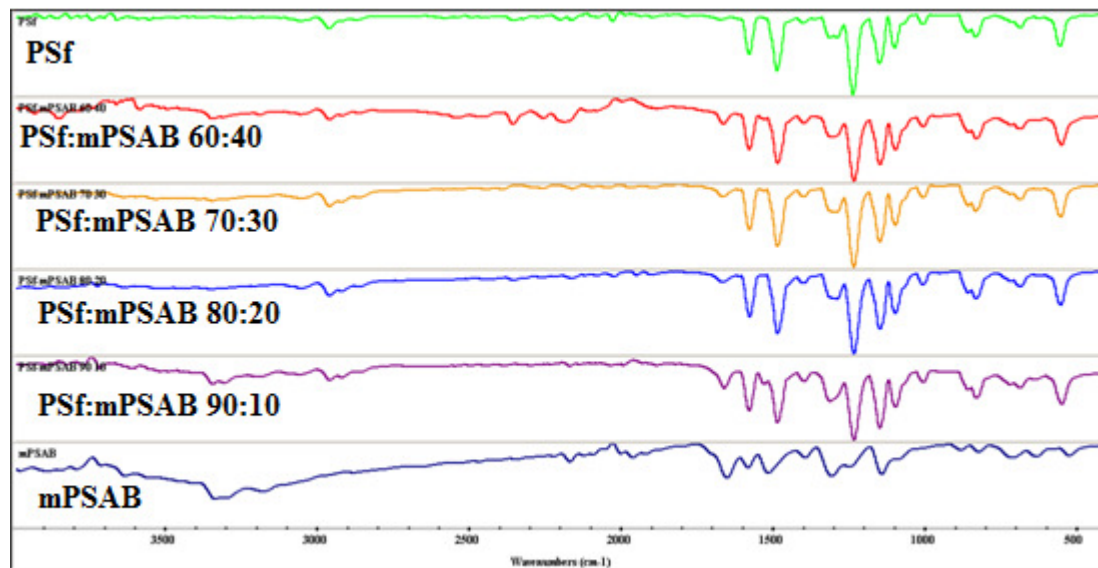
Figure 3.7 ATR-IR spectra of PSf:mPSAB blend membranes
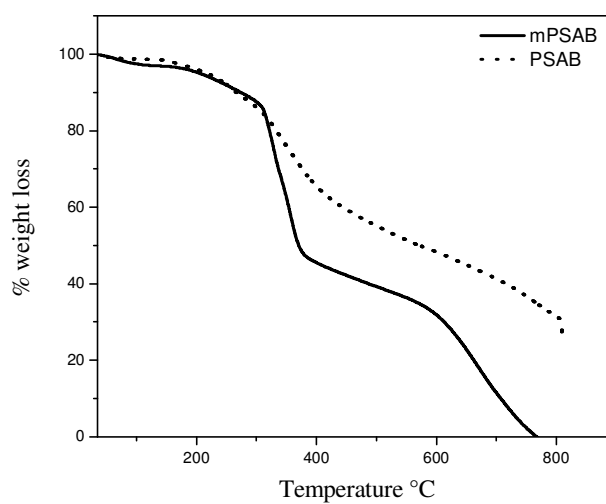
Figure 3.8 TGA curves of the polymers

TGA analysis was studied and Figure 3.8 showed TGA curves of polymers. There is no any weight loss upto 250 °C. After 250 °C, there is gradual decrease in the weights of both the polymers. In mPSAB around 325 °C there is sudden decrease in weight which is attributed to decomposition of side chains. After 350 °C, degradation of polymer backbone was observed in both the polymers.

3.1.2.2 Thermal properties of the membranes

The thermal behaviors of different blend membranes were studied from the DSC plots. Figure 3.9 and 3.10 shows the DSC graphs of PSAB and mPSAB membranes respectively. The T_g values of different composite membranes were measured with the rate of 10 °C per min and compared. From the thermal study, it was clearly observed that the T_g value of the blend membrane was different from that of PSf and it showed a single T_g value.
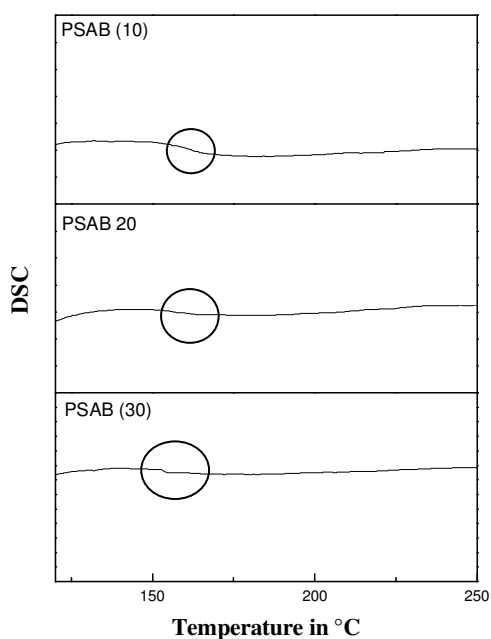
Figure-3.9 DSC curves of PSAB membranes
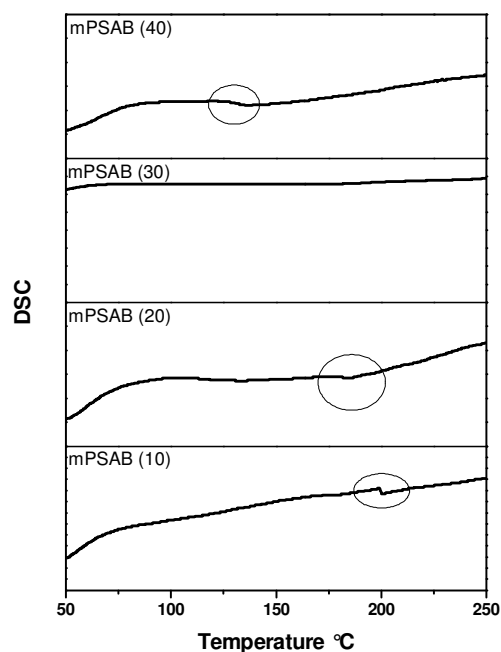
Figure 3.10 DSC curves of mPSAB membranes

This confirmed the formation of a blend membrane. As a result of many Van der Waals interactions or hydrogen bonding between two polymers, the individual components lose their identity thereby giving a single T_g peak. Although the T_g values of PSAB membranes increased with increasing concentration of PSAB, in mPSAB series, higher T_g was observed with higher concentration of polysulfone content.

3.1.2.3 Surface morphology of the membrane

Transport properties of the membranes are closely related to their morphological properties like surface porosity and variation of their inner pore structure. Scanning electron microscopy (SEM) serves as a powerful tool to characterize the microscopical pore structure of the membranes (Deng et al 2009).
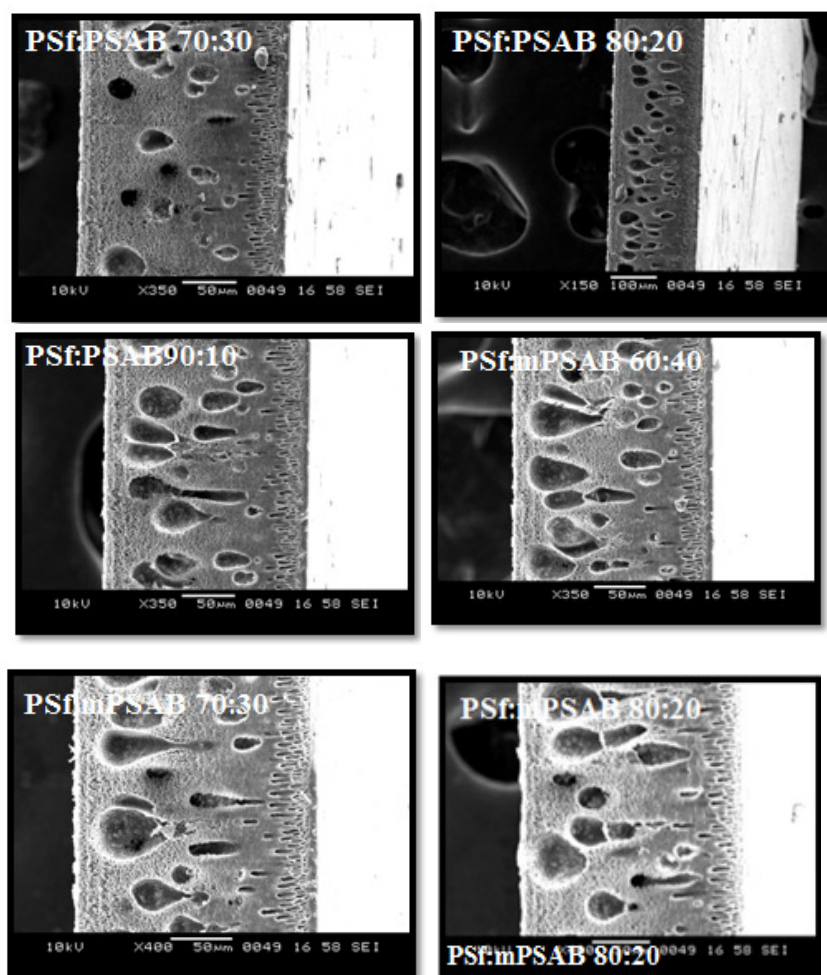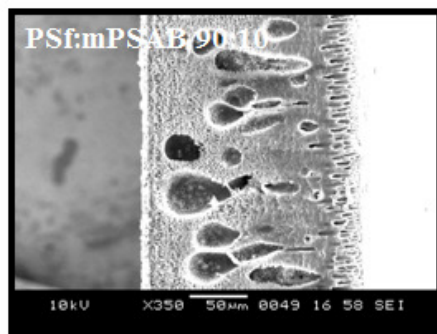
Figure 3.11 Cross sectional SEM images of membranes

3.1.2.4 Wettability study of the membranes

Hydrophilicity is directly related to the productivity of the membrane. More hydrophilic membrane results in better productivity. Wettability of the membrane can be studied using contact angle and water uptake study. Looking into the data, contact angle of the membrane was in the order of composition PSAB (10) > PSAB (20) > PSAB (30) and   mPSAB (40) > mPSAB (30) > mPSAB (20) > mPSAB (10), where figures in the parentheses indicate the content of PSAB and mPSAB. Figure 3.12 showed contact angle values of the membranes with water. In PSAB series it was observed that, with increase in the percent composition of PSf contact angle increased, whereas in mPSAB series, contact angle increased with increasing mPSAB concentration. In mPSAB the presence of one additional methyl group was responsible for decrease in the hydrophilicity of the membrane.

Hydrophilicity of the membrane can be explained by water uptake test. Affinity towards water is an important property for the water filtration membranes. However, hydrophilic materials may lead to large water uptake and at the same time membrane may lose its mechanical resistance.
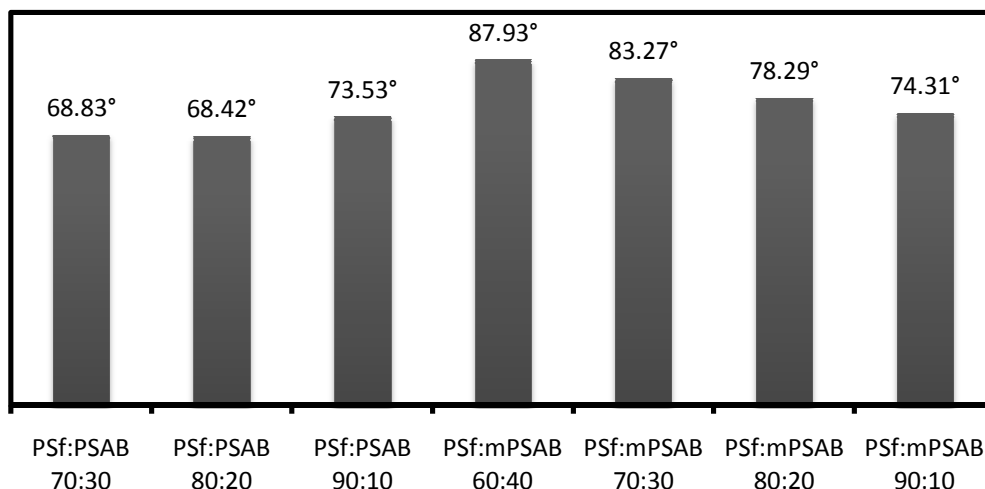
Figure 3.12 Contact angle of membranes

The uptake ratio is a parameter which is frequently used to characterize the affinity of the membranes towards water. The PSf:PSAB 70:30 showed highest water uptake in correlation with its lowest contact angle. Figure 3.13 showed, increasing the percentage composition of the PSAB, increased the water uptake of the membrane, In mPSAB series, with increase in mPASB composition decreasing water uptake trend was observed. While comparing the water uptake study of PSAB and mPSAB series of the membranes, mPSAB series showed less water uptake and high contact angle. Hence, it was concluded that PSAB blend membranes were more hydrophilic than the mPSAB blend membranes.

Water uptake test was carried out at different pH. The data shown in Figure 3.13 indicated a slight increase in water uptake ratio with the PSAB content in the initial blend. Also it was observed that at acidic and basic pH, membrane showed more water uptake as compared to neutral pH. Tendency of water uptake at different pH exhibited following trend, pH12 > pH10 > pH3 > pH7. The following theory was proposed in order to explain the above observation. Membrane can take up water by two ways, first due to absorption of water into the polymer matrix and second due to water retained by capillary structure of the membrane pores. The probability of opening of pores at different pH was

also considered. PSf:PSAB 70:30 membrane showed more water swelling and PSf:mPSAB 90:10 showed less water swelling as compared to membranes of other composition.
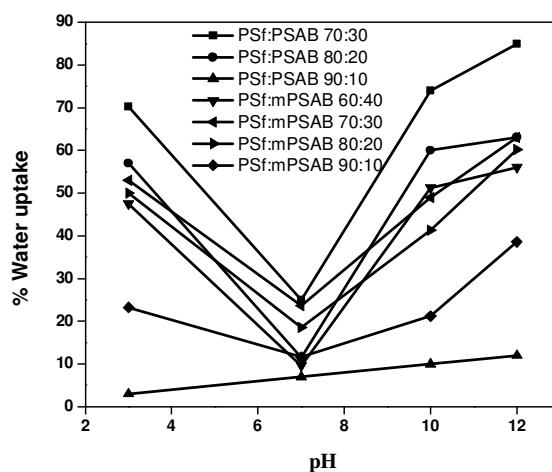
Figure 3.13 Water uptake of membranes in different pH

3.1.2.5 The performance study of the membranes

Pure water permeability was obtained by measuring the flux for pure water against operating pressure. As shown in Figure 3.14, the flux increased linearly with the operating pressure. The hydraulic permeability coefficient (L_p) was been calculated from the slope of the line obtained from the proportionality relationship between the water flux and the applied pressure as shown in Table 3.2.
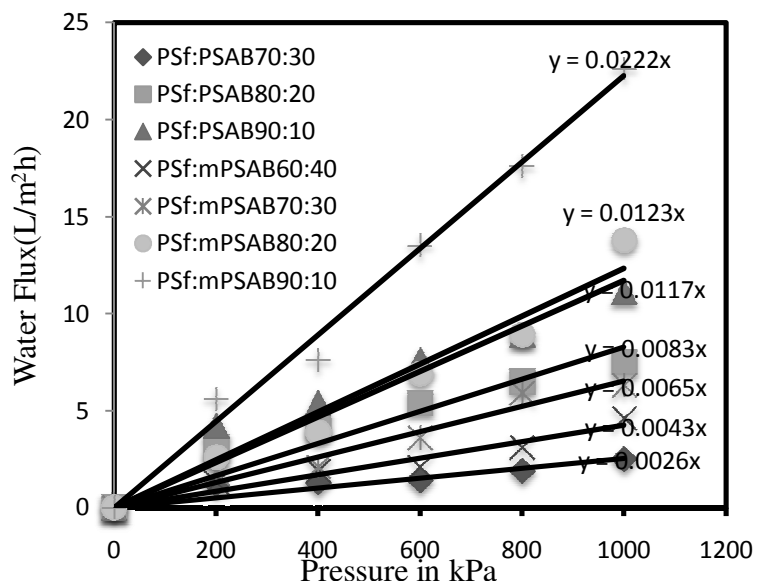
Figure 3.14 Water flux of membranes at different pressure

Table 3.2 Hydraulic permeability coefficient (L_p) values of membranes

Membrane	L_p (m/sPa)
PSf:PSAB 70:30	7.2×10^{-12}
PSf:PSAB 80:20	3.3×10^{-12}
PSf:PSAB 90:10	3.2×10^{-12}
PSf:mPSAB 60:40	1.1×10^{-12}
PSf:mPSAB 70:30	1.8×10^{-12}
PSf:mPSAB 80:20	3.4×10^{-12}
PSf:mPSAB 90:10	6.1×10^{-12}

The membranes showed increasing waterflux with increasing operating pressure. Figure 3.15 showed the MWCO of all the membranes. All the membranes exhibited nearly 90 % rejection of 1000 Da PEG solutions. Since all the membranes showed similar behavior, it was concluded that there is not much difference in pore size.
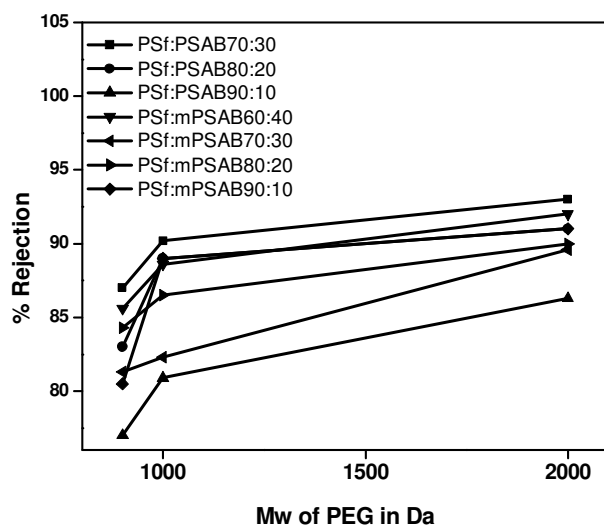
Figure 3.15 MWCO of membranes

The salt rejection experiment was carried out using 3500 ppm of NaCl solution in different pressure and pH. Figure 3.16 showed rejection of the membranes at different pressure. All the membranes showed same decreasing tendency with increasing pressure. It was thus concluded that high pressure lead to an increase in the pore size of the membrane. The membrane showed varied water swelling at different pH. It may be because of pore opening or chemical property of the polymers at different pH. Hence, the rejection of the membrane at different pH was carried out.

The data for salt rejection in Figure 3.17 suggested that, all the membranes showed more rejection in basic and neutral pH. In acidic pH the membrane pores opened to a greater extent leading to less rejection. Several factors contribute towards membrane
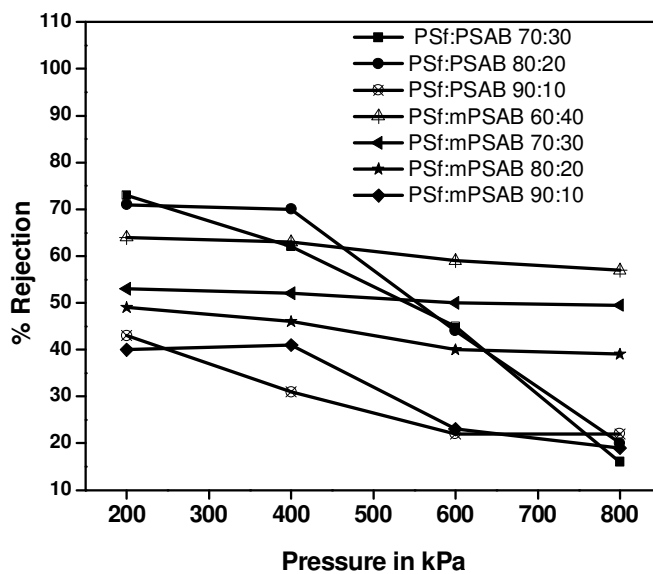
Figure 3.16 Salt rejection at different pressure
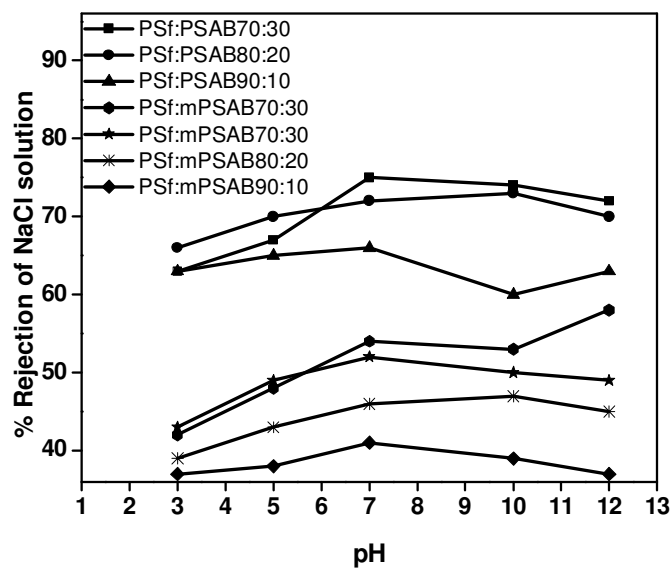
Figure 3.17 Rejection of NaCl in different pH

performance under different pH conditions. Literature showed that the presence of ions can affect the retention of uncharged molecules (Bergmann et al. 2005). Also studies

have correlated such changes in performance to the membrane charge density at different pH conditions (Manttari et al. 2006, Bergmann et al. 2005).

From Figure 3.17 it was clear that, in basic pH 11, membranes showed highest rejection. This is because, membrane surface became charged and the ionic interaction was more with feed sample. Also it followed that, if the feed sample had higher ionic concentration, it led to more rejection. Whereas in acidic pH, the amide and sulfonamide bonds in membrane matrix were broken, due to which the membrane structure was disturbed and it showed more opening which eventually led to less rejection. Increase in the percentage composition of the PSAB and mPSAB showed decrease in salt rejection, particularly in acidic pH. Also from the water uptake study it was concluded that the membranes showed more water uptake in acidic pH because they possessed larger pore size at acidic pH.
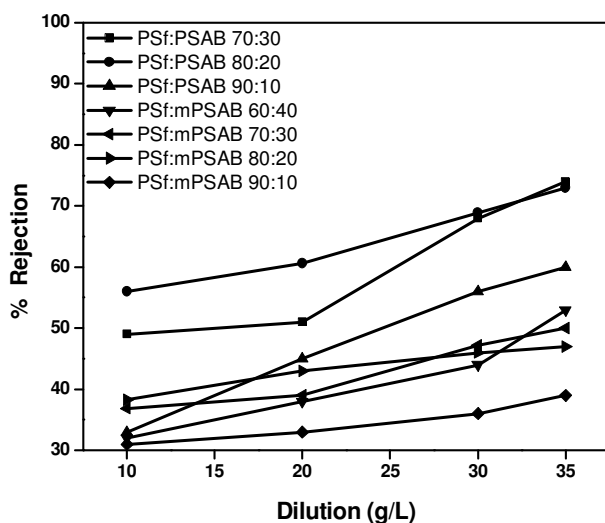
Figure 3.18 Effect of dilution on rejection

The ionic concentration of the feed immensely affects salt rejection hence the salt rejection at different feed concentration was studied. Figure 3.18 showed the effect of dilution on membrane rejection. It was observed, as the ionic concentration of the feed sample increases the rejection increases. All the membranes showed similar trait. The

feed sample having concentration of 3500 ppm showed more rejection than the other concentrations.

The effect of salt concentration on rejection could be explained by different mechanisms. Firstly, membrane pores were supposed to be more open due to swelling of the membrane by salt, as reported by many researchers (Ferger et al. 2000, Nilson et al. 2008, Bergmann et al. 2005, Escoda et al. 2010). Similarly, membrane thickness would also increase if membrane surface swelled. However, to our knowledge, there has been no direct observation to prove that membrane pores or thickness increased when salt was added. Freger (2004) detected that membrane thickness in 15 % (w/v) NaCl solution at pH = 3 and pH = 10 was thinner than that in pure water at pH = 7, suggesting that membrane did swell when the properties of solution changed. Moreover, for a membrane having an inter-connected porous structure, smaller solutes were expected to go through longer paths because they could permeate through the smaller pores of network (Bourance et al. 2007, Labbez et al. 2002), thus enlarging the effective membrane thickness as effective size of the solutes reduced. The above stated observations reasonably explained why the rejection values increased with increasing salt concentration.

3.1.2.6 Flux decline study

Since increase in rejection with higher concentration of salt was observed, study on the decline of flux was also carried out. Flux decline study was done using 2000 ppm of NaCl solution. The flux was determined at different intervals of the time starting from 60 min to 360 min with the time gap of 60 min. Figure 3.19 shows flux of the membrane at different intervals of time. Initially upto 300 min it was observed, there was an increase in the flux, however after 300 min it was constant and in some cases it was seen to decrease. This flux decline could be explained by a combination of two effects: the molecule should have the appropriate size to fill the membrane pores and adsorption process is enhanced by the hydrophobicity of the component. The rejection of the salt solution was 100 % after 240 min. Hence one can say that the higher rejection at higher concentration was due to membrane fouling.
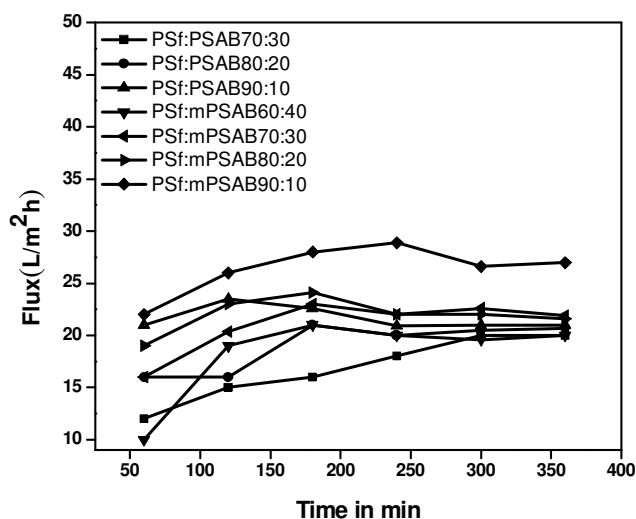
Figure 3.19 Flux decline result of membranes

3.1.3 Conclusions

The novel polymeric blend membranes were prepared by phase inversion technique and the performance was checked. All the membranes showed 1000 Da molecular weight cut-off for polyethylene glycol solution. Enhanced hydrophilicity was confirmed by water uptake and contact angle measurements. Water uptake is more in acidic and basic pH as compared to neutral pH, because unstable nature of amide and sulfonamide bond led to more porosity or increase in the pore size. The prepared membranes performed moderately for desalination of saline water. Enhanced salt rejection was effectively achieved by the novel blend membranes. Decrease in salt rejection was witnessed in acidic and basic pH and with dilution of feed sample.

3.2 POLYSULFONE AND POLY[(4-AMINOPHENYL) SULFONYL] BUTANEDIAMIDE BLEND MEMBRANES

In PSf and PSAB composite membranes, less salt rejection at higher pressure was observed whereas PSf and mPSAB membranes showed constant rejection even at higher pressure. This is because of the presence of alkyl group in the polymer, which gives mechanical strength to the membranes. With this objective in mind, following polymers were prepared.

Poly[(4-aminophenyl)sulfonyl]butanediamide (PASB) and methylated Poly[(4-aminopheonyl)sulfonyl]butanediamide (mPASB) novel polymers were prepared. The same procedure was followed to prepare these novel polymers but instead of aromatic acid chlorides (terephthalic acid chloride), aliphatic acid chloride (succinyl chloride) was used. The membranes were prepared by DIPS method, characterization and performance studies were done.

The novel polymers were prepared using succinyl chloride and sulfonamides. These polymers contained sulfonamide and amide linkages, thereby providing enhanced hydrophilicity to the membrane. Morever, aliphatic sulfonamides and amides are stronger than aromatic sulfonamides and amides. Hence, these polymers were designed for membrane preparation.

3.2.1 Experimental

3.2.1.1 Preparation of polymers

Polymers were prepared using Succinic acid chloride and Substitueted sulfonamides as monomers. 2 g (0.00985 moles) of freshly prepared succinic acid chloride was dissolved in 30 mL of NMP, to which 2 g (0.0116 moles) of substituted 4-amino-1-benzensulphonamide, 3.1 g (0.0232 moles) of LiCl and 2-3 drops of pyridine were added. The reaction mixture was then heated at 100 °C for 20 hrs. After cooling the reaction mass to room temperature, it was poured into ice cold water. The solid mass was separated by filtration, washed with water and finally purified by ethyl acetate washing. The product was dried in vacuum oven at 50 °C for 15 hrs. The dried solid product was

used for further characterization. Schematic representation of the reaction is presented in Figure 3.20
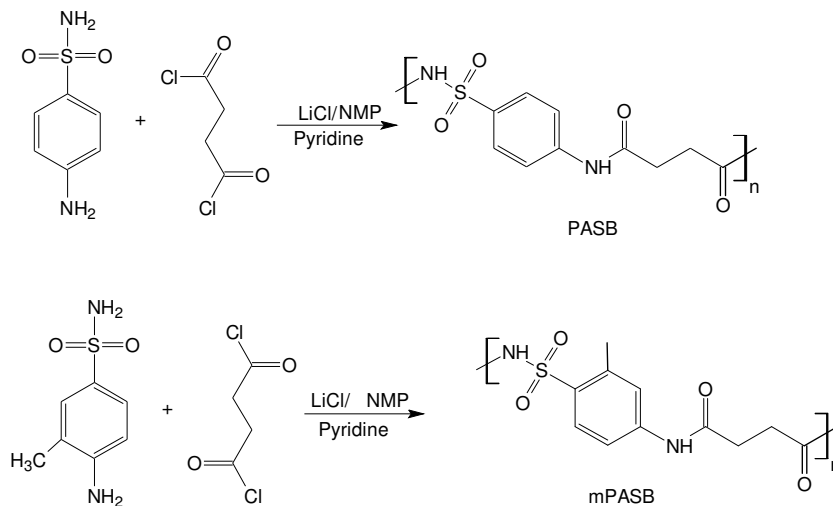
Figure 3.20 Schematic representation of polymer synthesis

3.2.1.2 Membrane Preparation

The membrane was prepared by DIPS method. The same procedure was used to prepare the membranes as reported in section 3.1.1.2. The different composition are tabulated in table-3.3.

Table 3.3 Composition of the polymers used for membrane preparation

Membrane	Polymers compositions		
	PSf	PSAB	mPSAB
PSf:PASB 60:40	60%	40%	-
PSf:PASB 70:30	70%	30%	-
PSf:PASB 80:20	80%	20%	-
PSf:PASB 90:10	90%	10%	-
PSf:mPASB 60:40	60%	-	40%
PSf:mPASB 70:30	70%	-	30%
PSf:mPASB 70:30	80%	-	20%
PSf:mPASB 70:30	90%	-	10%

3.2.2 Results and discussion

3.2.2.1 Characterization of polymer

Figure 3.21 shows ATR-IR spectra of the polymers. The spectra showed peak at 3341 cm^{-1} for the NH stretching, 1665 cm^{-1} for the C=O, 1139-1147 cm^{-1} due to O=S=O stretching and additional peak in mPSAB at 3073 cm^{-1} of CH$_3$ stretching.
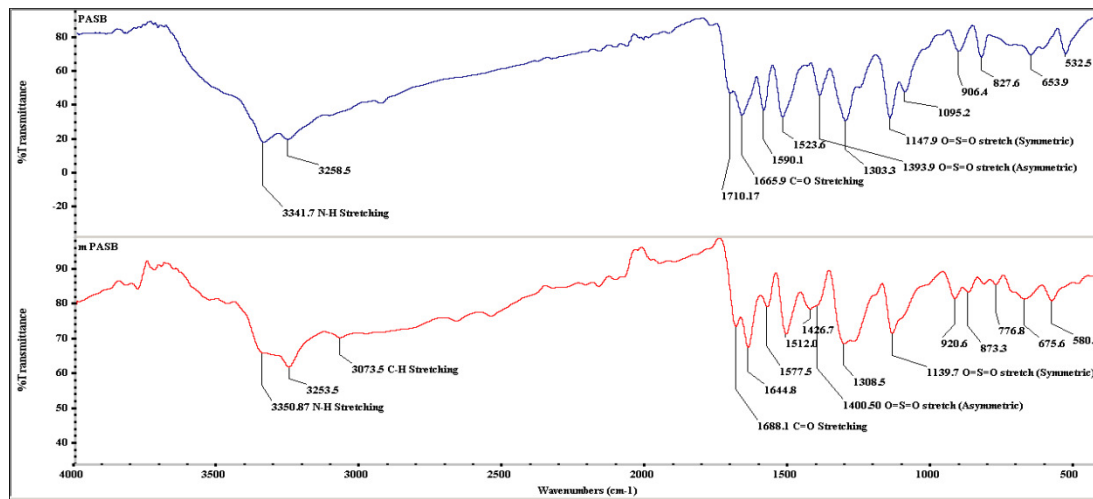
Figure 3.21 ATR-IR spectra of polymers
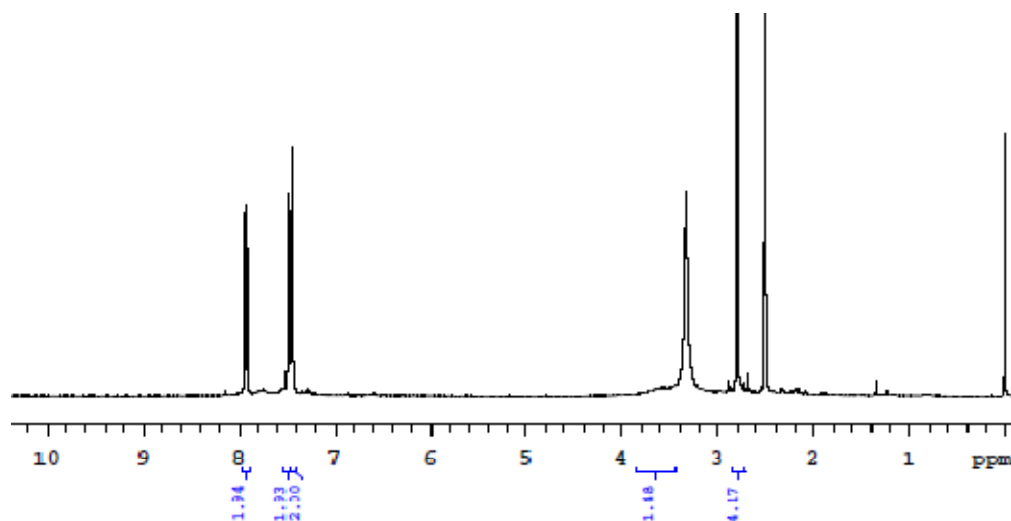
Figure 3.22 ^{1}H NMR spectrum of PASB polymer

Figure 3.22 shows ^{1}H-NMR spectrum of PASB. It is clearly observed that the peak at δ 7.5 and 7.9 corresponded to aromatic proton and bridge amide NH respectively, whereas terminal NH peak merged with the aromatic peaks. A peak at δ 2.9 corresponded to alkyl protons, all the values were in good agreement with desired product.

^{1}H NMR spectrum of mPASB (Figure 3.23) shows a multiplet at around δ 7.6 to 8 which included all aromatic protons as well as a -NH proton in it. A peak at δ 2.9 corresponded to ethyl protons. The methyl group attached to aromatic ring resonating at δ 2.5 merged with the DMSO peak. Hence the structure was confirmed.
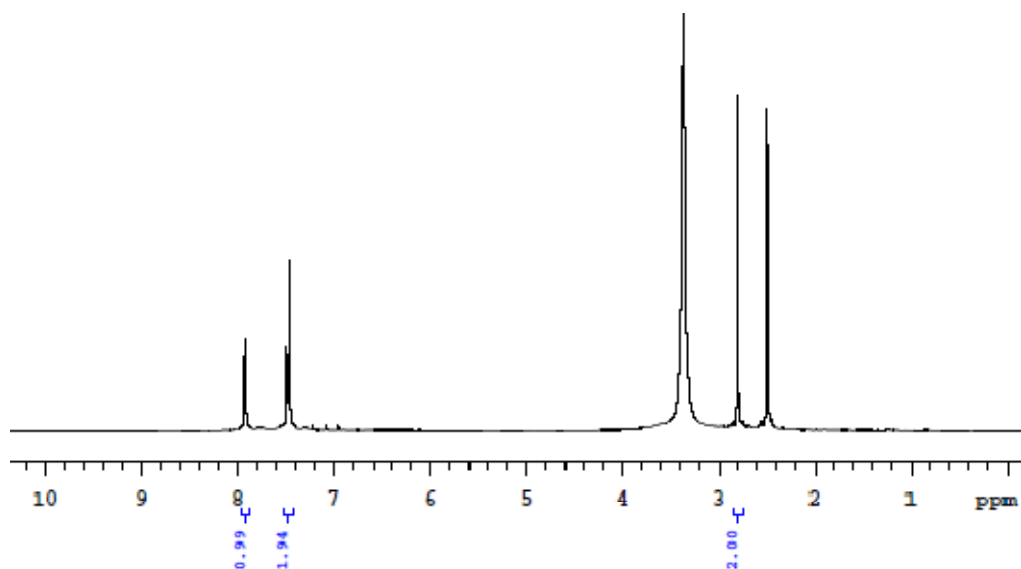
Figure 3.23 ^{1}H NMR spectrum of mPASB polymer

Molecular weight of the polymer was determined by GPC using polystyrene as a standard. PASB and mPASB showed Mw 110000 Da and 440000 Da with polydispersivity of 1.01 and 1.03 respectively.
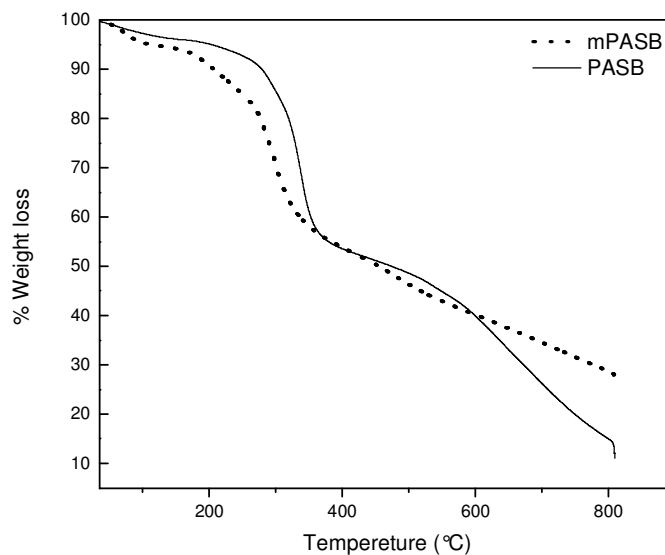
Figure 3.24 TGA of Polymers

From the thermograms it was observed that mPASB polymer was more stable than PASB because in mPASB, polymer was thermally stable upto 280 °C. After 280 °C, there was sudden weight loss in mPASB because of degradation of functional group. After 350 °C, degradation of polymer backbone occurred. In case of PASB, the polymer showed gradual decrease in weight throughout the temperature range.

3.2.2.2 Structural study of the membrane

The thermal behaviors of different blend membranes were studied from the DSC plots. DSC was recorded at a heating rate of 10°C min^{-1}. Scans were carried out from room temperature to 300°C in the absence of atmospheric oxygen. Figure-3.25 and 3.26 shows the DSC graphs of PASB and mPASB membranes. From the thermal study, it was clear that the blend membranes showed a single T_g value. This confirmed the formation of a blend, as a result of many Van der Waals interactions between two polymers.
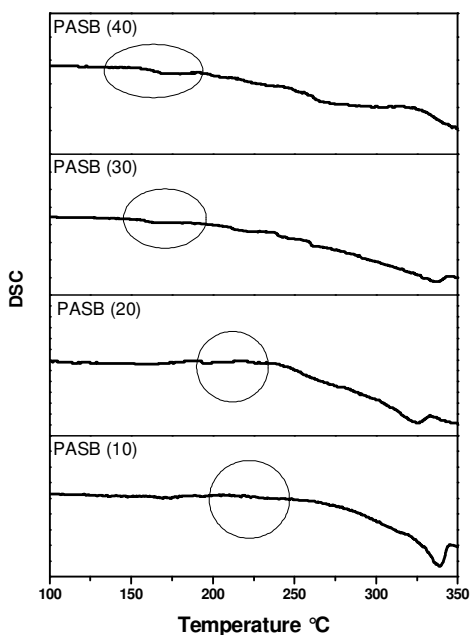
Figure 3.25 DSC curves of PASB membranes
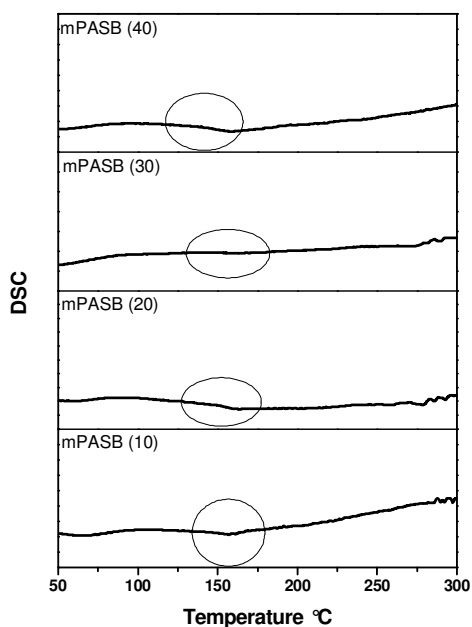
Figure 3.26 DSC curves of mPASB membranes

As shown in SEM photographs of Figure 3.27, the prepared membranes show typical asymmetric structure and fully developed pores, irrespective of the concentration of polymers present in casting solution. In the images three layers namely skin layer, middle layer and bottom layer were distinguished. Macrovoids are normally found in membranes prepared by DIPS method and low polymer concentration. The macrovoids are the important structural feature of water filtration membrane and play an important role in membrane performance. In this case, all the membranes showed good number of macrovoids.
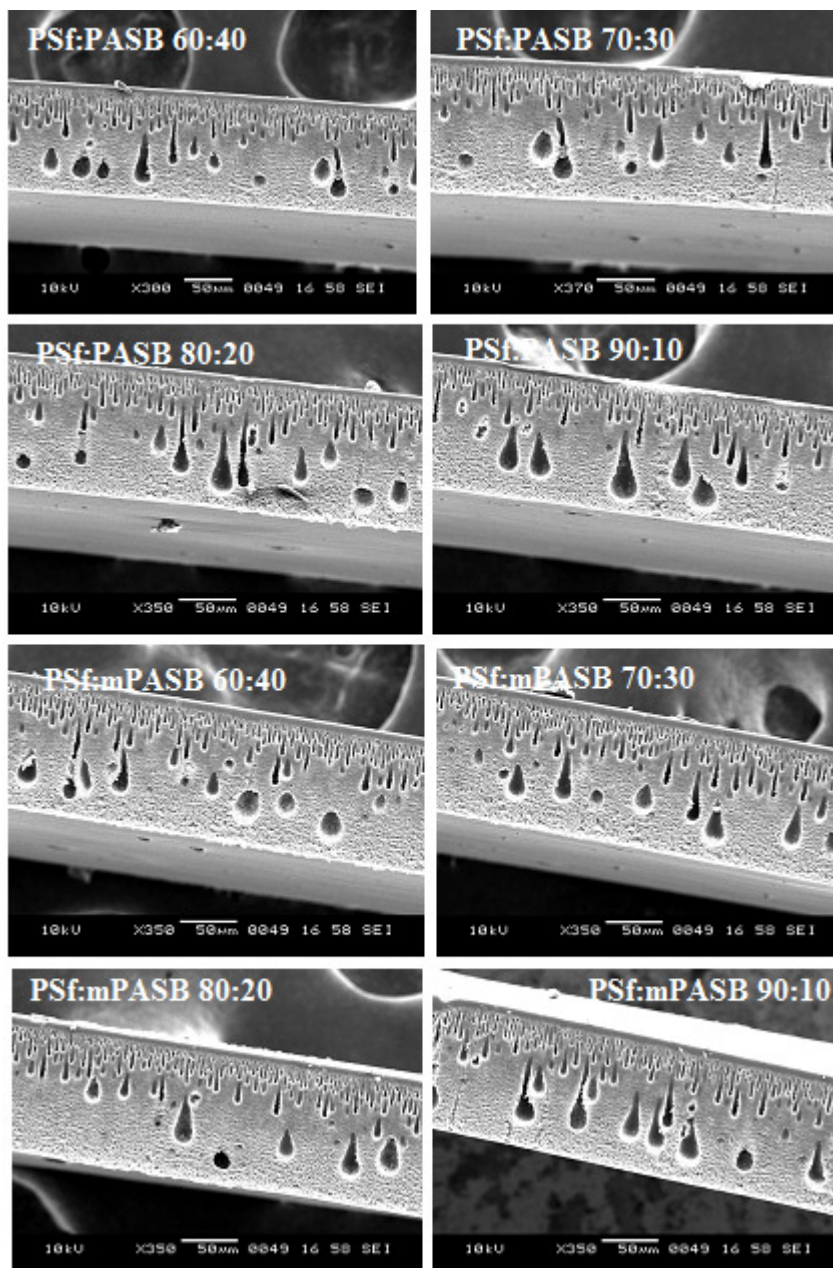
Figure 3.27 SEM images of membranes

3.2.2.3 Water uptake study and contact angle

Hydrophilicity of the membrane can be explained by contact angle and water uptake test. Table 3.4 shows the contact angles of the membranes. The contact angles of the PASB blend membranes were observed to be less than those of mPASB blend

membranes without exception, which indicated higher hydrophilicity of PASB than mPASB. A decrease in mPASB lowered the contact angle, while a decrease in PASB increased the contact angle. Affinity towards water is an important property for the water filtration membranes. However, hydrophilic materials may lead to large water uptake which may eventually lead to loss of mechanical resistance. The percentage water uptake is a parameter which is frequently used to characterize the affinity of the membranes towards water. From Figure 3.28, it is clear that an increase in the PASB content increased the water uptake. The same trait was observed in mPASB series also. While comparing the water uptake behavior in both series of membranes, mPASB series showed less water uptake, confirming higher hydrophilicty of PASB than mPASB.

Figure 3.28 Water uptake results of membranes against varying pH

Water uptake test was also carried out at different pH to study the membrane resistance towards pH. The water uptake data has been presented in Figure 3.28. In this case, there was no much effect of pH on water uptake. All membranes showed the same water uptake under different pH. It clearly indicated that the membranes had good resistance at different pH.

3.2.2.4 Performance of the membranes

Pure water permeability was obtained by measuring the flux for pure water against operating pressure. As shown in Figure 3.28, the flux increased linearly with the operating pressure. The hydraulic permeability coefficient has been calculated from the slope of the line obtained from the proportionality relationship between the water flux and the applied pressure using Spiegler-Kedem model. Table 3.4 represents hydraulic permeability coefficient of the membranes.

Table 3.4 Hydraulic permeability coefficient and contact angle of membranes

Membrane	L_p (m/Spa)	Contact angle °
PSf:mPASB60:40	7.9499×10^{-12}	57.18 ± 2
PSf:mPASB70:30	7.0635×10^{-12}	62.23 ± 2
PSf:mPASB80:20	6.5649×10^{-12}	62.7 ± 2
PSf:mPASB90:10	6.2325×10^{-12}	66.8 ± 2
PSf:PASB60:40	5.6508×10^{-12}	21.04 ± 2
PSf:PASB70:30	5.2353×10^{-12}	26.04 ± 2
PSf:PASB80:20	3.9611×10^{-12}	27.97 ± 2
PSf:PASB90:10	2.5207×10^{-12}	31.23 ± 2

From the data in Table 3.4, the decreasing order in L_p is PASB (40) > PASB (30) > mPASM (40) ≈ PASB (20) > mPASB (30) > PASB (10) > mPASB (20) > mPASB (10) where the figure inside the parantheses indicate PASB or mPASB content in the membrane. Looking into the data for the PASB series and mPASB series individually, L_p decreased with decrease in PASB and mPASB content since both PASB and mPASB are more hydrophilic than PSf. Comparing PASB and mPASB blend of same composition, the former has higher than the latter without exception, This is also expected since PASB is more hydrophilic than mPASB.

Figure 3.30 showed the separation of PEG of different molecular weights. The solute separation increased with increasing molecular weight as expected of 900 Da by

PSf:PASB 60:40 membrane. Considering the Stokes radii of the PEG solutes (eg. The Stokes radius of PEG 1000 Da is 0.79 nm) and the solute separation greater than 80 %, the membranes classified into the category of NF membranes.
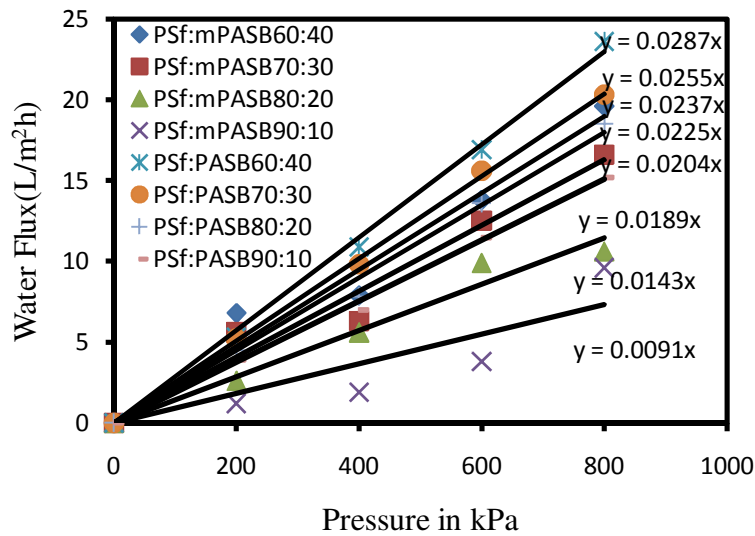
Figure 3.29 Water flux of membranes
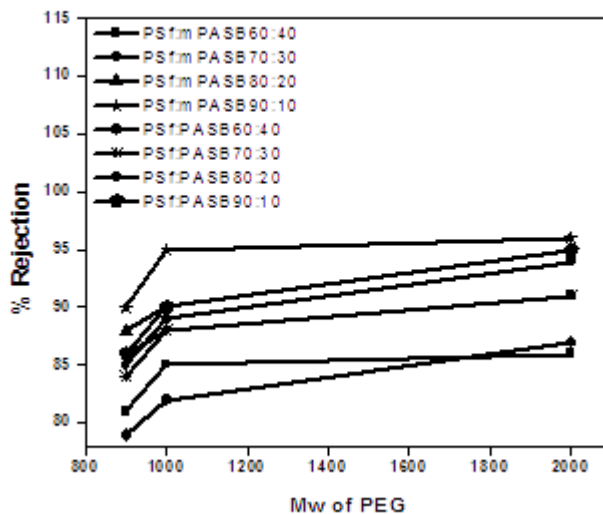
Figure 3.30 MWCO of membranes

From Figure 3.30, PEG 900 Da separation was as follows: PASB (40) < mPASB (40) < PASB (30) < PASB (20) < mPASB (30) ≈ PASB (10) <mPASB (20) < mPASB (20).

This is nearly the same as the decreasing order in L_p, with the exception of PASB (30) and mPASB (40). Thus the pores size also increased with increase in hydrophilicity and content of the additive.

The salt rejection experiment was performed using 3500 ppm of NaCl solution at different pressures. Figure 3.31 shows rejection of the membranes under different pressures. All the membranes showed similar tendency. The salt rejection did not change significantly with increasing pressure, whereas in case of water flux, it increased with increasing pressure. From this observation it was concluded that the prepared membranes exhibited good resistance over appreciable range of pressure.
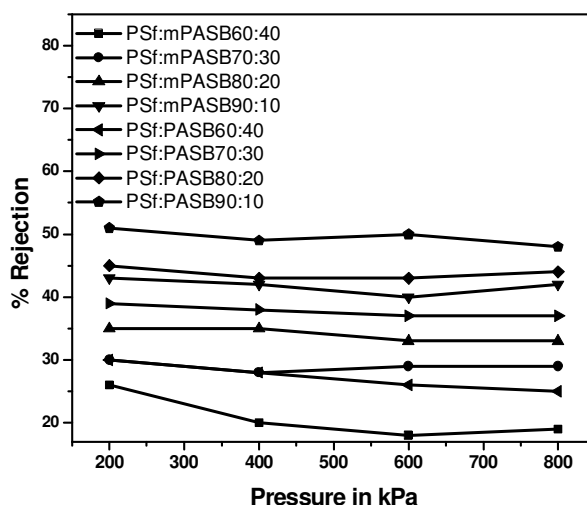
Figure 3.31 Salt rejection results at different pressure

From Figure 3.31, the increasing order of salt rejection is as follows: mPASB (40) < PASB (40) < mPASB (30) < mPASB (20) < PASB (30) < mPASB (10) < PASB (20) < PASB (10). Looking into PASB and mPASB series individually, the salt separation decreased as the additive content was increased. This was because of the increase in pore size with the increase in hydrophilicity of the membrane. However, interestingly salt separation of mPASB blend membrane was lower than PASB membrane of the same additive content, without exception, despite the fact that the latter membranes were more

hydrophilic and had large pore size. From this observation, it was concluded that the transport mechanism of electrolyte solutes such as NaCl is different from the nonelectrolyte solutes such as PEG.
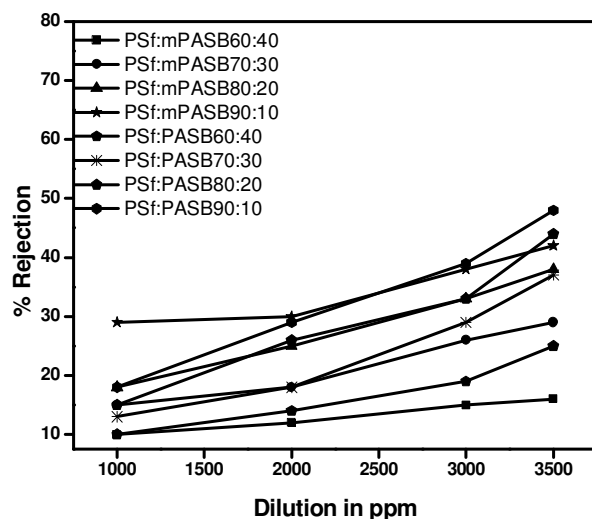
Figure 3.32 Salt rejection results at different dilution

PSf:PASB 60:40 membrane showed lower rejection owing to its large pore size in comparison with other membranes in the series. In both the series of the membranes, an increase in the PSf concentration resulted an increase in the rejection. The membrane PSf:PASB 90:10 showed maximum rejection of 52 %.

The concentration of the feed is also one of the important parameter that determines the rejection of the membrane. Figure 3.32 shows the rejection of membranes in different dilutions of feed solutions. All the membranes showed similar results, where, the increase in concentration increased the rejection.

3.2.3 Conclusions

All the prepared membranes showed better hydrophilicity as they contain hydrophilic sulfonamide bonds and reasonably good resistance towards high pressure filtration, where the hydrophilicity was confirmed by water uptake. All the membranes were found to be stable at different pH values and membranes showed 1000 Da

molecular weight cut-off. Membranes have performed excellently for desalination and the salt rejection of the membrane was enhanced in an effective way. The membrane Polysulfone:Poly[(4-aminophenyl)sulfonyl]butanediamide 90:10 showed maximum rejection and Polysulfone:Poly[(4-aminophenyl)sulfonyl]butanediamide 60:40 showed least rejection of sodium chloride solution. This is because with the increase in the concentration of PASB resulted in increasing of pore size of the membrane. There was no change in rejection was observed with increase of pressure. From the current study, it was very clear that the pore size of the membranes played a pivotal role in the performance of the membrane.

Abstract: In this chapter, Chitosan (CS) was modified into N-Phthaloyl chitosan (NCS). Polypropylene supported NCS membrane was prepared and the performance was compared with polypropylene supported CS membrane. Later, the PSf:NCS and sulfonated polysulfone (sPSf):NCS blend membranes were prepared and performance was studied and discussed.

4.1 NEW POLYPROPYLENE SUPPORTED N-PHTHALOYL CHITOSAN AND CHITOSAN MEMBRANES

Chitosan (CS) is a significant biomaterial that has been known from a long time. It is a linear copolymer of β-(1,4)-linked 2-acetamido-2-deoxy-β-D-glucopyranose and 2-amino-2-deoxy- β-D-glucopyranose. It has reactive hydroxyl and amine groups in its structure and hence has high charge density. The material is biodegradable in nature. Owing to its non-toxic nature, CS is extensively used primarily in pharmaceutical industry for efficient drug delivery. It is also used in other fields such as health care, food, beverages, cosmetics, toiletries, agriculture, waste water treatment and also for cell culture. Membranes prepared from CS have been developed for solution filtering, which can improve the quality of feed solution. CS membranes can be used in separation techniques such as ultrafiltration and reverse osmosis (Musale and Kulkarni 1996, Yang and Zall 1984).

The membrane process is governed by size exclusion mechanism, solute-solute and solute-membrane interactions that are dependent on membrane surface characteristics such as hydrophilic/hydrophobic balance, electrostatic charges on both membranes and the nature of the solute (Yang and Zall 1984, Vourch et al. 2005). CS is a hydrophilic material and in the acidic pH range it is positively charged due to protonation of $-NH_2$ groups (Wang et al. 2005), but in basic atmosphere deprotonation of the polymeric chain occurs. CS causes the fine sediment particles to bind together and is subsequently removed with the sediment during sand filtration. CS to a great extent removes phosphorus, heavy minerals and oils from the water. It is an important additive in the filtration process. Sand filtration alone is known to remove upto 50 % of the turbidity , while the CS with sand filtration removes up to 99 % turbidity .

Previous researchers (Yuana et al. 2005) have discovered that the hydrophilic property of CS often leads to problems in performance such as mechanical strength. To further enhance the performance of CS membranes, chondroitin sulfate was utilized to modify the CS membranes for preparing composite membranes with better hydrophilicity and biological compatibility (Yuana et al. 2005). The modification of the CS for membrane application may show better performance. Zheng et al. (2002) reported the synthesis of N,O-carboxymethyl Chitosan (NOCC) (Figure 4.1) and cellulose acetate blend film. NOCC, a water-soluble CS derivative, is a carboxylated CS having carboxymethyl substituent on some of the both amino and primary hydroxyl sites of the glucosamine units of the CS structure. In addition, it is hydrophilic and a typical kind of amphoteric polyelectrolyte with anticancer and antibacterial property. At the same time, it is found to be a potential candidate for microfiltration (Zhoa et al. 2003) and pervaporation (Lee 1993) by appropriate modification.
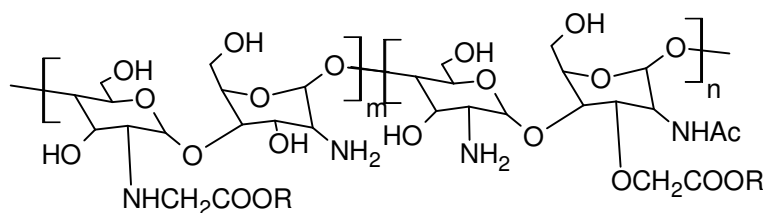
Figure 4.1 Structure of NOCC

Recently, Mu et al. (2012) modified CS using two misogynic units *6-((4'-methoxybenzoyl)oxy)-[1,1'-biphenyl]-4-yl)oxy)-6-oxohexanoic acid* (M1) and *6-(((8R,9R,10R,13S,14R,17S)-10,13-dimethyl-17-((S)-6-methylhepta-2-yl)-2,3,4,5,8,9,10,11,12,13,14,15,16,17-tetradecahydro-1H-cyclopenta[a]phenanthren-3-yl)oxy)-6-oxahexanoic acid* (M2) (Figure 4.2 and 4.3). These modified CS were coated on PSf UF membranes to reduce the pore size.
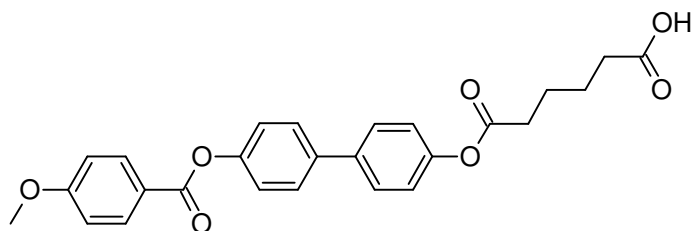
Figure 4.2 Structure of M1
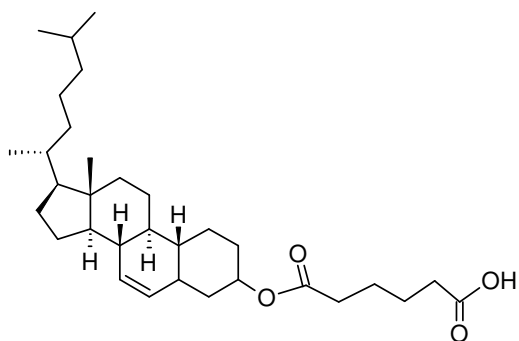
Figure 4.3 Structure of M2

These prepared membranes were used for desalination process. Extremely high flux, 2543.3 $Lm^{-2} h^{-1}$ was observed in NF membrane, and the rejection remained as high as 66.3 % at 0.4 MPa with 1000 mg/L NaCl solution.

Ohya et al. (1999) modified CS by grafting with styrene, wherein it increases the solubility of CS. Also it has been reported that the amine group of the CS was successively utilized for the CS modification.

In this approach, amine group is protected by N-Phthloylation. This is an effective method for homogenous modification of CS at amino site. This modification brings very drastic changes in the solubility of CS. This modification is very useful to prepare the blend membranes with PSf. The preparation properties of NCS membrane was studied and discussed.

4.1.1 Experimental

4.1.1.1 Preparation of NCS

CS modification was done according to the procedure reported by Ohya et al. (1999). In brief, 23.7 g CS from Sigma Aldrich (MW 5.4×10^5, 85 % degree of deacetylation) was reacted with 64.5 g phthalic-anhydride (Sigma Aldrich) in 100 mL Dimethylformamide (DMF) (Merck India) at 130 °C for 5 hrs under nitrogen atmosphere. The reaction mixture was poured into large amount of ice-cold water to precipitate NCS. It was then filtered and purified by ethanol and ethyl ether to obtain yellow solid with 80.6 % yield. The synthetic route for the same has been presented in Figure 4.4.
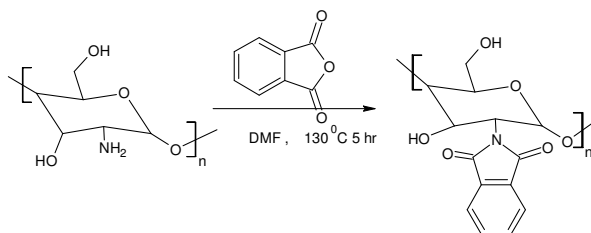
Figure 4.4 Schematic representation for the synthesis of NCS
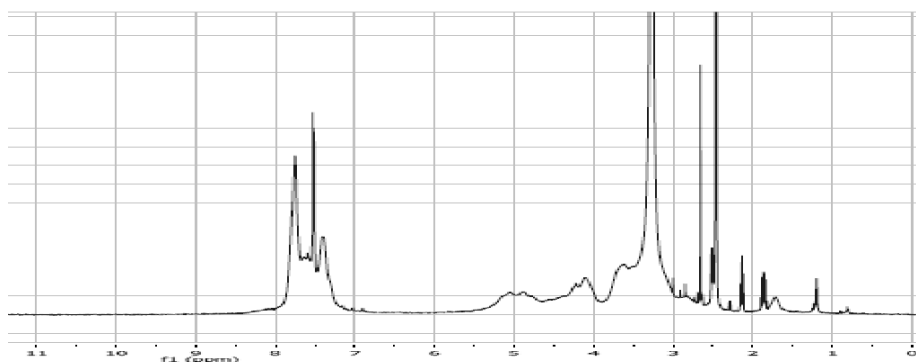
Figure 4.5 ^{1}H NMR spectrum of NCS

Figure 4.5, shows NMR spectrum of NCS. In the spectrum, presence of aromatic protons in the region 7.4 to 7.9 δ indicated the insertion of phthalic anhydride group into CS backbone. Whereas, the proton NMR of CS does not show any peak at this delta value

(Zhang et al. 2003). Hence it confirms the successful incorporation of phthalic anhydride group into CS molecule.
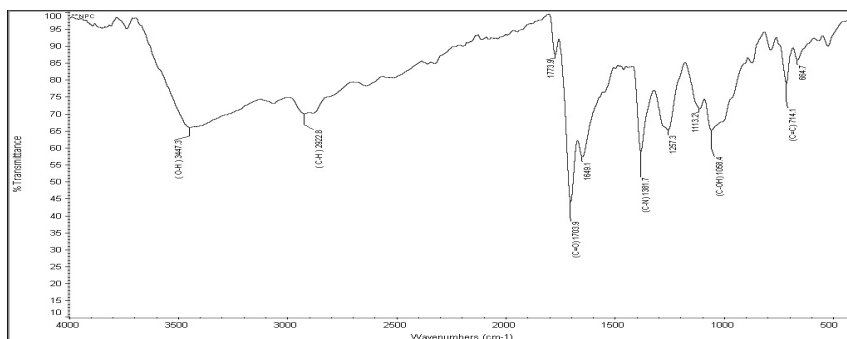
Figure 4.6 ATR-IR spectrum of NCS

Figure 4.6 represents FT-IR spectrum of NCS polymer. The peaks at 3447 cm^{-1} of OH group, 2922 cm^{-1} for C-H stretching, shoulder peak at 1703 cm^{-1} confirms the presence of imide C=O, 1381 cm^{-1} of C-N group and 1058 cm^{-1} of the C-O group.
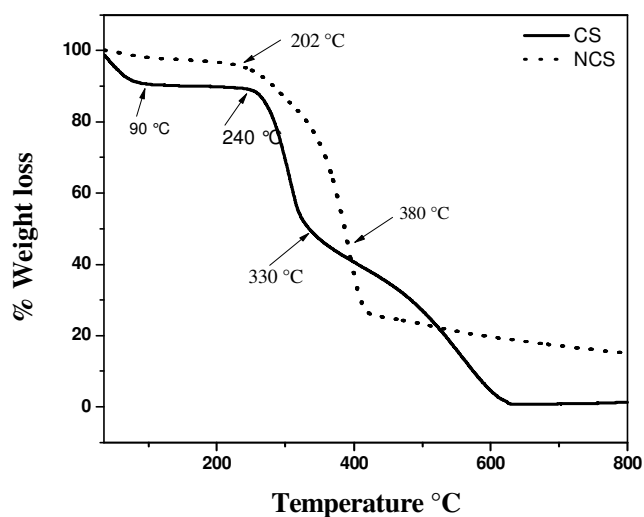
Figure 4.7 TGA of polymers

Thermographs of CS and NCS are shown in Figure 4.7. The CS showed slow weight loss starting from 90 to 240 °C due to the decomposition of polymer with low molecular weight followed by more obvious loss of weight starting from 240 to 330 °C.

This was attributed to a complex process including dehydration of the saccharide rings, depolymerization and decomposition of the acetylated and deacetylated units of the polymer (Zhang et al. 2003). A fast process of weight loss appeared in TG curve for NCS decomposing from 202 to 380 °C, due to the removal of a part of the polymer with low molecular weight by decomposition. The results demonstrate the loss of the thermal stability for NCS to the original CS. Introduction of phthloyl group into polysaccharide structure disturbed the crystalline structure of CS, especially through the loss of hydrogen bonding.

4.1.1.2 Membrane preparation

NCS membrane was prepared by Temperature Induced Phase Separation (TIPS) method. The different concentration of NCS solution was prepared using NMP and DMF. Solution was spread in to the glass plate of 14 cm^2 area. The solution was allowed to dry at   60 °C under vacuum for the evaporation of solvent upto 24 hrs. The membrane was very thin and it was not possible to use it for filtration process. Different experiments were tried to increase the thickness of the membrane. Table-4.1 and 4.2 summarizes the details of experiment with an aim to increase the thickness of the membrane.

Table 4.1 Preparation of NCS membrane using NMP as solvent

Sl. No.	Concentration of casting sol^n.	Variation in drying temp	Casting sol^n. used	Thickness in mm	Remarks
1	5 %	60 °C for 24 hrs	2 mL	-	No membrane
2	5 %	60 °C for 24 hrs	4 mL	-	No membrane
3	5 %	40 °C for 24 hrs	2 mL	0.10	Thin membrane
4	5 %	40 °C for 24 hrs	4 mL	0.15	Thin membrane
5	10 %	40 °C for 24 hrs	2 mL	0.22	Thin membrane
6	10 %	40 °C for 24 hrs	4 mL	-	Thin membrane
7	20 %	40 °C for 24 hrs	2 mL	0.13	Thin membrane
8	20 %	40 °C for 24 hrs	4 mL	-	Brittle membrane

Table 4.2 Preparation of NCS membrane using DMF as a solvent

Sl. No.	Concentration of casting sol^n.	Variation in drying temp	Casting sol^n. used	Thickness in mm	Remarks
1	10 %	40 °C for 24 hrs	2 mL	-	Thin membrane
2	10 %	40 °C for 24 hrs	4 mL	-	Thin membrane
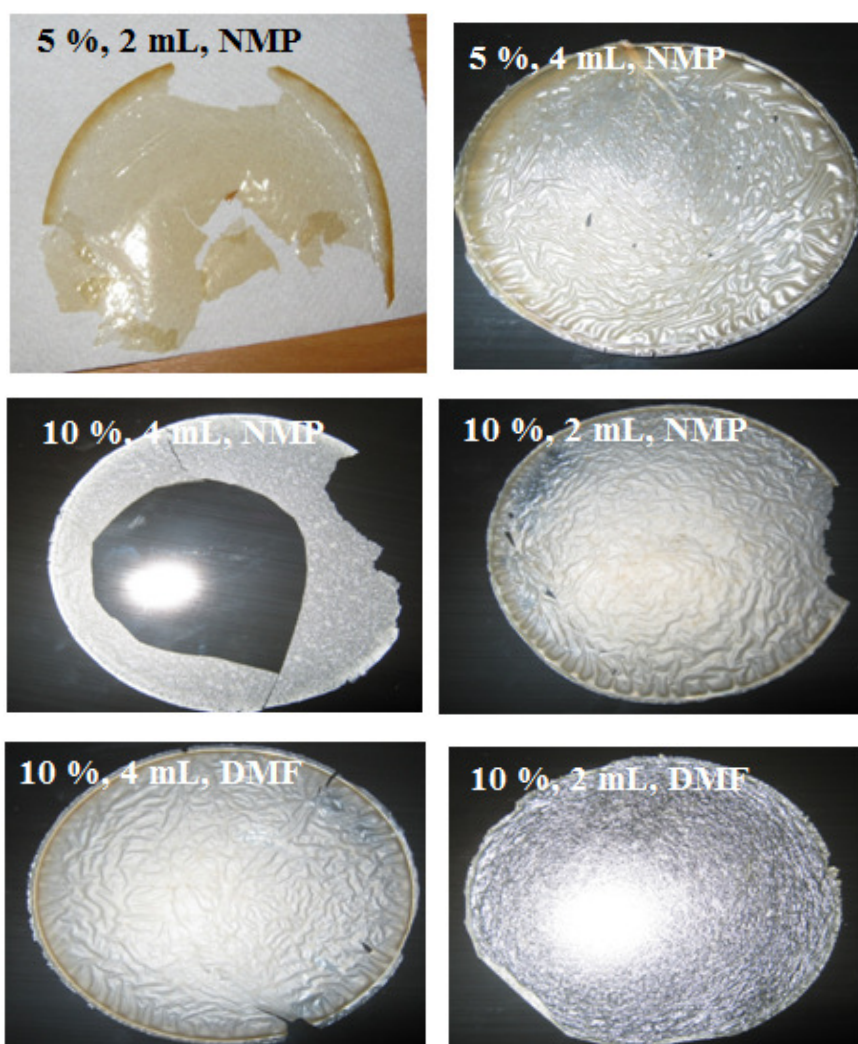
Figure 4.8 Digital images of membranes

As such, neat NCS membranes were mechanically unstable and preparation technique was also observed to be very tedious. Figure 4.8 shows digital images of the

NCS membranes and one can observe that they are very thin. In order to overcome this practical difficulty, the polypropylene supported NCS membranes were prepared and for the sake of comparison, polypropylene supported CS membrane was also synthesized. Performance of both the membranes were discussed.

4.1.1.3 Preparation of supported CS membrane

CS (Degree of deacetylation 75 %) from Sigma Aldrich (M_w 20000 Da) and polypropylene support was taken for the membrane preparation. Polypropylene support was Cranemat KC, which was a gift sample from Dr. Michael Guiver (National research council-Canada). CS was dissolved in 2 % acetic acid solution (2 % m/v) at room temperature. After filtering the resultant solution through G3 sand filter, solution was spread on to the surface of the polypropylene supported membrane and allowed to dry at 80 °C for 48 hrs. The thickness was found to be 4 mm. After drying, membrane was dipped in 4 % of NaOH solution to neutralize the acetic acid present in the membrane for one hour and then membrane was washed with distilled water until pH of the washed water reached 7. Membrane was dried at room temperature for 48 hrs. Before characterization of the membrane, it was immersed in distilled water for 1 hr.

4.1.1.4 Preparation of NCS supported membrane

The same support and procedure was used to prepare NCS supported membrane. 5 % NCS solution was prepared using NMP. After filtering the resultant solution through G3 sand filter, it was spread on to the surface of the polypropylene support and allowed to dry at 80 °C for 48 hrs. The thickness was found to be 4 mm. After complete drying, the membrane was stored in distilled water for further characterization.

4.1.2 Results and discussion

4.1.2.1 Morphology of the membrane

Scanning electron micrographs of the typical supported membrane are presented in Figure 4.9 and 4.10. It was obvious from the pictures that, CS was cast as a thin layer on top of the polypropylene substrate. Figure 4.9 (**a**) shows the morphology of membrane prepared by phase inversion technique. Polypropylene substrate clearly shows the
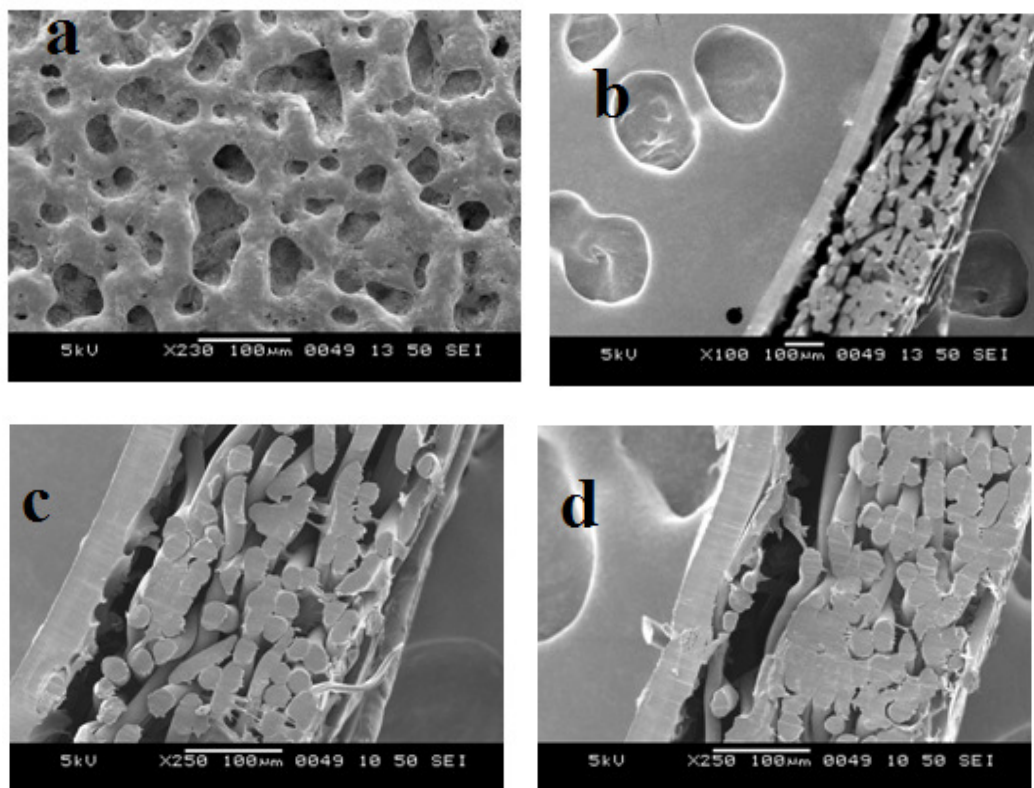
Figure 4.9 SEM images of membrane (**a**) surface of membrane (**b, c & d**) cross section of membrane
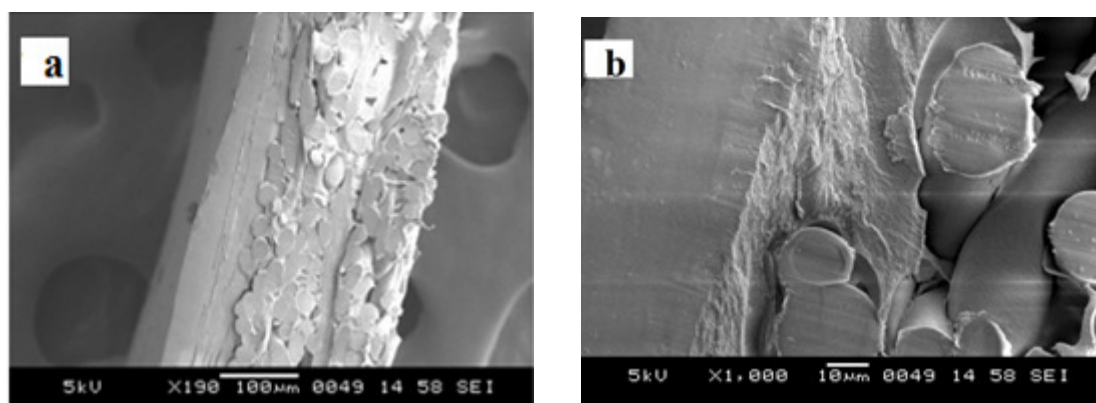
Figure 4.10 (**a and b**) Cross section of NCS support membrane

presence of microfibers. The thickness of top CS skin layer was approximately 10 µm as observed from SEM image (Figure 4.9 (**c**)). Figure 4.9 (**b, c**) shows the surface of the

membrane; as CS solution cast on to the polypropylene support membrane, it adheres to the surface of support.

Figure 4.10 shows cross section SEM image of the NCS membrane. Here it is difficult to distinguish two layers in membrane. In NCS membrane, the casting solution penetrated into the fibers present in support and looked like a rigid wholesome mass. The CS solution was prepared in 1 % acetic acid and since the polypropylene support is hydrophobic in nature, CS solution did not penetrate easily into fibers resulting in clear skin layer formation. Whereas, in the case of NCS, the casting solution was prepared in NMP-an organic media, so the casting solution entered easily into the fibers and became a rigid mass on drying.

4.1.2.2 Thermal analysis of the membrane

Figure 4.11 shows DSC curve for CS support membrane. DSC experiments were carried out with the heating rate of 10 °C per min.
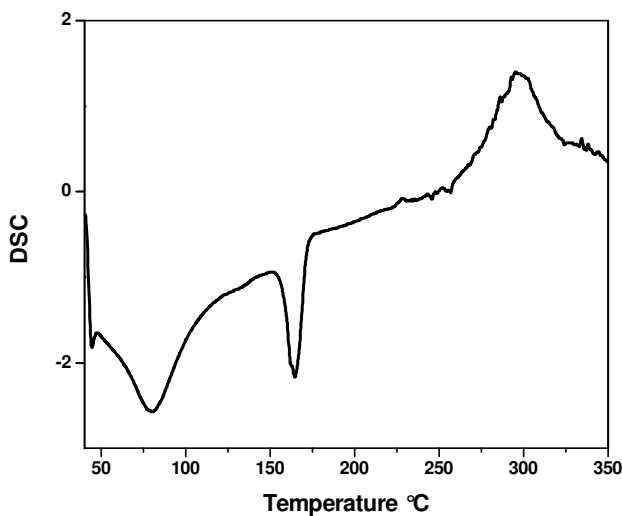
Figure 4.11 DSC curve of CS membrane

It showed two separate T_g values, one near 90 °C due to CS and the other peak at around 170 °C corresponding to the polypropylene support. The presence of two different T_g values clearly indicated that the two polymers have not blended with each other instead they are just adhering to one another on the surface through some molecular

interactions thereby maintaining their individual identity. This is also evident from the SEM image of the membrane.

Figure 4.12 shows DSC curve for NCS support membrane. DSC experiments were carried out with the heating rate of 10 °C per min. It showed two separate T_g values, one near 110 °C was due to NCS and the other peak around 170 °C corresponded to the supporting polypropylene. This is because here also NCS solution just penetrated into the fibers and through some molecular interaction it adhered to the support membrane. So both the polymeric materials maintain their identity thereby showing separate T_g.
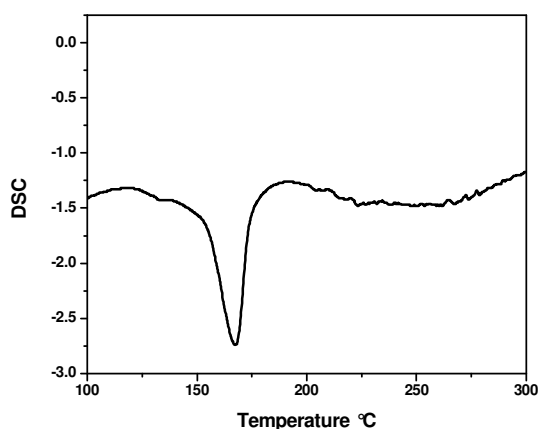
Figure 4.12 DSC curve of NCS membrane

4.1.2.3 Water uptake behavior and contact angle measurement

To investigate water uptake behavior at various pH values, the membranes were immersed in 5, 7, 9, and 11 pH solutions. The membranes were swollen considerably in the selected pH scale. Figure 4.13 shows the pH-dependent water uptake behavior of fully swollen membranes. Both the membrane showed a lower water uptake ratio at pH 7, 9 and 11 as compared with pH 5. The pH sensitivity of the membranes was due to the inherent nature of CS itself (Risbud et al. 2000, Kim et al. 2000, Lee et al. 1997, Roberts 1992 and Herber et al. 2003). It exhibits pH-responsive behavior as a weak poly base due to the large number of amino groups in its backbone. Acidic media has a pronounced effect on swelling behavior compared to the neutral and basic media. The protonation of

the –NH$_2$ group in membranes ensured chain relaxation, leading to efficient solvent diffusion. In neutral and basic media, the swelling was mainly driven by solvent diffusion, but the chain relaxation effect due to protonation of amino groups was absent. In addition, the samples with higher porosity had higher extent of swelling, which seemed to preside over the diffusion of solvent in the matrix. Amide linkages are very active in acidic pH as compared to basic. Hence, NCS membrane showed more hydrophilicity in acidic pH. When water uptake of NCS was compared to CS, CS showed more water uptake because of the presence of more free amino groups than that of NCS which increased the possibilities of formation of hydrogen bonding.
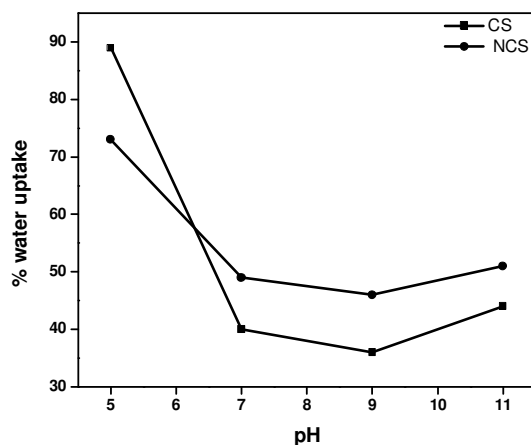
Figure 4.13 Water uptake behavior of membranes in different pH
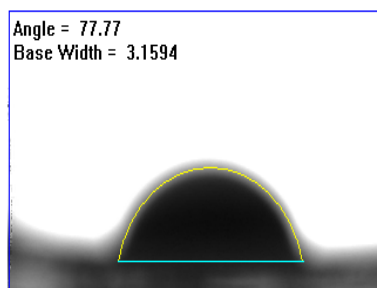
Figure 4.14 Contact angle of CS membrane
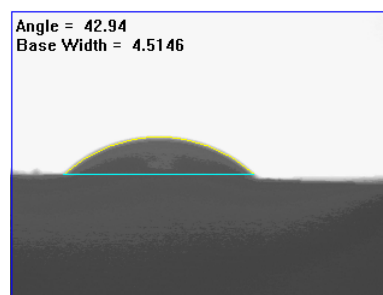
Figure 4.15 Contact angle of NCS membrane

The contact angle is another important parameter for measuring surface hydrophilicity (Khayet et al. 2002, Palacio et al. 1999). In general, smaller contact angle

corresponds to more hydrophilic material. Contact angle of the CS membrane is 77.77° and that of NCS is 42.94° as shown in Figure 4.14 and 4.15.

4.1.2.4 Performance of the membrane

Water permeability of the membrane was studied using dead end flow cell for different pressure ranging between 200 kPa to 800 kPa. Figure 4.16 shows the water flux result. Water flux showed a linear increase with an increase in pressure. Water permeability coefficient of the membrane was calculated using the slope and it was found to be 2.229×10^{-11} m/sPa and 2.77×10^{-11} m/sPa for CS and NCS membranes respectively.
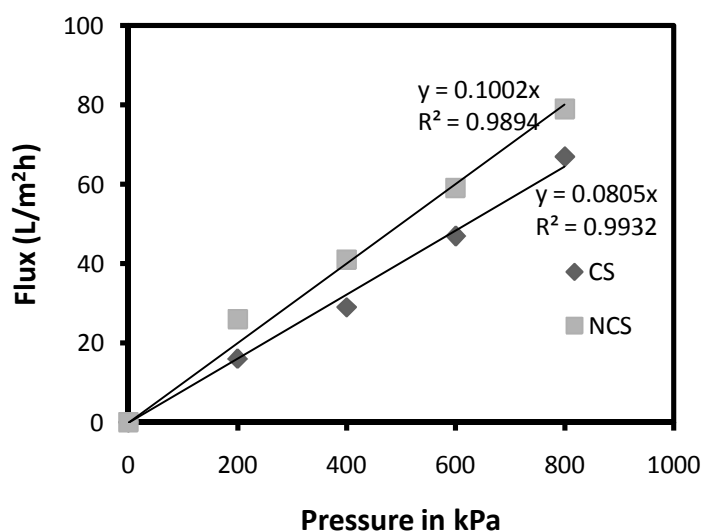
Figure 4.16 Water flux results of membranes
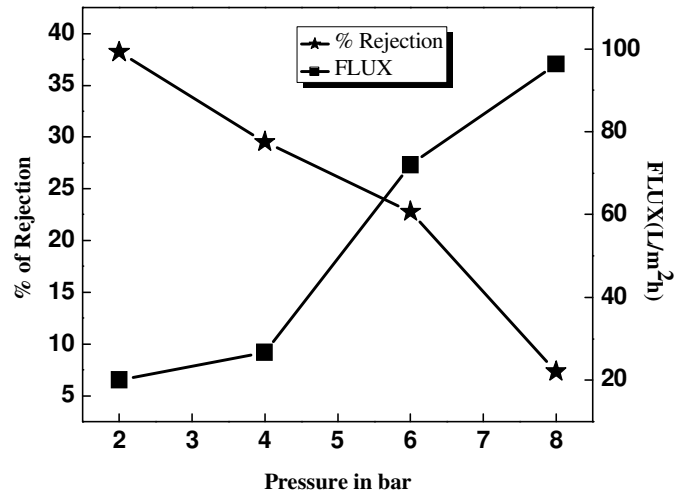
Figure 4.17 Rejection and flux of CS membrane for NaCl solution at different pressure
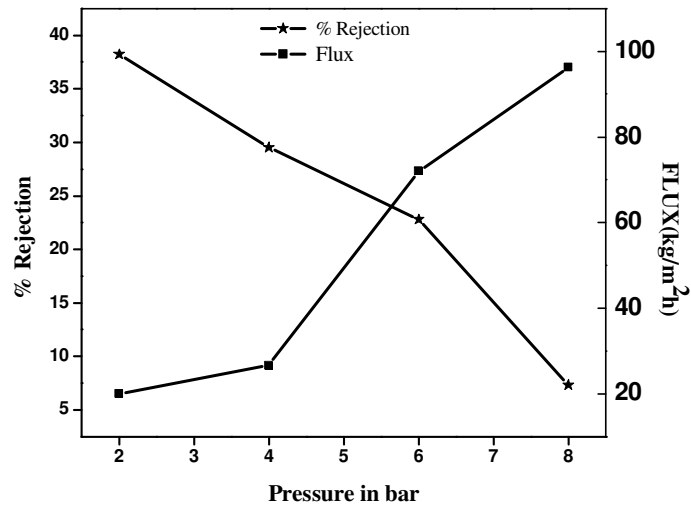
Figure 4.18 Rejection and flux results of NCS membrane for NaCl solution at different

pressure
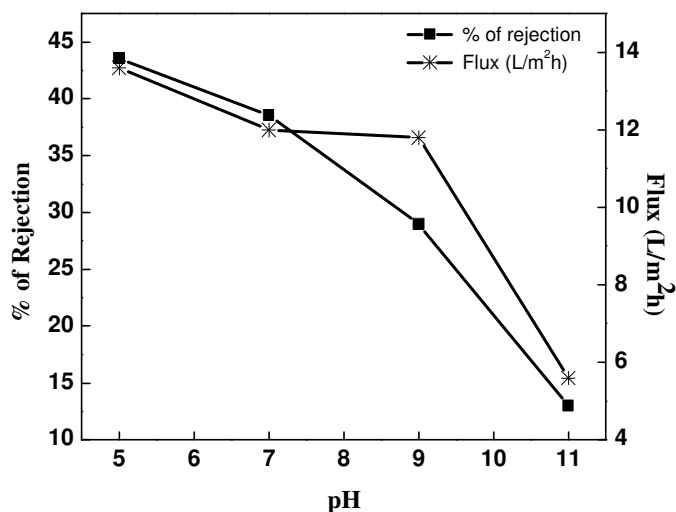
Figure 4.19 Rejection and flux of CS membrane for NaCl solution in different pH

Rejection of the NF membrane to inorganic electrolytes is related to the ion valency and size (Petersen 1993).
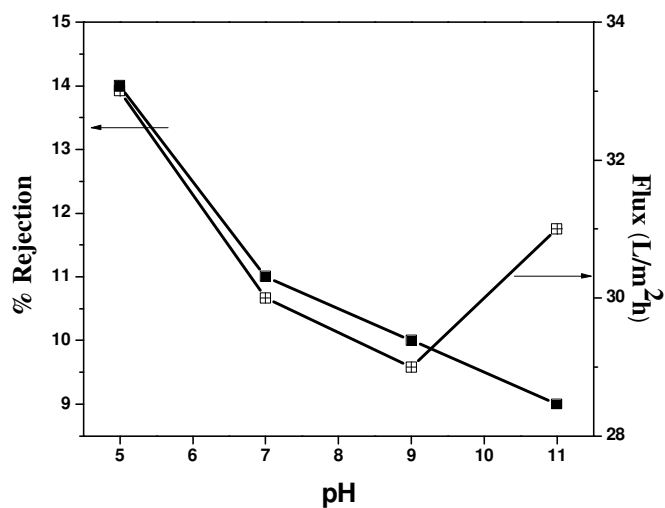
Figure 4.20 Rejection and flux of NCS membrane for NaCl solution in different pH

The transport mechanism and electrolyte rejection of amphoteric NF membranes are convection (C), diffusion (D) and electro migration (EM) (Fievet et al. 2005). The effect of ionic charge should be considered as a dominant factor for the filtration of

inorganic electrolytes of low concentration (Wang et al. 2002). Rejection increases with membrane charge density regardless of the electrolyte and permeate volume flux since fewer co-ions can enter the membrane pores.

Figure 4.17 shows performance of the CS membrane at different pressure. The CS membrane showed about 40 % salt rejection at lower pressure. Figure 4.18 shows performance of the NCS membrane. The NCS showed about 14 % of rejection at lower pressure. Rejection experiments were carried out in different pH as well as at different pressure using 3500 ppm of NaCl solution. The rejection study in different pH was carried out at 200 KPa. Figure 4.19 shows percent rejection and flux of the CS membrane in different pH. Membrane behavior for the different pH solution was studied. At acidic pH, CS having NH_2 group in its backbone gets protonated and the membrane surface becomes positively charged, as a result of hydrophilic surface. Hence it showed highest rejection in acidic pH than at basic. This is due to the fact that the presence of positive charge on the membrane surface facilitated the exchange of anion thereby showing highest rejection. In basic pH, the free NH_2 groups remained intact and hence showed less rejection. In NCS, due to the absence of free amine group, no charge is created on the surface and hence showed less rejection in general. Figure 4.20 shows rejection and flux of the NCS at different pH.

4.1.3 Conclusions

The supported membranes, particularly, Chitosan membrane showed good performance in acidic pH compared to the basic and neutral. In acidic medium at pH 5, membrane showed 45 % salt rejection with the flux of 43 L/m^{2}h, whereas in pH 11, it showed 12 % salt rejection with the flux of 5 L/m^{2}h. The membrane showed a low swelling ratio at pH 7, 9, and 11 as compared with pH 5. It showed 90 % water swelling in pH 5, whereas contact angle was observed to be 77.77°. N-Phthaloyl chitosan membrane exhibited average performance in comparison with Chitosan membrane but the hydrophilicity was better than Chitosan membrane.

4.2 POLYSULFONE AND N-PHTHALOYL CHITOSAN BLEND MEMBRANES

In previous section, properties of CS and NCS membrane supported on polypropylene base were studied. In order to study the property of hydrophilicity of NCS to a greater extent, blend of PSf and NCS membranes at different compositions were carried out. The structure of the membrane was studied by ATR-IR, DSC and SEM. Further they were verified by means of water flux study, dielectric constant and filtration using mono and divalent salt solutions.

4.2.1 Experimental

4.2.1.1 Preparation of membranes

PSf (M_w 35000 Da) and the prepared NCS were dissolved in NMP in different ratios and stirred at 60 °C for 24 hrs to get clear homogenous solution. The ratio of the polymers are tabulated in Table 4.3. The viscous solution thus obtained was filtered by G4 sand filter before casting. The membrane was prepared by casting viscous solution onto a glass plate. The thickness of the wet membrane was maintained at 0.2 mm. Glass plate was air dried at 25±1 °C for 30 seconds for evaporation of solvents in air and then was immersed into a coagulation bath containing water as non-solvent bath for 30 min. Demixing of solvent and non-solvent in the coagulation bath resulted in the phase inversion process and membrane peeled out from the glass plate. Finally the obtained membrane was washed and stored in distilled water for further characterization.

Table 4.3 Composition of the polymers for membrane preparation

Membrane	Polymer concentration	
	PSf	NCS
PSf:NCS 80:20	80 %	20 %
PSf:NCS 85:15	85 %	15 %
PSf:NCS 90:10	90 %	10 %
PSf:NCS 95:05	95 %	05 %

4.2.2 Results and Discussion

Figure 4.21 represents the ATR-IR spectra of the membranes. The characteristic peaks of the NCS at 3345 cm^{-1}-3361 cm^{-1} of the OH group, 2965 cm^{-1}-2968 cm^{-1} of the C-H group and C=O peak shifted to the lower side of 1664 cm^{-1} to 1679 cm^{-1}. C-N and C-OH groups shifted to the 1013 cm^{-1} to 1041 cm^{-1} and 737 cm^{-1} to 738 cm^{-1} respectively. The presence of strong peak at 1241 cm^{-1} to 1243 cm^{-1} is attributed to the ether C-O-C stretch of the PSf moiety and the peak at 1169 cm^{-1} to 1170 cm^{-1} due to O=S=O stretching.

Cross section images were taken at lower magnification. Figure 4.22 **a-d** represents the cross section images of the membranes. Increase of NCS concentration resulted in diminishing of finger-like structure, however resulted in formation of thick sponge like structures. This observation was explained on the basis of phase separation process. In this case, the increase of NCS concentration decreased the exchange between solvent in the casting solution and water and thereby weaker stress derived from the
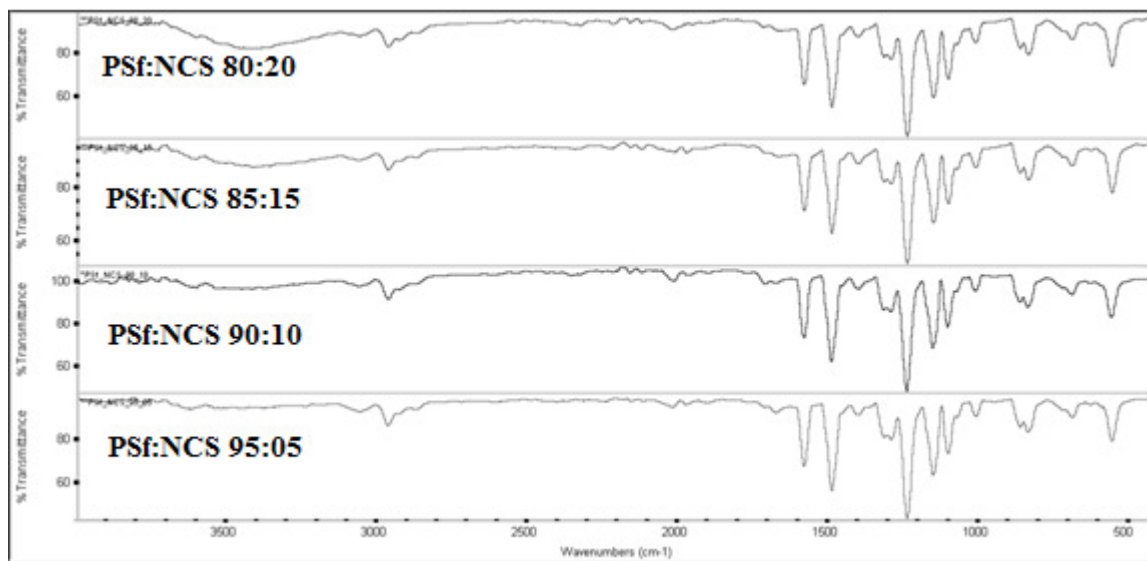
Figure 4.21 ATR-IR spectra of membranes
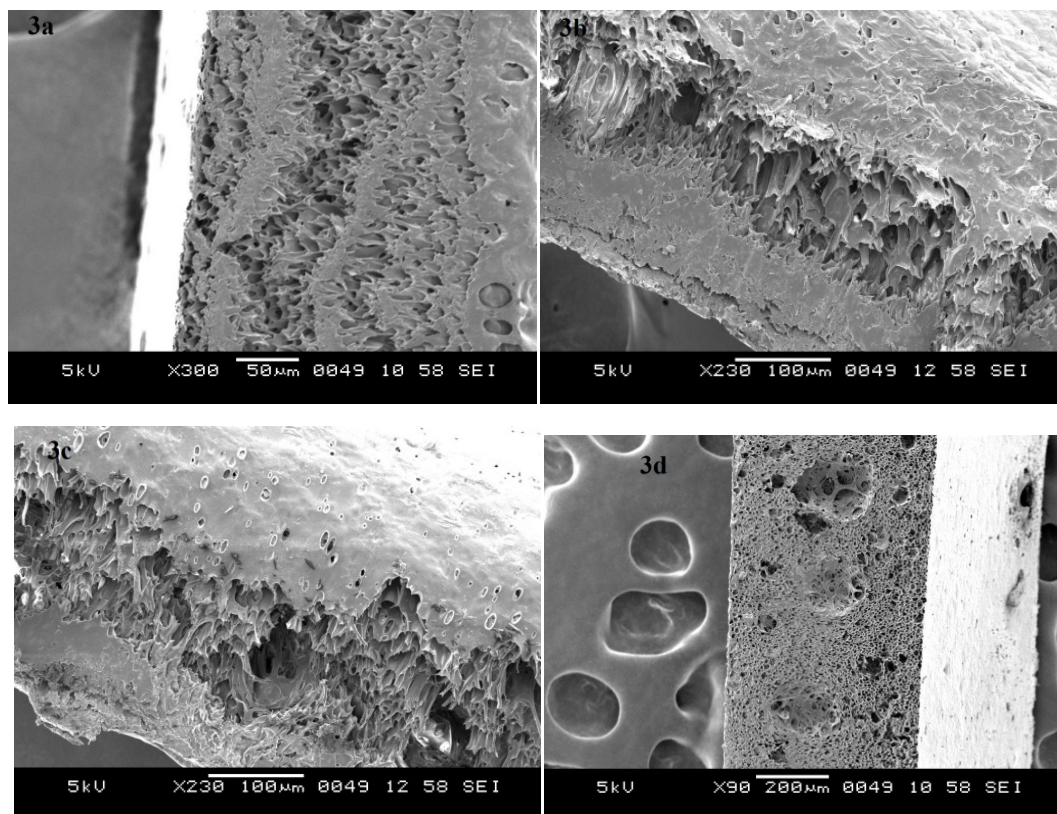
Figure 4.22 Cross sectional SEM images of membranes (**a**) PSf:NCS 80:20 (**b**)PSf:NCS 85:15 (**c**) PSf:NCS 90:10 (**d**) PSf:NCS 95:15

shrinkage of polymer-rich phase led to limited phase separation. Therefore the sponge-like structure was more dominant.

Pure water permeability was obtained by measuring the flux for pure water against operating pressure. As shown in Figure 4.23, the flux increased linearly with the operating pressure. PSf:NCS 95:05 composition showed the lowest flux and PSf:NCS 80:20 showed highest flux. The hydraulic permeability coefficient of the membrane has been shown in Table 4.4. The increasing NCS composition in the membrane increased the water flux and hence the hydraulic permeability coefficient.
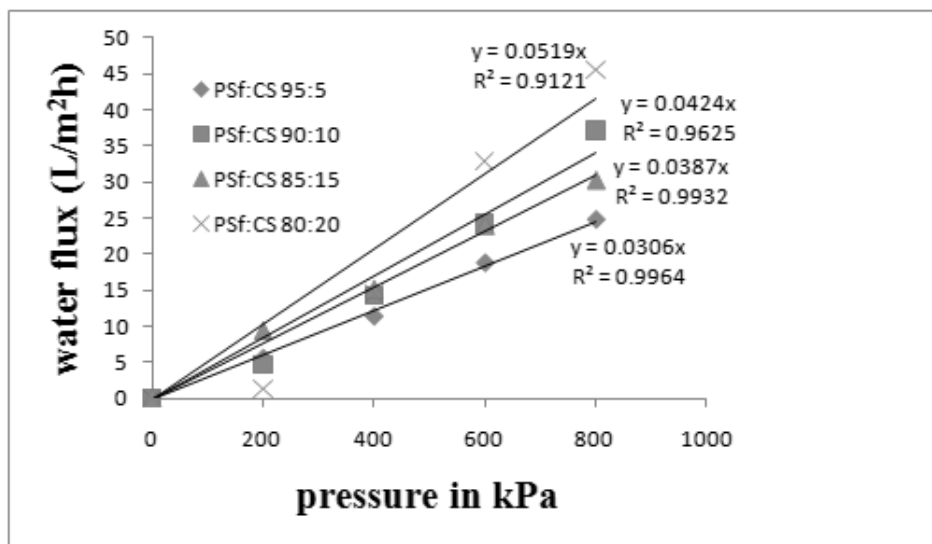
Figure 4.23 Water flux of blend membranes

Figure 4.24 represents the dielectric spectrum which are independent of the frequencies between 4×10^6-7×10^6 Hz. Among the four compositions, the membrane PSf:NCS 80:20 showed the smallest dielectric constant. Membranes PSf:NCS 95:05 and PSf:NCS 90:10 possessed the same and maximum dielectric value. As discussed by Jaleh et al. (2010), the maximum dielectric constant represented smallest void area of the membrane and this was confirmed by minimum water flux shown in Figure 4.23.

Table 4.4 Contact angle and hydraulic permeability coefficient of membranes

Membrane	Contact angle ^{o}	L_p in (m/sPa)
PSf:NCS 95:05	89±2	8.48×10^{-12}
PSf:NCS 90:10	86±2	0.11×10^{-12}
PSf:NCS 85:15	75±2	0.12×10^{-12}
PSf:NCS 80:20	73±2	0.14×10^{-12}
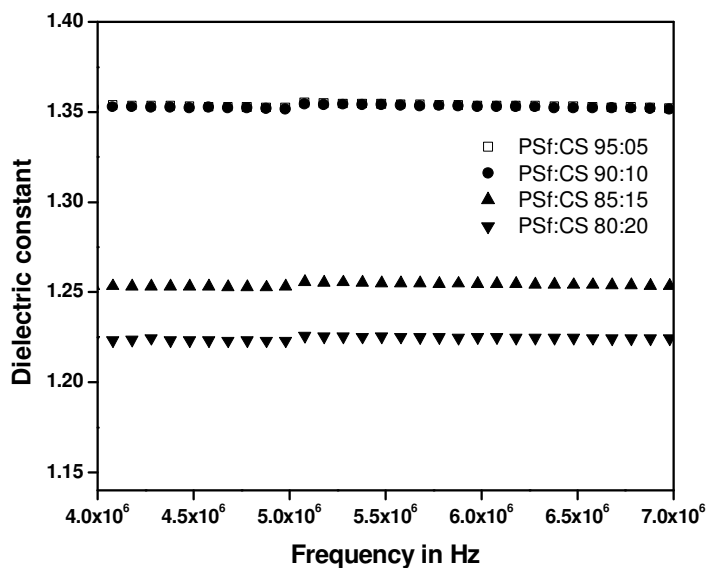
Figure 4.24 Dielectric constant of membranes

Figure 4.25 shows the water swelling study under different pH. pH variation was done by using conc. HCl and 4 % NaOH solution. The membrane PSf:NCS 80:20 showed highest water swelling than the other membranes at all pH. All membranes showed similar pattern in the water uptake. Higher NCS concentration corresponded to higher swelling percentage. Contact angle of the membranes was studied, the results of which are shown in Table 4.4. As anticipated, the membrane PSf:NCS 80:20 showed smallest contact angle whereas highest contact angle was measured in case of PSf:NCS 95:05 membrane. Since PSf is hydrophobic material, the addition of relatively hydrophilic NCS resulted in decrease of contact angle. In the pH range of 4-5, membranes showed highest water swelling. This was due to the amide bond in NCS, which readily underwent protonation and leading to higher water swelling, whereas in higher acidic pH 3, the unstable amide bond was broken resulting in low water swelling. In neutral and basic pH, no such phenomenon was observed and hence the water swelling was less.
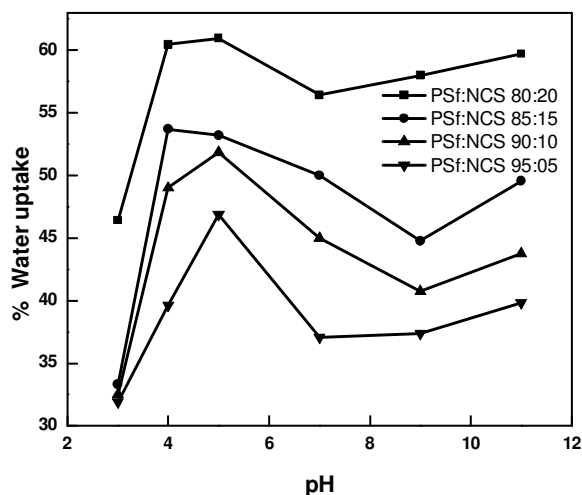
Figure 4.25 Effect of pH on water swelling

The prepared membrane was further investigated by filtering PEG solutions of known molecular weight. Figure 4.26 represents rejection of PEG according to the molecular weight used. The membrane PSf:NCS 95:05 showed PEG (6000 Da) rejection of 80 %, while for PEG (10000 Da), it was found to be nearly 90 % rejection. The remaining membranes possessed larger pore size and hence exhibited less PEG rejection in correlation with the NCS content.

Salt rejection of the membranes is presented in Figure 4.27 (**a-c**). A declining tendency towards salt rejection under high applied pressures was observed in all cases. It must have been due to some convection flow, leading to an increase in permeate salt concentration. While comparing among the electrolytes used, the rejection observed decreased in the following order $MgSO_4 > Na_2SO_4 > NaCl$ as shown in Figure 4.27 (**a-c**). Higher rejection of $MgSO_4$ over $NaCl$ was explained using size exclusion principle. As SO_4^{2-} is larger in size than that of Cl^-, it showed greater rejection. The membrane PSf:NCS 95:05 showed maximum rejection of 93 % for $MgSO_4$, 76.11 % for Na_2SO_4 and 70.12 %, for NaCl respectively. The PSf:NCS 80:20 showed least rejection for $MgSO_4$, Na_2SO_4 and NaCl at about 28.5 %, 22.5 % and 13.6 % respectively. These results

confirmed that the membrane PSf:NCS 95:05 possessed the smallest pore size compared to membranes with other compositions. This was evident from MWCO study of the membrane also.
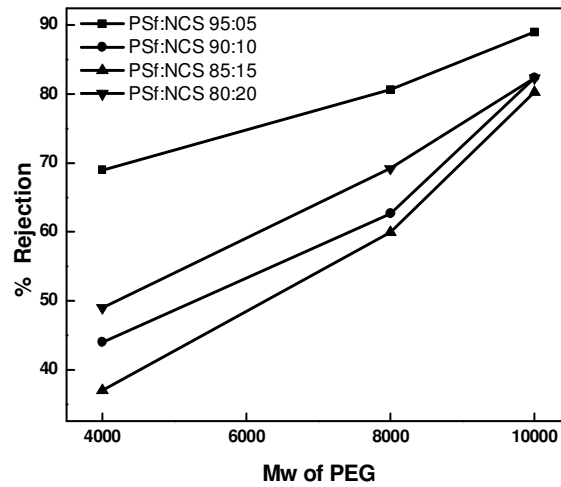
Figure 4.26 MWCO of membranes
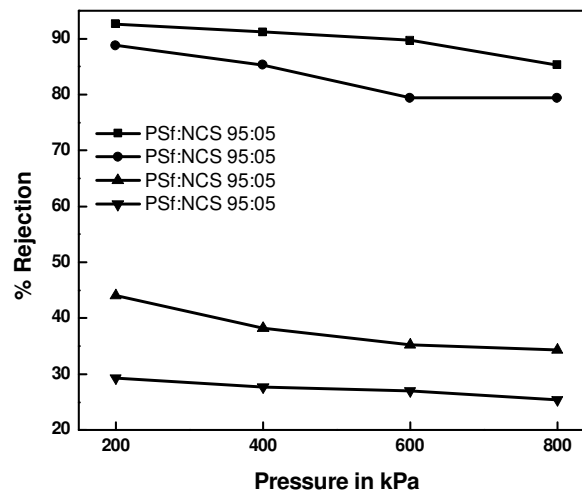
Figure 4.27 (**a**) MgSO$_4$ rejection
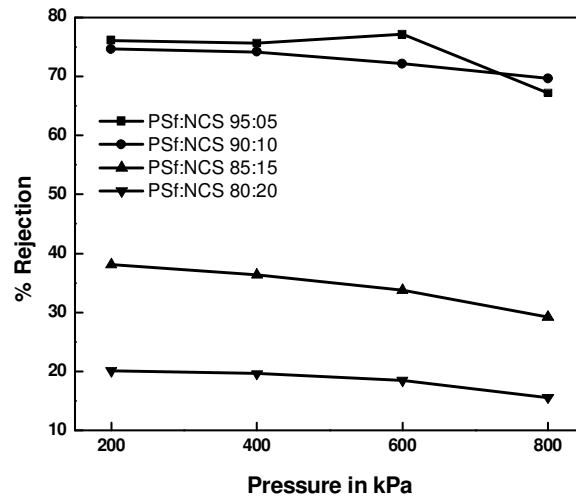
Figure 4.27 (**b**) Na$_2$SO$_4$ rejection

It is interesting to point out that, greater MgSO$_4$ rejection in membrane PSf:NCS 95:05 than membrane PSf:NCS 90:10 indicated that, the former had smaller pore size than the latter, whereas the comparative pore size between these two membranes could not be easily distinguished if NaCl was used for testing.
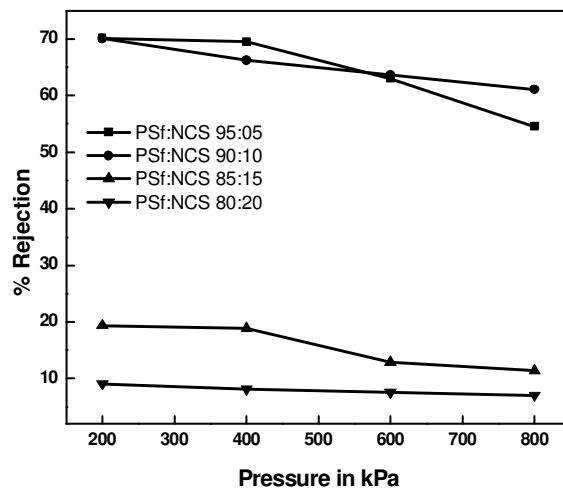
Figure 4.27 (**c**) NaCl rejection

4.2.3 Conclusions

Synthesized membranes behaved as nano and ultra-filtration membrane according to the N-Phthaloyl chitosan content. The increase in N-Phthaloyl chitosan content induced membrane hydrophilicity, leading to water swelling and membrane pore size enlargement. In addition, the membrane swelling property was observed to be pH dependent. The lowest swelling occurred at pH 3, maximum value of 65 % being observed at pH 5-6. Membrane Polysulfone:N-Phthaloyl chitosan 95:05 and 90:10 were categorized as nano-filtration membranes showing 95 % of megnisium sulphate rejection, 78 % of sodium sulphate rejection and 75 % of NaCl rejection respectively. The Polysulfone:N-Phthaloyl chitosan 85:15 and 80:20 were classified as ultrafiltration membranes with much smaller rejection for the above salts.

4.3 SULFONATED POLYSULFONE AND N-PHTHALOYL CHITOSAN BLEND MEMBRANE

Prompted by the previous results, sulfonation of the PSf was carried out in order to introduce negative charge on membranes. With the hope of enhancing the efficiency, the resulted sPSf was used for fabrication of ion exchange membranes with NCS.

Chen et al. (1996) reported preparation of sulfonated polysulfone (Figure 4.28) /polysulfone and aminated polysulfone (Figure 4.29)/polysulfone blend membranes. These blend membranes showed improved performance in comparison with that of the original polysulfone membranes. Sulfonation is one of the favorable method to introduce negative charge on the polymers. Charged membranes were well facilitated for the ion exchange process. Ion-exchange membranes have also been used in electrodialysis of brackish water desalination for several decades. For the desalination application, it is essential for ion-exchange membranes to possess high selectivity and productivity.
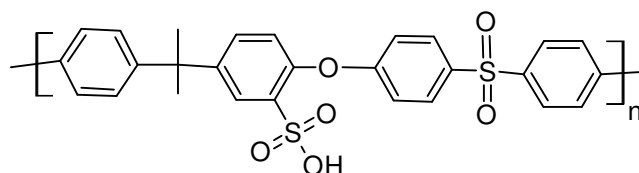
Figure 4.28 Structure of sulphonated polysulfone
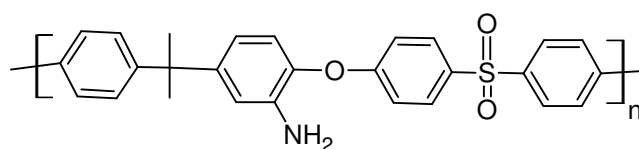
Figure 4.29 Structure of aminated polysulfone

To date, most of the ion-exchange membrane studies have focused on Nafion, sulfonated polystyrene and sulfonated poly (phenylene oxide) based material systems. Experiments with ion exchange membranes were described as early as 1890 by Ostwald. Work by Donnan a few years later led to development of the concept of membrane potential and the phenomenon of Donnan exclusion.

Intially, charged membrane were made from the natural materials or chemically treated collodion membranes however, their mechanical and chemical properties were

very poor. Nonetheless, as early as in 1939, Manegold and Kalauch (1939) suggested the application of selective anionic and cationic exchange membranes to separate ions from the water.

Hence, PSf was sulfonated and NCS blend membranes were prepared. The chemical and physical properties of the prepared membranes, such as: water flux, swelling ratio, ion-exchange capacity, diffusion potential, MWCO, and salt rejection of NaCl, Na_2SO_4 and $MgSO_4$ solutions were studied.

4.3.1 Experimental

4.3.1.2 Preparation of sPSf

PSf (MW 35000 Da) was sulfonated according to the procedure described by Chao et al. (Chao and Elsey 1982). Dried PSf of 10 g was dissolved in 100 mL of anhydrous 1,2-dichlorethane in a 250 mL two-neck round bottom flask equipped with condenser and nitrogen purge inlet. The synthetic path has been presented in Figure 4.30. The resulting solution was purged with nitrogen for 1 hr and 2.6 mL of chlorosulfonic acid diluted in 20 mL of 1,2- dichloroethane was added dropwise for 30 min. The amount of intermediate product was dependent on the mole ratio of sulfonating agent and polymer-repeating units. The resultant solution was vigorously stirred for 12 hrs at 30 °C. After the completion of reaction, sPSf was isolated from the solution by precipitation with methanol and then the polymer was washed with deionized water for several times and dried at 60 °C under vacuum to attain constant weight. Degree of sulfonation was determined by titration method and was found to be 49 %.
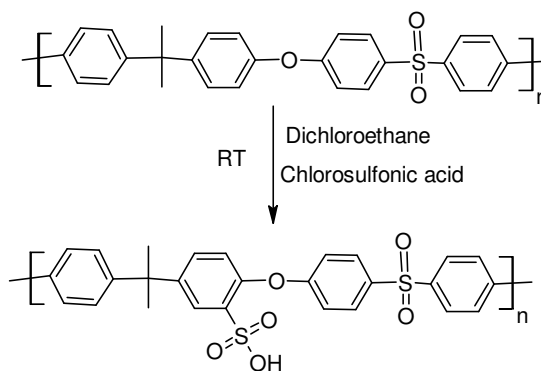
Figure 4.30 Schematic representation of sulfonation of PSf

4.3.1.3 Preparation of blend membranes

sPSf:NCS blend membranes were prepared by phase inversion method. Different ratios of sPSf and NCS was dissolved in N-methyl pyrolidone (NMP) at 60 °C for 24 hrs until a viscous and clear solution was obtained. The different ratio of polymers are tabulated in table 4.5. The solution was filtered by G4 sand filter immediately. The solution was cast on a glass plate using glass rod. The thickness of the wet membrane was maintained to 0.2 mm. It was then air dried for 30 seconds and immersed in a coagulation water bath at room temperature for 30 min after which membrane got separated from the glass plate. It was washed several times with distilled water to remove the excess of NMP and then stored in distilled water until further characterization.

Table 4.5 Composition of the polymers for membrane preparation

Membrane	Polymer concentration	
	sPSf	NCS
sPSf:NCS 60:40	60 %	40 %
sPSf:NCS 70:30	70 %	30 %
sPSf:NCS 80:20	80 %	20 %
sPSf:NCS 85:15	85 %	15 %
sPSf:NCS 90:10	90 %	10 %
sPSf:NCS 95:05	95 %	05 %

4.3.2 Results and discussion

4.3.2.1 Characterization of sPSf

FT-IR spectrum of sPSf was measured for confirmation of the product. Figure 4.31, showsed the peaks of sPSf. Strong characteristic peaks at 1010 and 1097 cm^{-1} were observed in the sulfonated polymers, corresponding to symmetric and asymmetric stretching of the sulfonate group respectively. The presence of strong peak at 1241 cm^{-1} to 1243 cm^{-1} was attributed to the ether C-O-C stretch of the PSf moiety and the peak at1169 cm^{-1} to 1170 cm^{-1} due to O=S=O stretching. Aromatic C–H stretch could be detected at 1141 cm^{-1}. Figure 4.32 shows ATR-IR spectra of the membranes.
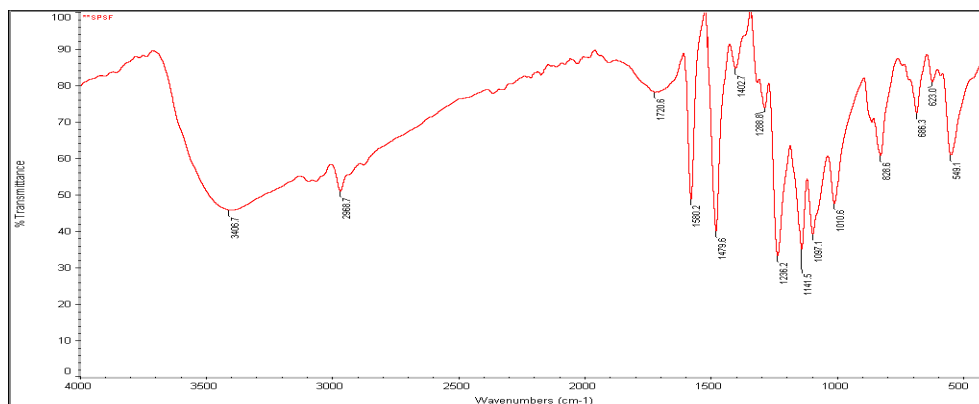
Figure 4.31 FT-IR spectrum of sPSf
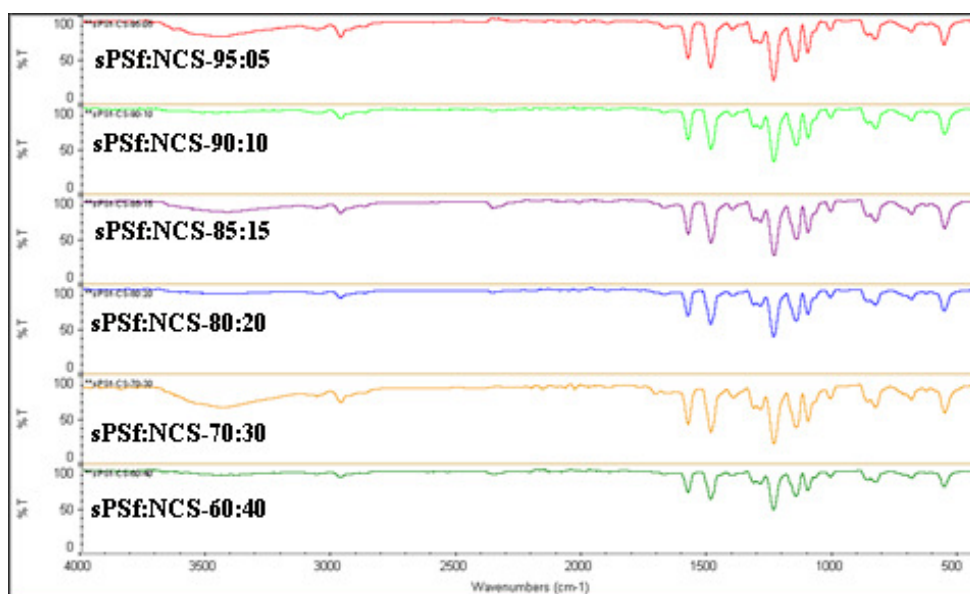
Figure 4.32 ATR-IR spectra of membranes

TGA analysis of PSf and sPSf polymers are reported in Figure 4.33. The parent PSf is a highly thermo-stable polymer, of which the 5 % weight loss temperature is above 500 °C and there is only one weight loss step that is ascribed to the decomposition of polymer main chain. For sPSf three transitions of weight loss in three separate temperature ranges were distinguished in the figure. The first step around 100 °C related to the loss of the absorbed water. The second one, between 235 °C and 387 °C, was attributed to decomposition of the $-SO_3H$ groups. The third thermal degradation of sPSf at about 450 °C was assigned to the degradation of the polymer main chain.
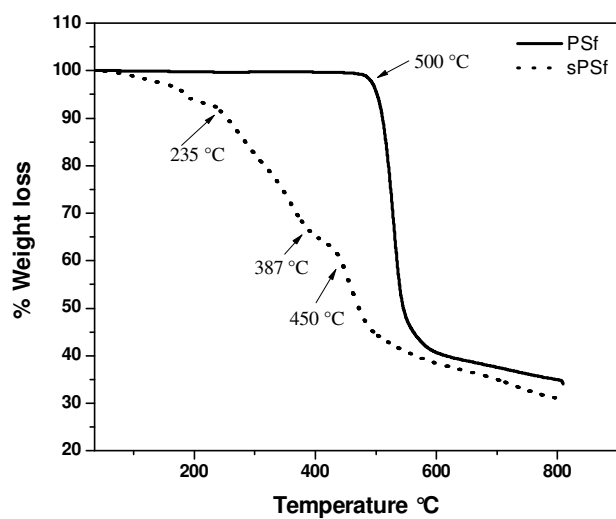
Figure 4.33 TGA curves of PSf and sPSf
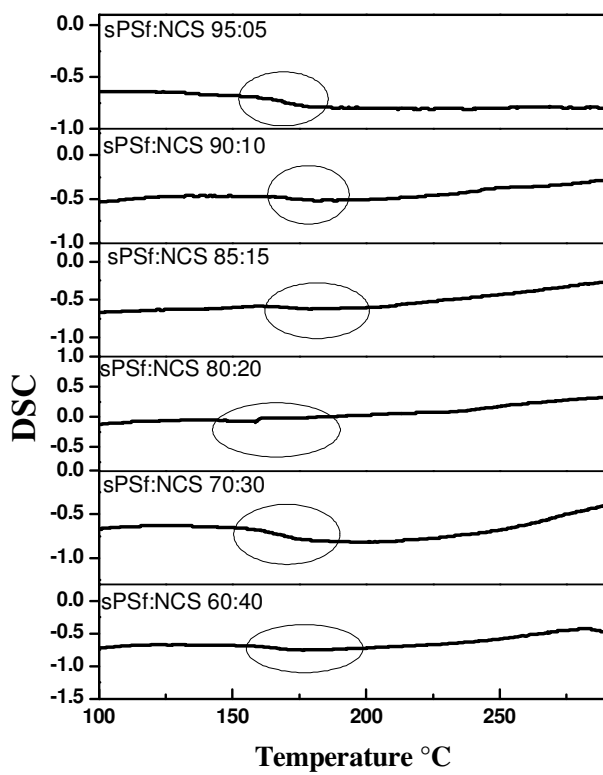
Figure 4.34 DSC curves of membranes

The thermal behaviors of different blend membranes were studied using DSC. DSC was recorded at a heating rate of 10 °C min^{-1}. Scans were carried out from 30 °C to 300 °C under the absence of atmospheric oxygen. Figure 4.34 shows the DSC graphs of membranes. From the thermal study it was clear that, the T_g value of the blend membranes showed a single T_g value. This confirmed the formation of blend, as a result of many Van der Waals interactions between two polymers.

4.3.2.2 IEC, water uptake and contact angle measurements

The ion-exchange capacity (IEC) provides information on the charge density in the membranes which is an important factor related to the conductivity and transport properties of the membranes. The ion-exchange capacity, hydraulic permeability and contact angles of the membranes are summarized in Table 4.6. IEC and hydraulic permeability coefficient increased with increase in concentration of sPSf due to presence of more hydrophilic sulfonic acid groups in the polymer matrix. This is consistent with increase of water swelling of the membranes with higher content of sPSf, indicating higher hydrophilicity. The hydrophilicity was also confirmed by contact angle measurement. Contact angle decreased with increase of the concentration of sPSf. Water uptake test was done at different intervals of time. Figure 4.35 shows percent water uptake with time interval of 60 mins. It was clear that after 12 hrs membrane showed same water uptake.

Table 4.6 Physical properties of membranes

Membrane	IEC (mM/g)	Hydraulic permeability coefficient m/sPa	Contact angle °
sPSf:NCS60:40	0.083	3.51×10^{-12}	87.48 ± 2
sPSf:NCS70:30	0.136	6.08×10^{-12}	83.01 ± 2
sPSf:NCS80:20	0.169	9.41×10^{-12}	82.32 ± 2
sPSf:NCS85:15	0.175	3.14×10^{-11}	78.36 ± 2
sPSf:NCS90:10	0.176	4.86×10^{-11}	78 ± 2
sPSf:NCS95:05	0.177	8.86×10^{-11}	76.63 ± 2
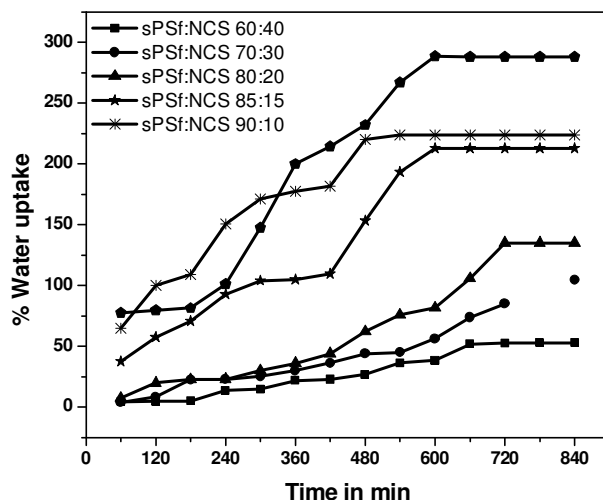
Figure 4.35 Water uptake v/s time

4.3.2.3 Diffusion potential of the membranes

As shown in Table 4.7, the membrane sPSf:NCS 90:10 showed highest diffusion potential and membrane sPSf:NCS 60:40 showed least diffusion potential. Membrane diffusion potential was affected by sulfonation of PSf, it increased with the sPSf concentration. In the case of sPSf:NCS 95:05, diffusion potential was less because of larger pore size.

Table 4.7 Diffusion potential of sPSf:NCS blend membranes

Membrane	Diffusion potential in mV
sPSf:NCS60:40	14.6
sPSf:NCS70:30	42.43
sPSf:NCS80:20	53.06
sPSf:NCS85:15	53.36
sPSf:NCS90:10	71.7
sPSf:NCS95:05	31.3

4.3.2.4 Performance of the membrane

Membranes based on sPSf:NCS blend membranes were prepared in different compositions and the maximum possible composition was found to be 60:40. The water flux of membranes is an essential parameter, which is useful for any industrial process. Water flux was influenced by the composition of the membrane material (Mahendran et al. 2004). It was studied using dead end flow cell at different pressure ranging between 200 kPa to 800 kPa. Figure 4.36 shows the water flux results.

It is evident from the study that increase of pressure increased the water permeation linearly. Water permeability coefficient of the membrane was calculated using the slope and tabulated in Table 4.6. The membrane pore size was confirmed by water permeability coefficient values. In the present study, water permeability coefficient increased with an increase in the composition of sPSf. The membrane sPSf:NCS 95:05 showed highest water permeation, indicating that the membrane had largest pore size. This was confirmed by small diffusion potential and hence it could not be effectively used for salt rejection.
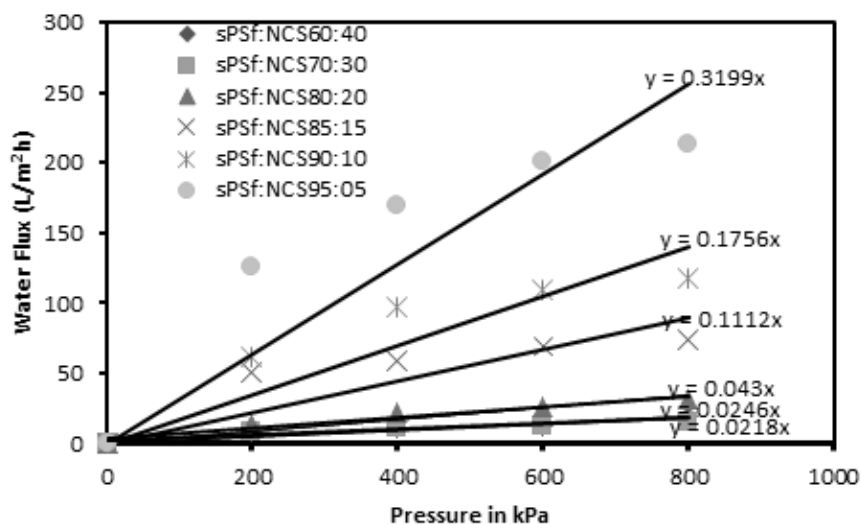
Figure 4.36 Water flux study at different pressure
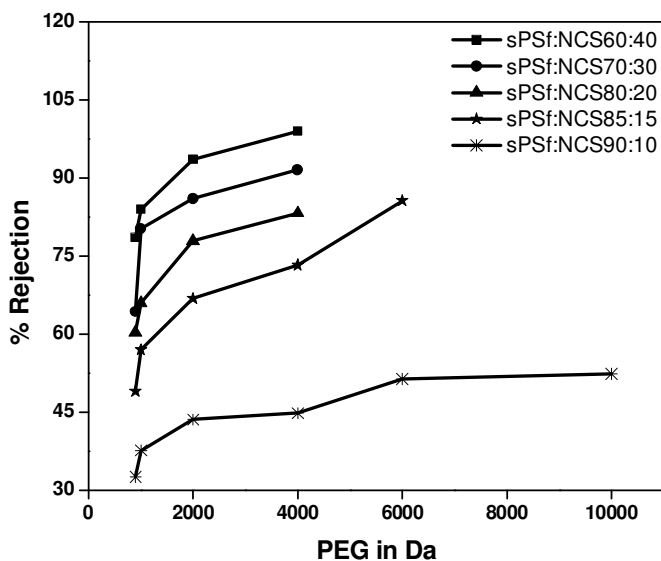
Figure 4.37 MWCO of membranes

The MWCO values are shown in Figure 4.37. The MWCO was determined for pore size of the blend membranes. The membrane 60:40 composition showed 1000 Da cut off value. It was observed that increase in the composition of sPSf, increases the MWCO. From the water flux and water swelling study, it was confirmed that membrane pore area was increased with increase in composition of sPSf. Membrane sPSf:NCS 90:10 showed MWCO greater than 10,000 Da, which was too large to be used for salt rejection.

In desalination, nanofiltration membranes were preferred over reverse osmosis as relatively high flux can be obtained with reasonable rejection of solute at comparatively less operating pressure. Performance study was done using 1000 ppm of NaCl, Na_2SO_4 and $MgSO_4$ solutions. Salt rejection of the membranes has been presented in Figure 4.38 (**a-c**). It was interesting to observe that, there was a tendency to decline in salt rejection under higher applied pressures in all cases. This was due to increase in the pore size at higher pressure. From the rejection study, it was clear that rejection decreased in the order of $MgSO_4 > Na_2SO_4 >$ NaCl as shown in Figure 4.38 (**a-c**).
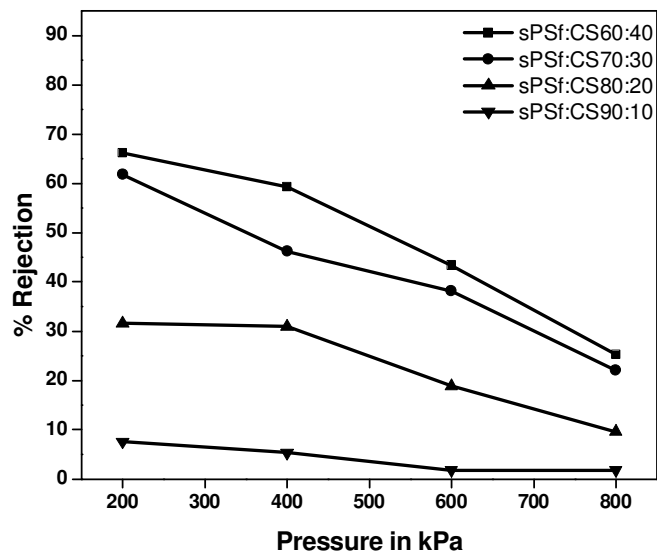
Figure 4.38 (**a**) Rejection results of NaCl
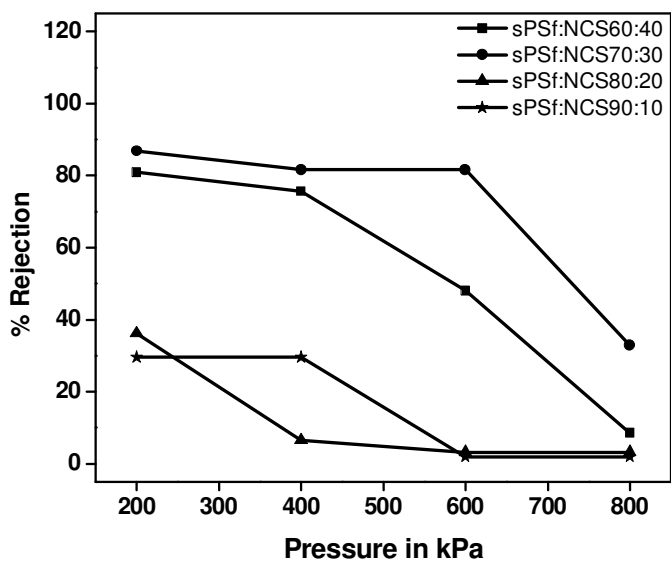
Figure 4.38 (**b**) Rejection results of Na_2SO_4
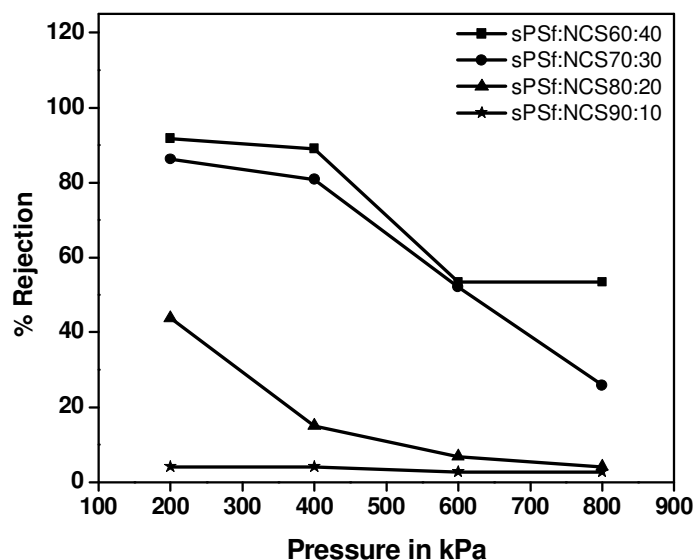
Figure 4.38 (**c**) Rejection results of MgSO$_4$

Higher rejection of MgSO$_4$ over NaCl was explained using size exclusion principle, as MgSO$_4$ is larger in size than that of NaCl. Donnan exclusion is less effective in bulk concentration of solute. This is because at higher concentration, the time taken by the solute to reach the membrane surface is faster (Xu and Lebrun 1999). It is believed that with increase in ionic strength, tendency of magnesium ions to reach membrane surface increased as a result of which the rejection of magnesium ions increased (Xu and Lebrun 1999).

The membrane sPSf:NCS 60:40 showed the highest rejection of 92 % for MgSO$_4$, 86.11 % for Na$_2$SO$_4$ and 66 % for NaCl respectively. The sPSf:NCS 90:10 showed smallest rejection for MgSO$_4$, Na$_2$SO$_4$ and NaCl at about 34.1 %, 26.6 % and 7.6 % respectively. These results confirmed that the membrane sPSf:NCS 60:40 possessed the smallest pore size compared to the others.

4.3.3 Conclusions

The forgoing discussion concludes that sulphonated polysulfone: N-Phthaloyl chitosan blend nanofiltration membranes are cation exchange membranes for

desalination. Membrane diffusion potential and ion exchange capacity of the membrane confirmed that the prepared membrane had negative charge. Hydrophilicity and membrane charge are greatly affected by sulfonation of polysulfone and tends to increase with the sulphonated polysulfone concentration. Hydrophilicity of the membrane was studied by water swelling test and contact angle measurement. In the molecular weight cut-off study, the membrane 60:40 composition showed 1000 Da of molecular weight cut-off. It has been observed that, increase in the concentration of sulphonated polysulfone, increases the molecular weight cut-off. Using these statistics, it was concluded that the content of sulphonated polysulfone affects the performance of the membrane.

Abstract: In this chapter, the effect of surface modification on the membrane performance was discussed. Three types of surface modification were done, namely, chemical modification, vapor phase deposition of metals and N^+ beam irradiation on to the membrane surface. The surface morphology and performance difference of the membrane after and before modification was compared and discussed.

The intention of surface modification of a membrane is to introduce additional interactions (affinity, responsiveness or catalytic properties) for improving the selectivity or creating an entirely novel separation function which ensures an increase in the productivity. The key feature of a successful surface functionalization lies in the synergy between the useful properties of base membrane and novel functional polymer (layer). This is best achieved by functionalization, which essentially preserves the bulk structure of the base membrane. In a more general context, surface modifications of polymers have attracted much attention in last decade. Often, two alternative approaches are distinguished. 'Grafting-to' is performed by coupling polymers to surfaces, whereas in 'Grafting-from', monomers are polymerized using an initiation at the surface. The structure of the polymer plays an important role in 'Grafting-to' surface modification. It can be well controlled by synthesis and also characterized in detail. However, the grafting density which may be achieved on the surface are limited and the coupling reactions typically require special efforts. In contrast, the synthesis of surface anchored polymers via 'Grafting-from' is often less controlled with respect to polymer structure. Inspite of this drawback, a very wide variation of grafting densities and chain lengths can be obtained under relatively convenient reaction conditions. In order to achieve the ultimate aim of membrane surface modification, often two or multi stage methodology provides an optimum solution.

Recently, surface modification of membranes is thought to be important to the membrane industry for process development. Surface functionalization has already become a key technology, the major aim being performance improvement (flux and selectivity) by reduction of unwanted fouling. The major drawback of membrane fouling

during separation by membranes can be reduced to an appreciable extent by surface modification technique.

Surface hydrophilicity plays a central role for flux and selectivity. Membrane researchers and manufacturers have for example, tried to graft different kinds of hydrophilic polymers (with different functional groups) onto the membranes or tried to blend polymers to increase hydrophilicity. During these processes, sometimes a change in charge density is achieved which may be beneficial (Gopal et al. 2007). The aim of surface modification of a membrane is largely two-fold:

1. Minimization of undesired interactions (adsorption or adhesion, or in more general terms membrane fouling) that reduce the performance of the membrane and

2. Improvement of selectivity or even the formation of entirely novel separation functions (Ulbricht 2006).

This can be achieved via introduction of additional (tailored) interactions (affinity, responsiveness or catalytic properties). Novel membranes with high selectivity for isomers, enantiomers or special biomolecules are in high demand. Consequently, particular attention should be paid to truly molecule-selective separations i.e., advanced nanofiltration and ultrafiltration membranes. In addition, a membrane selectivity that can be switched by an external stimulus or can adapt to the environment/process conditions would be an important feature. Such novel developments may seem futuristic, but it is clear that if such advanced or novel selective membranes were available, they would immediately find applications in many fields such as analytics, screening, membrane reactors or bio-artificial membrane systems (Kato et al. 2003).

Many factors need to be considered in the overall process of membrane modification, such as uniformity, reproducibility, stability, process control and reasonable cost together with precise control over functional groups, which is a big challenge. A lot many number of surface modification techniques have been developed till date. Surface grafting has emerged as a simple, useful and versatile approach to

improve surface properties of polymers for many applications. Grafting has several advantages:

1. The ability to modify the polymer surface to have distinct properties through the choice of different monomers.

2. The controlled introduction of graft chains with high density and exact localization to the surface without affecting bulk properties.

3. Long-term chemical stability, which is assured by covalent attachment of graft chains (Minko 2006).

Many modification techniques have been used to significantly modify membranes including radical polymerization (Belfer, et al. 2001), low temperature plasma (Ang 2000), layer-by-layer alternating polyelectrolyte deposition (APD) (Greene and Tannenbaum 2004), ionizing radiation (Kim 1990 and Wanichapichart and Lu 2011) and photochemical techniques (Hilal 2003). The latter factor contrasts with physically coated polymer chains that can in principle be removed rather easily.

Chennamsetty et al. (2006) reported commercial sulfonated polysulfone water treatment membrane modified by ion beam irradiation. After the irradiation, ATR-FTIR was used to identify chemical structure changes incurred by the modification. Some of the sulfonic groups on the surface of the membrane were broken due to ion beam irradiation which resulted in cross-linking of the polymer. These changes modified the surface morphology of the membrane and also decreased the negative charge of the membrane.
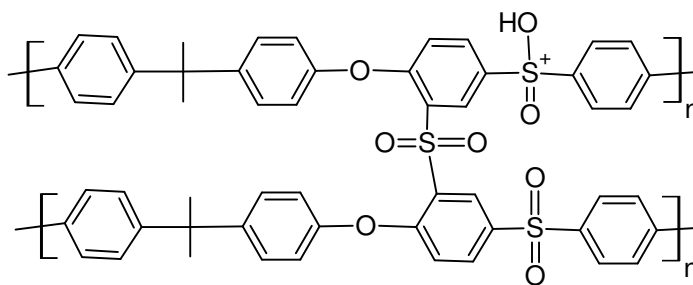
Figure 5.1 Structure of the cross-linked polysulfone

Yu et al. (2011) prepared commercial thin-film composite aromatic polyamide (Figure 5.2) reverse osmosis membranes modified by depositing N-isopropylacrylamide-co-acrylic acid copolymers (P(NIPAm-co-AAc)) (Figure 5.3) on the membrane surface. The modified membranes showed improved membrane properties. The effect of surface modification on membrane salt permeability was investigated through permeation tests with different salts under different pH. The membrane modification was found to decrease the salt permeability of NaCl and Na_2SO_4 under neutral and alkaline conditions, the decrease was significant for Na_2SO_4 than for NaCl.
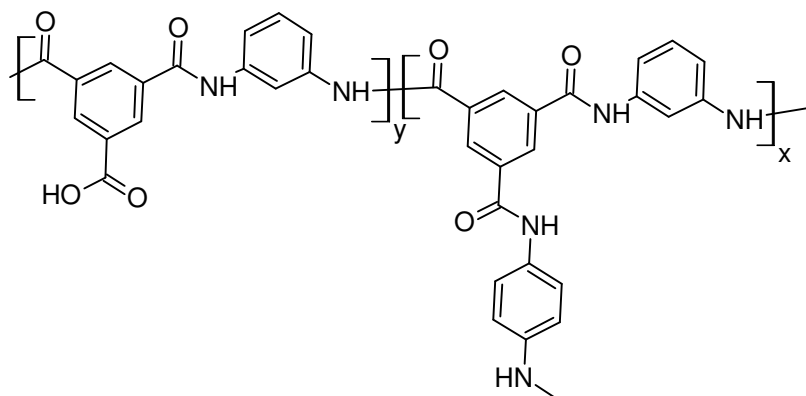
Figure 5.2 Structure of aromatic polyamide
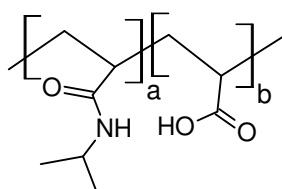
Figure 5.3 Structure of N-isopropylacrylamide-co-acrylic acid

Yu et al. (2011) extended his same work and modified same polyamide membrane using a thermo-responsive polymer poly(N-isopropylacrylamide-co-acrylamide) (P(NIPAM-co-Am)) (Figure 5.4). It was found that membrane modification improved the water permeability and fouling resistance to bovine serum albumin (BSA) due to the increased membrane surface hydrophilicity. The phase transition of thermo-responsive polymer surface coating layer above Lower critical solution temperature

(LCST) facilitated removal of foulant located on membrane surface (Figure 5.5). Furthermore, the in situ membrane surface modification approach would be of particular interest for treating existing commercial membranes in their original module assembly.
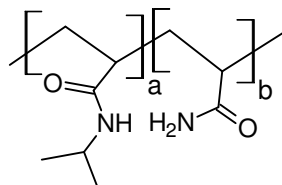
Figure 5.4 Poly(N-isopropylacrylamide-co-acrylamide)
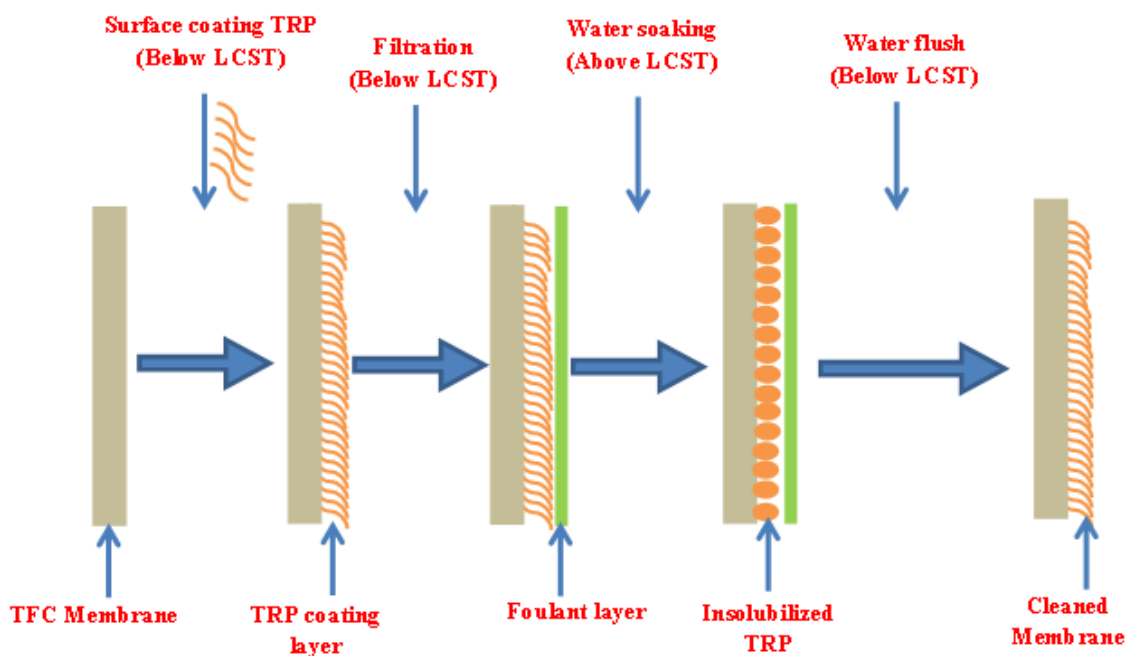
Figure 5.5 Schematic representation of surface modification of (TFC) membrane

Wu et al. (2012) reported grafting-to approach was experimentally simpler and provided better control of grafted polymer, but it usually suffered from lower grafting density. Novel three-step method for polyacrylamide grafting-to the polypropylene macroporous membrane was carried out by marrying click chemistry with reversible addition-fragmentation chain transfer radical polymerization (Figure 5.6) The permeation performances of the modified membranes were tested by the filtration of protein dispersion. The protein filtration experiments show that, in comparison with the

unmodified membrane, the modified membrane can effectively reject proteins due to the densely grafted polymer chains.
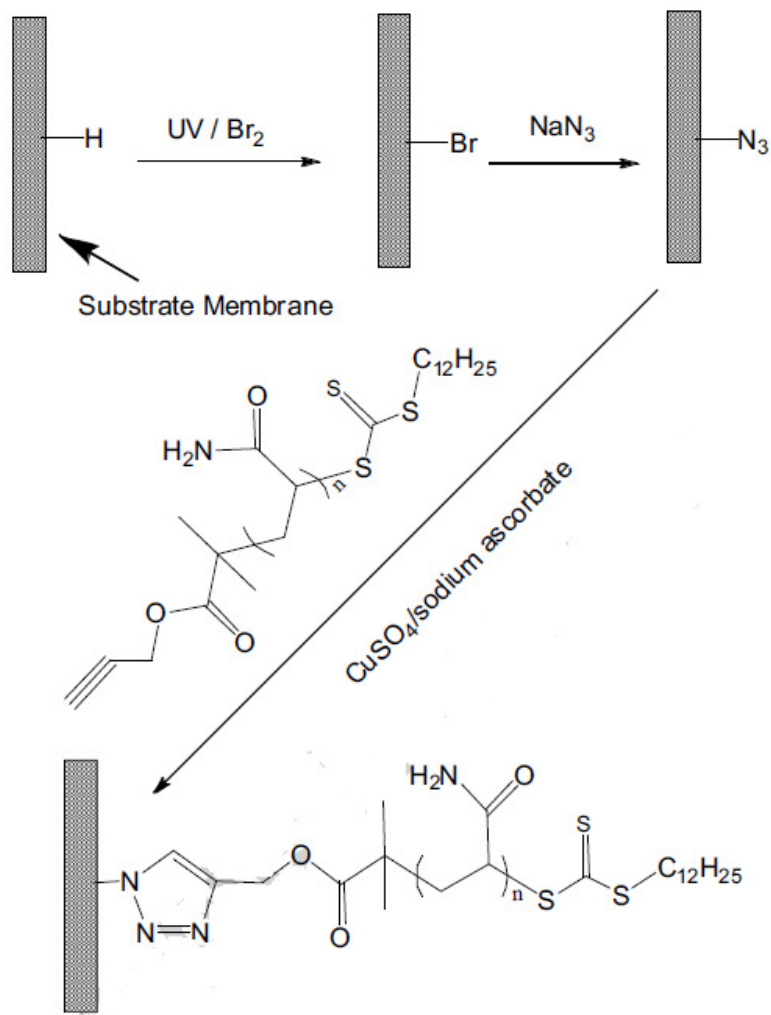
Figure 5.6 Schematic representation of reversible addition–fragmentation chain-transfer polymerization (RAFT) by click chemistry

Keeping in view the advantages offered by surface modification techniques it was, proposed to bring about chemical modification, Beam irradiation and Physical Vapor Deposition of the membrane surfaces in order to improve their performance.

5.1 CHEMICAL MODIFICATION OF POLYSULFONE AND POLY (ISOBUTYLENE-ALT-MALEIC ANHYDRIDE) BLEND MEMBRANE

Chemical modifications to a solid surface are as numerous as the reactions in an organic chemistry book. However, organic reactions are in solution i.e., are homogeneous, whereas polymer surface modifications are necessarily heterogeneous, i.e. are at the interface between two phases. The rates and yields of heterogeneous reactions tend to be lower than those of the corresponding homogeneous reactions. The innate solvent resistance and lack of reactivity of engineering polymers (relatively inert and insoluble synthetic polymers) mean that fairly aggressive and/or specialized procedures are required to achieve surface modification.

Chemical modification result in general oxidation forming carbonyl groups, hydroxyl groups and carboxylic acid groups on the polymer surface. When the treatment mixture includes sulfuric acid, sulfonation also occurs (Fischer and Eysel 1995). The introduction of these oxygen containing functional groups increases the polarity and the potential for hydrogen bonding, which in turn improves wettability and adhesion. Over exposure to the treatment conditions tends to damage the polymer surface by producing microscopic pits (Blais et al 1974). This surface pitting or etching can be beneficial to both wettability and adhesion properties. An interesting feature of oxidized polymer surfaces is worthy of note. Oxidized surfaces are higher in energy than the original unoxidized surface and may experience a phenomenon called surface reconstruction.

This is the reorientation and diffusion of the polar oxygen functionalities away from the surface and into the bulk leaving lower-energy, hydrophobic segments exposed. This phenomenon was noted early by Ter-Minassian-Saraga et al. (Baszkin et al. 1976 and 1977). It has been studied more recently by Gagnon and McCarthy (1984) Whitesides and coworkers (Holmes-Farley et al. 1987).

Polysulfone membranes have been subjected to reaction schemes that attach propyl sulfonate (Higuchi et al. 1988, 1990 and 1991), isopropyl alcohol (Higuchi et al.

1990), chloromethyl functional groups (Higuchi et al. 1992) as well as hydrophilic derivatives of the chloromethyl group. These modifications have been found to influence performance characteristics such as flux, solute rejection, solute MWCO and mixed solute separation.

Dai et al. (2004) proposed a new economic and convenient method to modify the surface of microporous polypropylene (PP) membranes with phospholipid. The process included the photo-irradiated graft polymerization of N,N-dimethylaminoethyl methacrylate (DMAEMA) and the ring-opening reaction of the grafted polyDMAEMA with 2-alkyloxy-2-oxide-1,3,2-dioxophospholanes (AOP). Four AOPs, whose alkyloxy groups consisted of dodecyl, tetradecyl, hexadecyl and octadecyl moieties were used to convert the grafted polyDMAEMA to phospholipid polymers. Figure 5.7 represent schematic representatives for the approach to prepare phospholipid-modified membrane
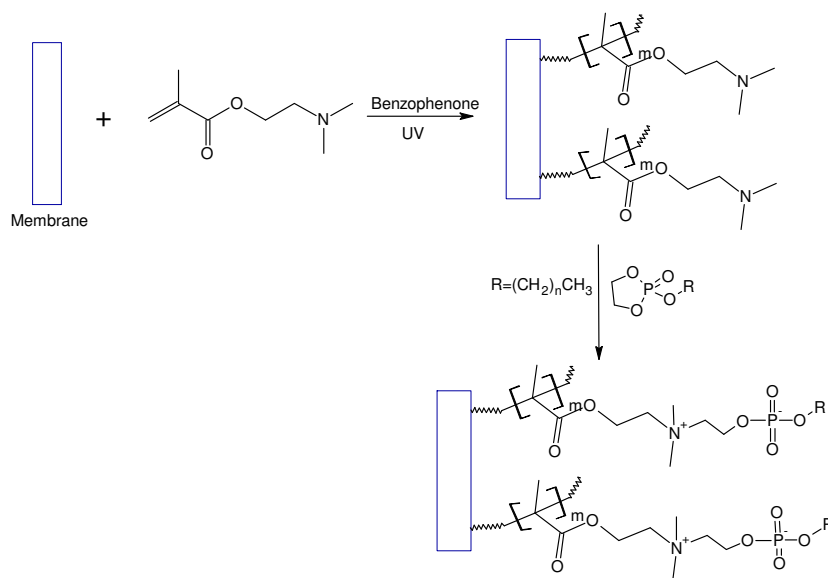
Figure 5.7 Schematic representation of phospholipid-modified membrane

One such type of chemical modification was presented here. Polyisobutylene-alt-maleic anhydride (PIAM) (Figure 5.8a), Polystyrene-alt-maleic anhydride (PSAM) (Figure 5.8b) and its derivatives have shown increased interest in recent years due to their potential applications as drug carrier (Henry et al. 2006), nanotechnology (Malardier-

jugroot et al. 2005, Tain et al 2006), biomaterial carrier (Yoshimaga et al. 1997) and anti-rejection for cross-species transplantation (Vetere et al. 2002).
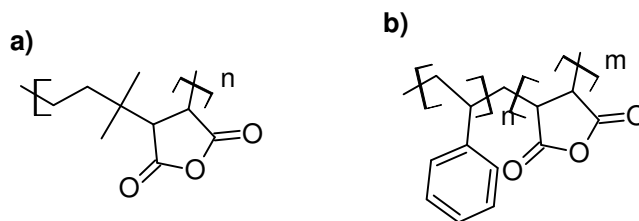
Figure 5.8 Structure of a) PIAM b) PSAM

PIAM has aliphatic chain and repeating anhydride group which breaks into two carboxylic acid groups when it comes in contact with water (Anita et al. 2009). Carboxylic acid group imparts surface charge to create Donnan effect and also enhances the hydrophilicity of the membrane. Hence, PIAM is considered to be a potential material to prepare membrane with a chance of introducing some charge onto the membrane surface.

5.1.1 Experimental

5.1.1.1 Membrane preparation

PSf (M_w 35,000 Da), PIAM were obtained from Sigma Aldrich, (India). NMP of analytical grade purity was obtained from Merck, India and was used without further purification. Both PSf and PIAM in required amounts were dried in vacuum oven for 10 hours. Different concentration of PSf and PIAM was dissolved in specified amount of NMP and heated at 60 °C. The solution was continuously stirred for 20 hrs to obtain complete dissolution. Further, polymer solution was spread on a glass plate using a casting knife. Excess of solvent was removed by heating it in a hot air oven and allowed to cool at 30 °C, there on dipped in coagulation bath containing water. Demixing of solvent and non-solvent in the coagulation bath resulted in the phase separation and the membrane gets peeled out from the glass plate. The obtained membrane was dipped in distilled water for another 24 hrs and was washed several times. Further, the membrane was immersed in 0.1 % NaOH solution for 20 hrs to break the anhydride group of PIAM

(Figure 5.9) and was washed and stored in distilled water. Using the above procedure, membranes having different composition of PSf and PIAM were prepared and subjected to further characterization.
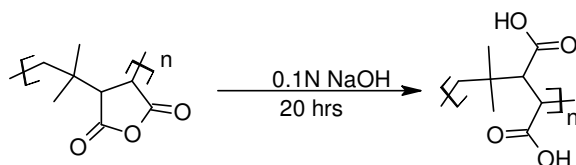
Figure 5.9 Schematic representation of PIAM polymer after alkali treatment

5.1.2 Results and discussion

5.1.2.1 ATR-IR spectra of membranes

ATR-IR spectra of polymer composites are shown in Figure 5.10, from which it is clear that, as the percentage of PIAM increases, the intensity of peak at ~1777 cm^{-1} increases.
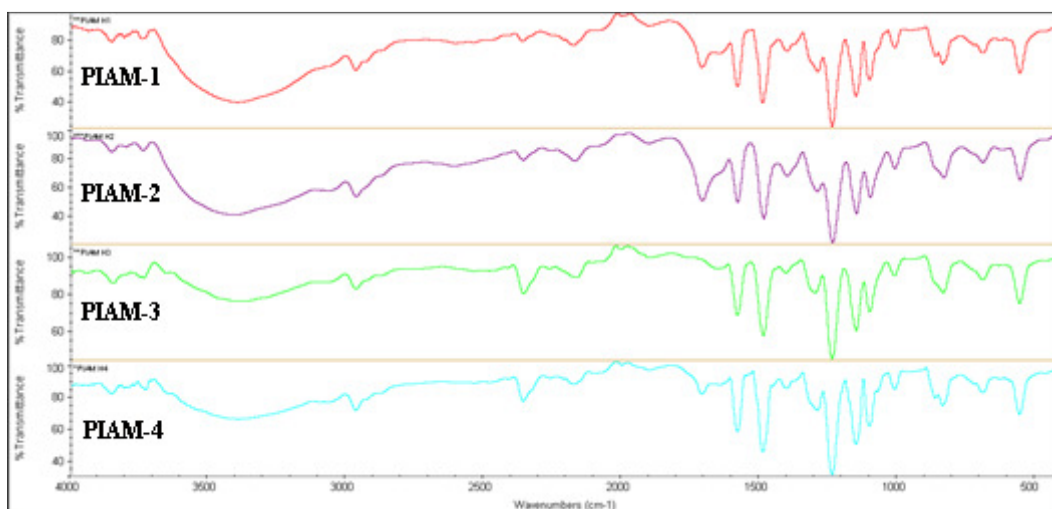
Figure 5.10 ATR-IR spectra of membranes

This was attributed to an increase in carbonyl group of the membrane; also peak at ~2966 cm^{-1} attributed to –OH stretching of acid group showed increased intensity as the composition of PIAM increased. This proves that as the blend membrane was dipped in 0.1 % NaOH for 20 hrs, the anhydride group was broken due to hydrolysis forming two

110

acid groups. The presence of strong peak at ~1235 cm^{-1} is assigned to the ether C-O-C stretch of PSf moiety and peak at ~1147cm^{-1} is due to O=S=O stretching.

5.1.2.2 Thermal properties of membrane

Thermal behavior of different blend membranes were studied from the DSC plots. Figure 5.11 shows the DSC graphs of PIAM membranes. T_g of different composition membranes were measured and compared. T_g of PIAM is 141 ^{o}C. It was observed that, with higher PSf content in the membrane the T_g also increases.
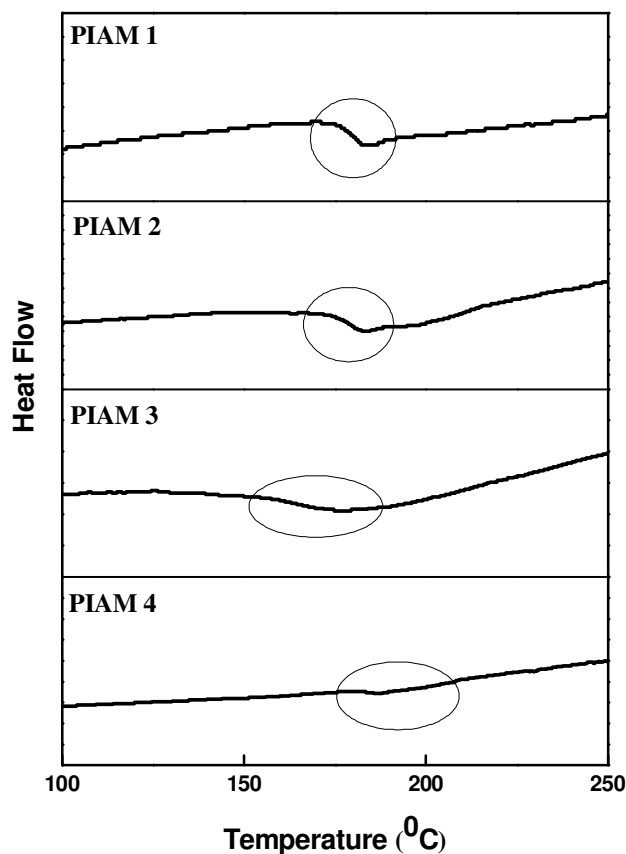
Figure 5.11 DSC curves of membranes

5.1.2.3 Water uptake and Contact angle measurement

Table 5.1 represents the water uptake results of the membranes with increasing amount of PIAM. This effect was found to depend on the carboxylic acid group in PIAM. Carboxyl groups increases the hydrogen bonding capability of the membrane surface. Hence water uptake decreases with decreasing concentration of PIAM. PIAM-1 membrane had maximum PIAM content, hence it showed maximum water uptake.

The contact angle is an important parameter for measuring surface hydrophilicity. (Khayet et al. 2002, Palacio et al. 1999) In general, a smaller contact angle corresponds to more hydrophilic materials. As can be seen from Table 5.1, increasing PIAM concentration decreases the contact angle. However, increasing PIAM concentration increases the water uptake and IEC. Formation of carboxylic acid group in the membrane increases with concentration of PIAM. Carboxylic acid group showed enhanced hydrophilicity. PIAM-1 showed 47.40° and PIAM-4 showed 67.92°. This proves the enhanced hydrophilicity of the membranes.

5.1.2.4 Ion exchange capacity

Ion exchange capacity of membrane proves the presence of carboxylic acid group in the membrane. The percentage composition of PIAM used was less than PSf, so the IEC is poor. The measured IEC values are shown in Table 5.1. PIAM-1 showed maximum IEC whereas PIAM-4 showed less IEC. IEC decreases with decreasd in the PIAM content.

Table 5.1 Physical properties of membranes

Sl. No.	Membrane composition PSf:PIAM	Membrane code	Water uptake (%)	IEC (mmol/g)	Contact angle °
1	60:40	PIAM-1	54%	0.98	47.40
2	70:30	PIAM-2	50%	0.97	50.68
3	80:20	PIAM-3	20%	0.69	65.97
4	90:10	PIAM-4	14.5%	0.55	67.92

5.1.2.5 Morphology studies

Scanning electron microscopy is a powerful tool to study the morphology of the membrane. These morphological features are typically observed in membrane and are
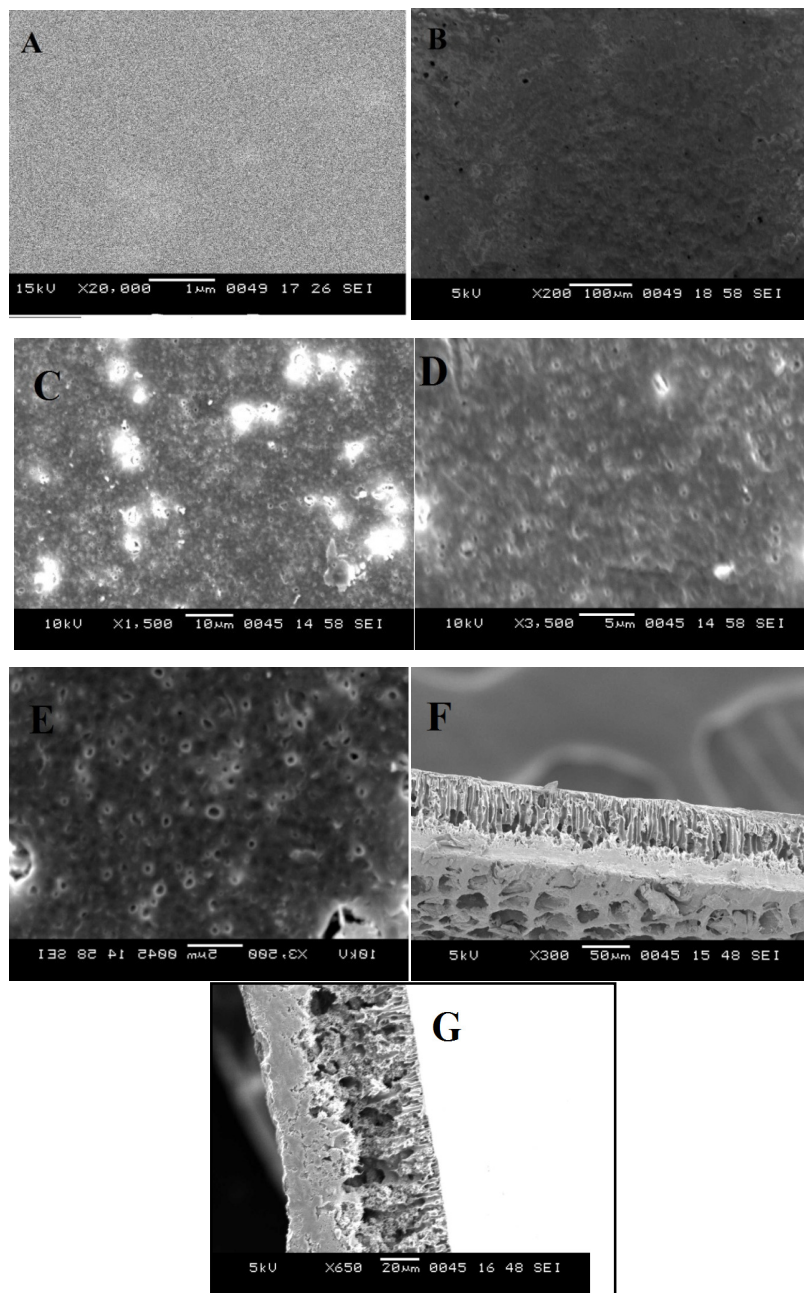
Figure 5.12 SEM images of the membranes; (**a**), (**b**) Surface image of PIAM-1 (**c**) Surface image of PIAM-2 (**d**) Surface image of PIAM-3 (**e**) Surface image of PIAM-4 (**f**) Cross section of PIAM-1 (**g**) Cross section of PIAM-2

known to be derived from liquid-liquid phase demixing process. To develop high performance polymer membranes, it is essential to design suitable molecule and morphological structure of membrane for their applications. It can be seen from the cross section of these four membranes that they have relatively similar structures, having three layers i.e., top layer, intermediate layer and sub layer with finger like projection and spongy structure. Surface view shows smooth surface with small pores. The SEM images have been presented in Figure 5.12.

5.1.2.6 Performance of membrane

The results of the membrane before alkali treatment showed that the rejection of electrolyte solution decreases in the following order $MgSO_4 > Na_2SO_4 > NaCl$ as shown in Figure 5.13. Higher rejection of $MgSO_4$ over Na_2SO_4 and NaCl can be explained using size exclusion principle, as SO_4^{2-} divalent ions are larger in size than Cl^- ion. The rejection after alkaline treatment is shown in Figures 5.15. The rejection decreased in the order of $Na_2SO_4 > MgSO_4 > NaCl$. It can be explained on the basis of charge interaction and size exclusion mechanism. Separation of charged ions of electrolyte occurs due to their interaction with fixed charge present on the membrane. Interaction between carboxylic acid group on the surface of the membrane and cations like Na^+ decreases the pore size of the membrane from which the SO_4^{2-} ion cannot pass. Hence, Na_2SO_4 showed more rejection than that of NaCl (Yan et al. 2006). $MgSO_4$ showed higher rejection than that of NaCl because of size exclusion mechanism. Charge interaction increased with an increase in concentration of PIAM.
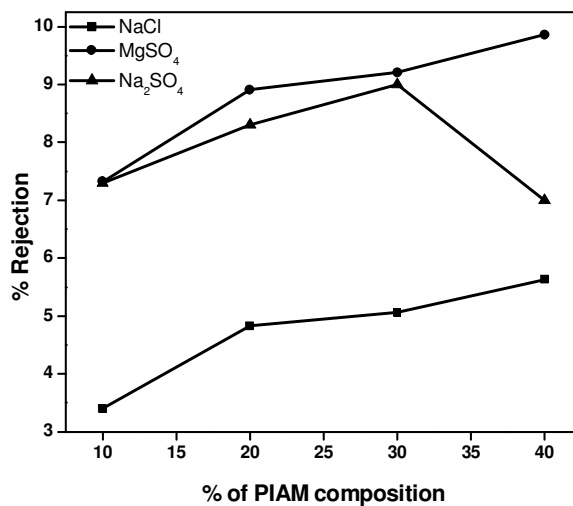
Figure 5.13 Salt rejection of membranes before alkali treatment
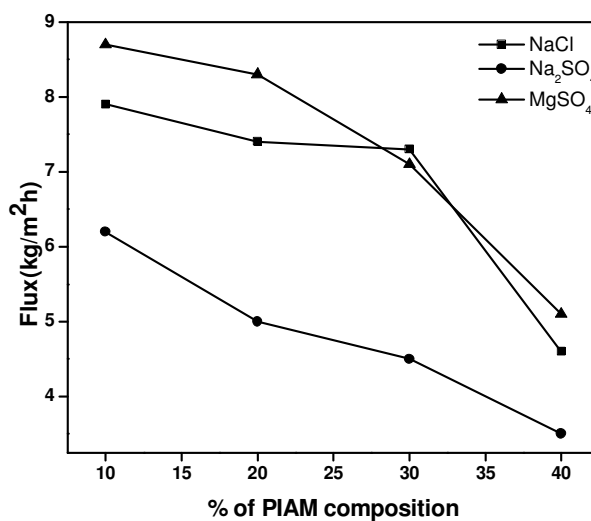
Figure 5.14 Flux of membranes before alkali treatment

More number of carboxylic acid groups was formed in PIAM-1 still PIAM-2 showed more rejection because formation of more carboxylic acid groups led to increase

in pore size. Figure 5.14 and 5.16 represents the flux of NaCl solution before and after the alkali treatment
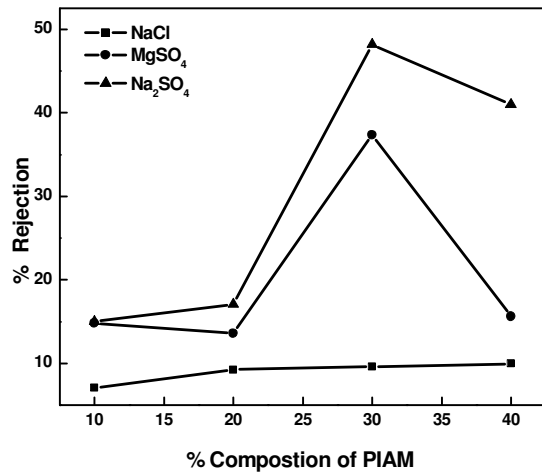
Figure 5.15 Salt rejection of membranes after alkali treatment
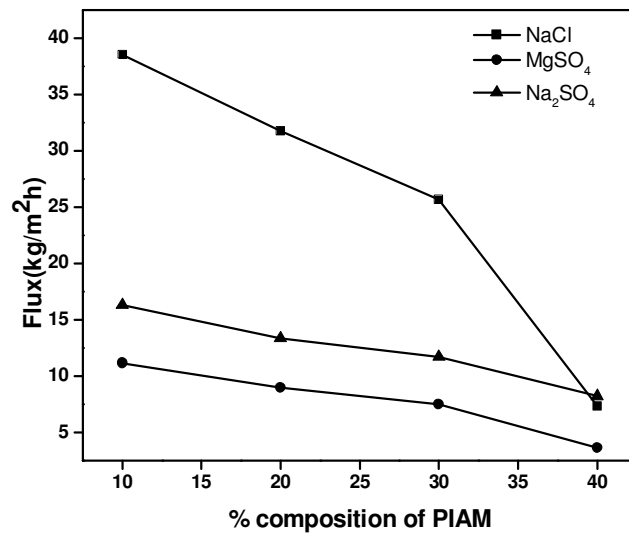
Figure 5.16 Flux of membranes after alkali treatment

5.1.3 Conclusions

In the present work, new polyisobutylene-alt-maleic anhydride and polysulfone nanofiltration membranes of different compositions were prepared by diffusion induced phase separation method. Membranes were characterized by ATR-IR, SEM and DSC studies. These membranes were also tested for salt rejection, flux and water swelling studies. From the results, it was evident that before the alkali treatment salt rejection and flux was less. However, alkali treatment resulted in hydrolysis of the anhydride bonds to form the acid groups. Among the tested salt solutions, sodium sulphate showed maximum salt rejection due to the Donnan effect. Higher concentration of polyisobutylene-alt-maleic anhydride resulted in higher flux due to increased surface charge as a result of carboxylic acid groups formed by base hydrolysis of anhydride group. Thermal properties showed that, higher the composition of the Polysulfone, higher was the T_g value. Hydrolysis of anhydride bonds by alkaline treatment is a promising method for increasing the flux and salt rejection of nanofiltration membranes.

5.2 PHYSICAL MODIFICATION OF MEMBRANE BY PHYSCIAL VAPOR DEPOSITION METHOD

Physical vapor deposition (PVD) on the membrane is one of the surface engineering techniques. This process is used to form optical interference coatings (Kaminska et al. 2003), mirror coatings (Hass et al. 1956), decorative coatings (Reiners et al. 1994), permeation barrier films on flexible packaging materials (Chahroudri et al. 1991), electrically conducting films (Jayaraj et al. 2001), wear resistant coatings (Rickerby et al. 1990) and corrosion protective coatings (Udayashankar et al. 2008). It involves changing the properties of the surface and near-surface region in a desirable way. In this process a material is added to the surface and the underlying material (substrate) is covered and not detectable on the surface. An atomistic film deposition process is one, in which the overlay material is deposited atom-by-atom. Deposition can range from single crystal to amorphous, fully dense to less dense, pure to impure and thin to thick. Generally the term "PVD" is applied to layers which have thickness of the order of several microns or less and may be as thin as a few atomic layers, For the membranes it can be restricted to the nano level thickness. Often the properties of the deposited membrane are affected by the properties of the underlying material (substrate) and can vary with the thickness of deposition (Figure-5.17).

Recent studies of membrane modifications have focused on blending with inorganic materials; addition of inorganic fillers has led to increased membrane permeability and improved control of membrane surface properties (Aerts et al. 2001, Bottino et al. 2001). Inorganic materials that can be blended with polymers include silica (Bottino et al. 2002), zirconium oxide (Taurozzi et al. 2008), silver nanoparticales (Wara et al. 1995), aluminium oxide (Lin et al. 2003) and small inorganic salts, such as lithium (Strapnik et al. 2002). There is no specific report of metal deposition on the membrane using PVD. Hence the introduction of PVD process to decrease the pore size was carried out.
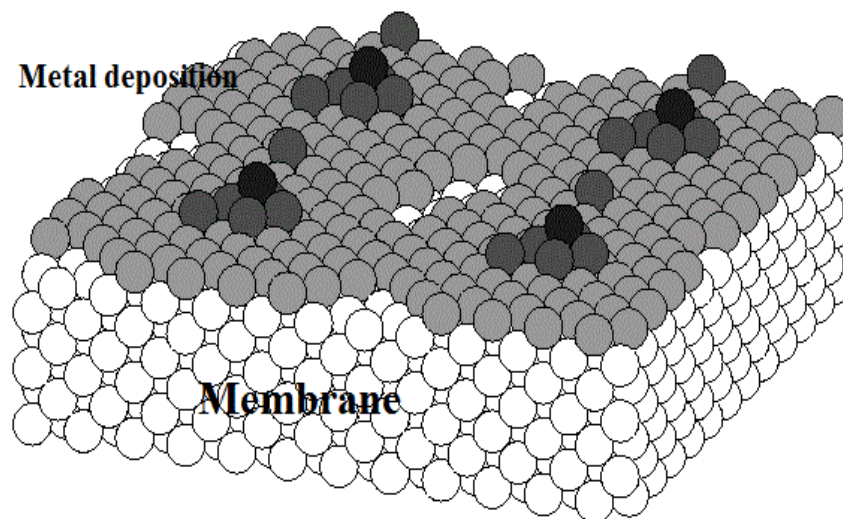
Figure 5.17 Representation of metal coating on membrane surface

(Source: http://www.sandia.gov/surface_science/pjf/Kabstracts/germann.htm)

The surface modification was carried out by means of aluminum coating on microporous PSf membrane by PVD method. PSf is a remarkable membrane material that has been known for a long time because of its flexible nature. Aluminum coating on membrane decreases the pore size which is highly effective in improving membrane performance.

5.2.1 Experimental

5.2.1.1 Membrane preparation

PSf (M_w 35,000 Da) was obtained from Sigma-Aldrich Co, Germany. NMP was procured from Merck India, Ltd. The chemicals were used without any further purification. Solution containing 20 wt % of PSf (2 g) in 8 mL of NMP was prepared by mild stirring for 24 hrs at a constant temperature of 60 °C. The obtained viscous solution was cast over glass plate using K-Control coater purchased from United Kingdom. Further, this casted membrane was kept in an oven at 180 °C for about 2 min to evaporate the excess of solvent and finally membrane was separated by dipping in water. It was stored in double distilled water until further characterization.

5.2.1.2 PVD of aluminium

The deposition of Aluminium was done by evaporating Al (Merck, 99.99 %) in an Indian high vacuum pump, IHVP box coater model-IVP 12A4BC. Figure 5.18 shows schematic representation PVD process cell. In order to get a very thin coating, time of deposition was restricted. The thickness of the deposited film was found to be 45 nm as indicated by online thickness monitoring system which includes a crystal oscillator. The deposition carried out in a vacuum less than 10^{-5} mbar inside a custom made vacuum chamber equipped with rotary and a diffusion pump with deposition time of 3 min. Membrane was mounted at a distance of 20 cm from the source to avoid possible heating and was rotated using a substrate rotation assembly to ensure better uniformity. The membrane was then washed with water to remove aluminum present on the surface.
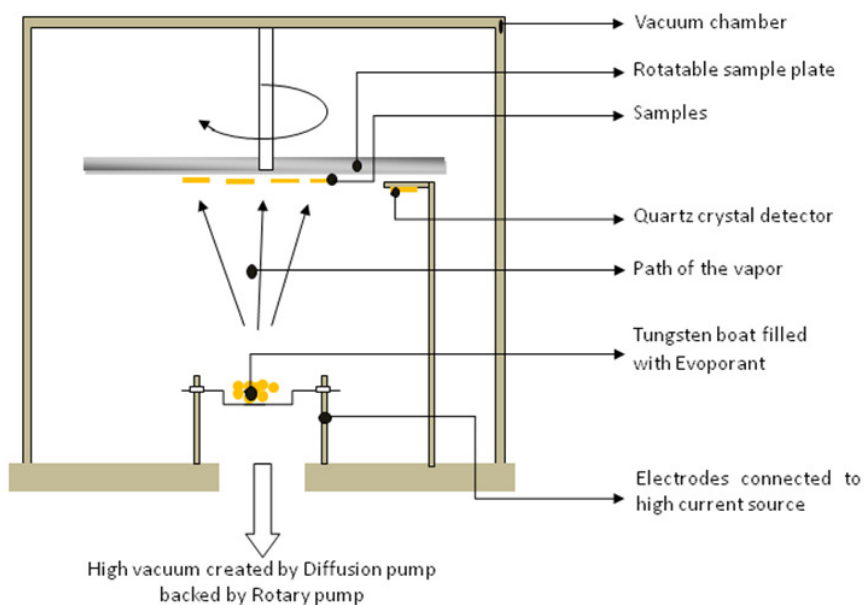
Figure 5.18 Schematic representation PVD process cell

5.2.2 Results and discussion

5.2.2.1 Thermal study

Thermal analysis was performed on the PVD membrane in order to investigate the interaction between the polymer and the metal particles. Thermograms were recorded during heating at a controlled rate to evaluate their thermodynamic properties. Sample

was heated from 35 °C to 600 °C at the rate of 10 °C/min. Figure 5.19 shows that, the deposition of aluminium increased the T_g of the membrane. T_g of PSf was 195 °C whereas PVD membrane showed T_g of 265 °C (Table 5.2).
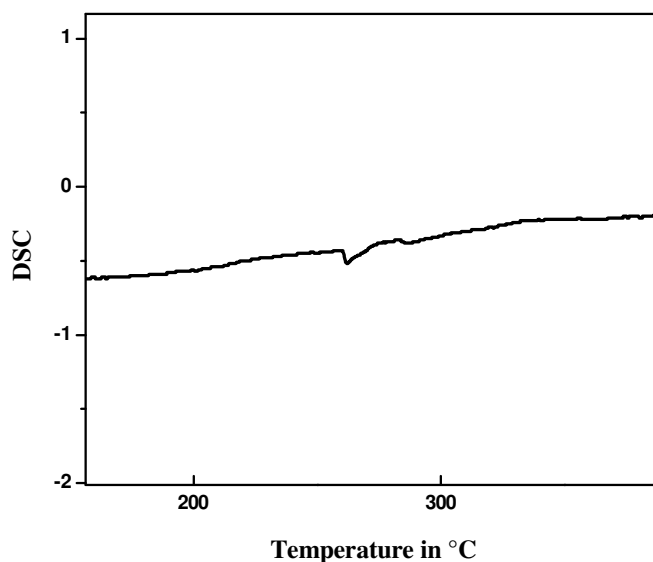
Figure 5.19 DSC curve of membrane

5.2.2.2 Water swelling and contact angle measurement

Contact angle is an important parameter for measuring the surface hydrophilicity, lower contact angle indicates the hydrophilic nature of the membrane. As shown in Table 5.2, the PVD membrane showed more contact angle i.e., 89.45° whereas, PSf membrane showed 66.84°. Deposition process increased the roughness on the membrane surface which increased the contact angle.

Table 5.2 Water uptake, contact angle and T_g of membranes

Membrane	Water uptake in %	Contact angle °	T_g
Before PVD	54	66.84	195° C
After PVD	33	89.94	265° C

Water swelling study is very important to the water filtration membranes. PSf membrane showed more water uptake than the PVD membrane. In PSf membrane, pores

are in micro size hence water can easily enter into the pores. Whereas in PVD membrane, pores are reduced to smaller size resulting in smaller water uptake.

5.2.2.3 Surface morphology of the membrane

AFM pictures showed more roughness (Figure 5.20 (**a–d**)) on the PVD membranes than the PSf membrane. The comparison of Figure 5.20 **a** and **b** showed the deposition of the aluminium on the membrane pores. In Figure 5.20 **a**, pores were clearly noticeable whereas, in Figure 5.20 **b** pores were not observed. Figure 5.20 (**c**, **d**) shows the roughness of the membranes.
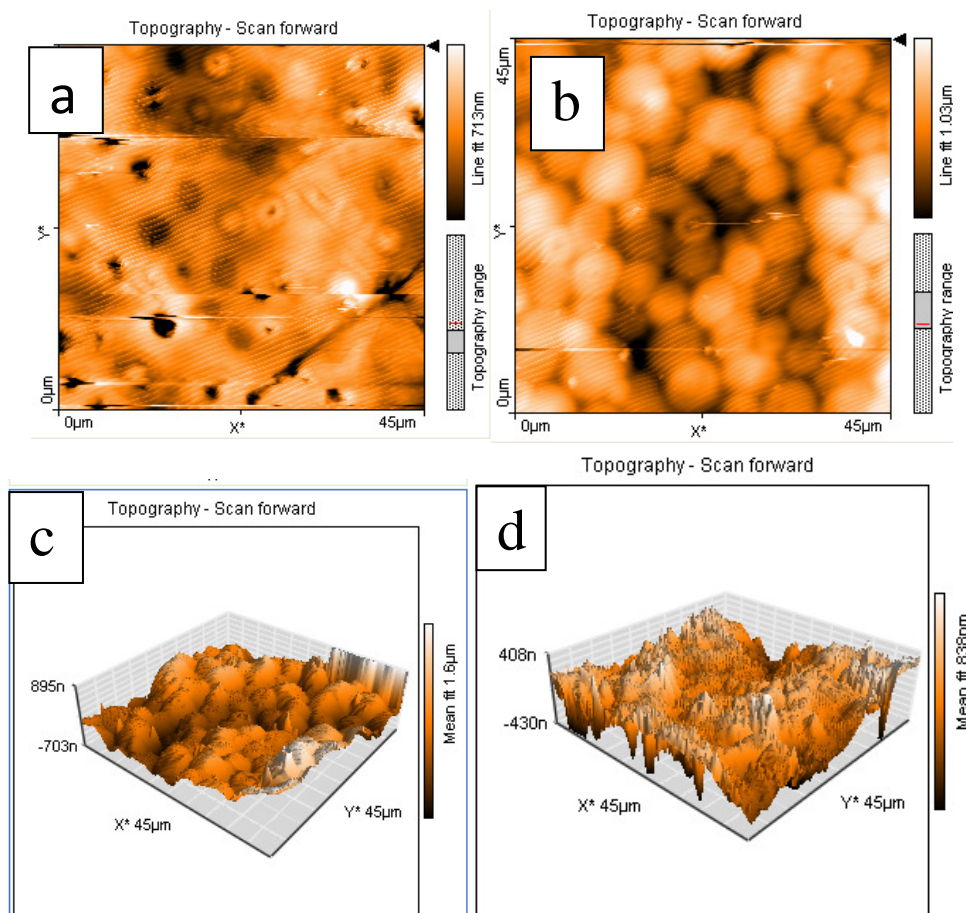
Figure 5.20 (**a**) AFM images showing surface profile of PSf membrane (**b**) AFM image showing surface profile of PSf membrane after PVD (**c**) 3D AFM of PSf membrane after PVD (**d**) 3D AFM of PSf membrane

Figures 5.21 (**a-e**) shows SEM images of the PVD membrane. SEM pictures clearly showed that, micro pores were filled with aluminum thereby reducing the pore size of the membrane. Before deposition of metal, the pore size was above 100 nm but after deposition the pores were filled with aluminum increasing the mechanical strength and reducing the pore size.
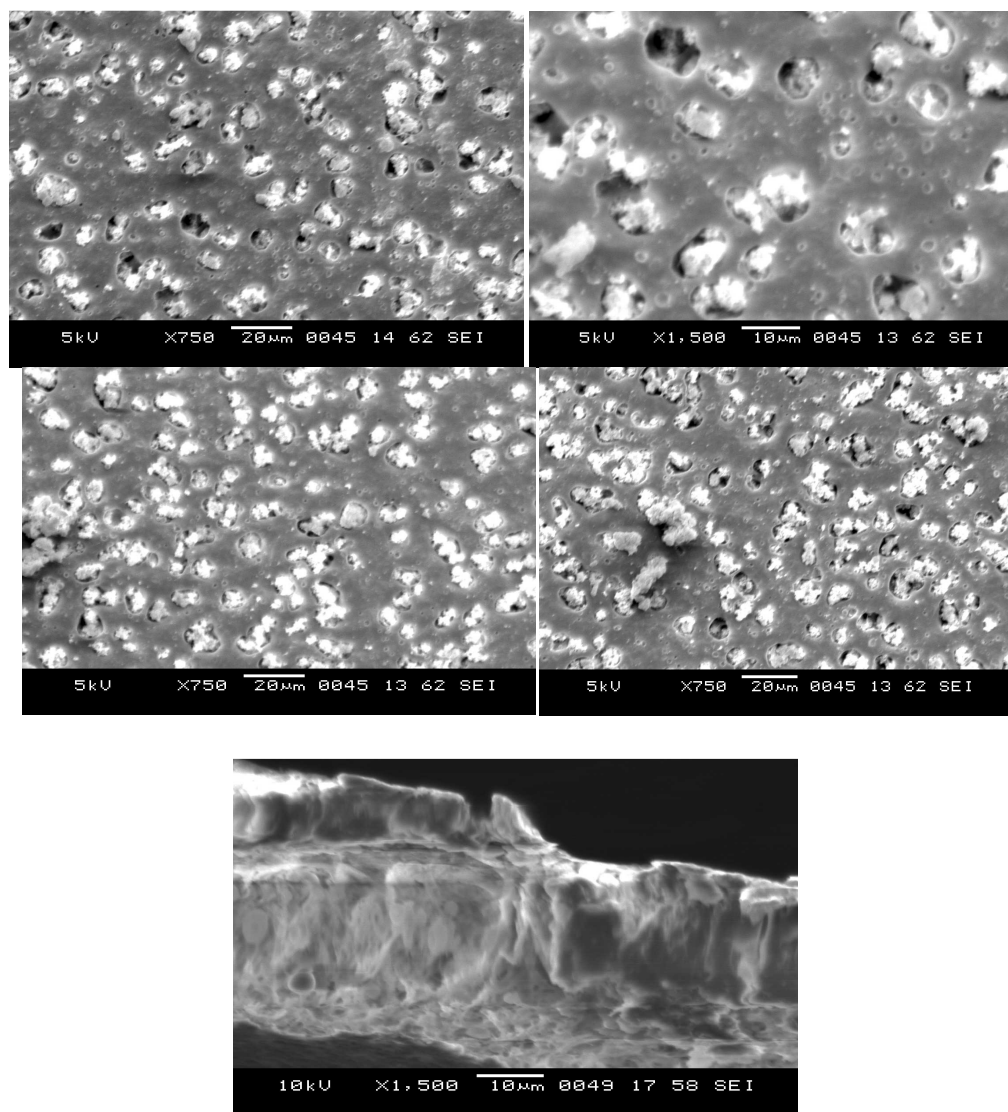
Figure 5.21 (**a-e**) SEM images of membranes

This also changed the shape of microvoids along with changes in the thickness of the membrane. Average thickness of the membrane was approximately (107±20) μm whereas, after deposition it was increased to (125±20) μm, i.e., an increase of 15–19 % of thickness was observed. Cross section image of the membrane clearly showed distribution of the aluminum particles in the microvoids.

5.2.2.4 Performance study of the membrane

Pure water flux was obtained by measuring the flux for pure water against operating pressure. As shown in Figure 5.22, the flux increased linearly with the operating pressure. This linear behavior is described by a slope close to pure water permeability, according to the Spiegler–Kedem model. The hydraulic permeability coefficient of the PSf membrane is $1.10324 \cdot 10^{-10}$ m/sPa. After PVD, it decreased to $9.141 \cdot 10^{-12}$ m/sPa. Hence exhibited NF membrane's permeation.
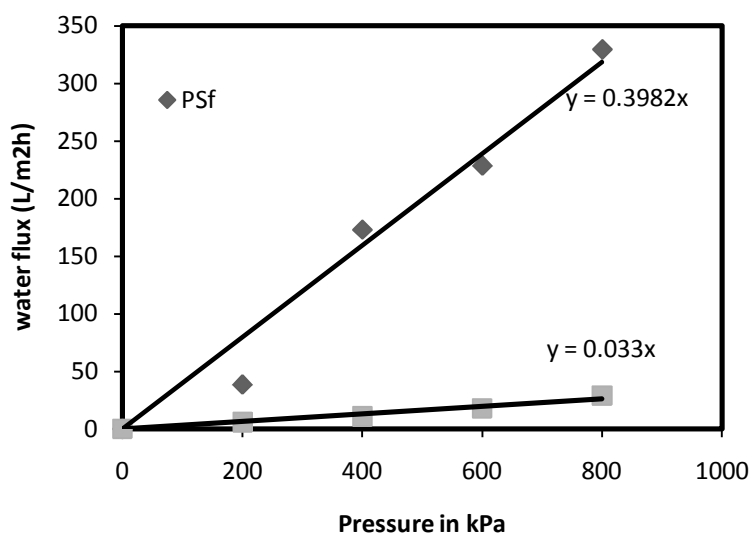
Figure 5.22 Water flux of membranes

Performance study of the membrane was carried out by dead end flow cell, with 3500 ppm of NaCl solution at different pressures ranging from 2 to 8 bar. Figure 5.23 represents the rejection and flux of PVD membrane. The membrane showed rejection and flux of 42.22 % and 16.4 L/m^{2}h respectively at 2 bar pressure. SEM images of membrane clearly showed the insertion of aluminium into the pores thereby reducing the pore size

resulting in more rejection and less flux. Due to size exclusion principle, smaller sized water molecule permeates into the membrane and NaCl particles are rejected. Surface roughness is a major factor which decides the performance of the membrane. If roughness is more, rejection is also more as evident from AFM images and rejection results. Increase in the pressure decreased the salt rejection with simultaneous increase in flux. Results clarified that, increase in flux decrease the salt rejection.
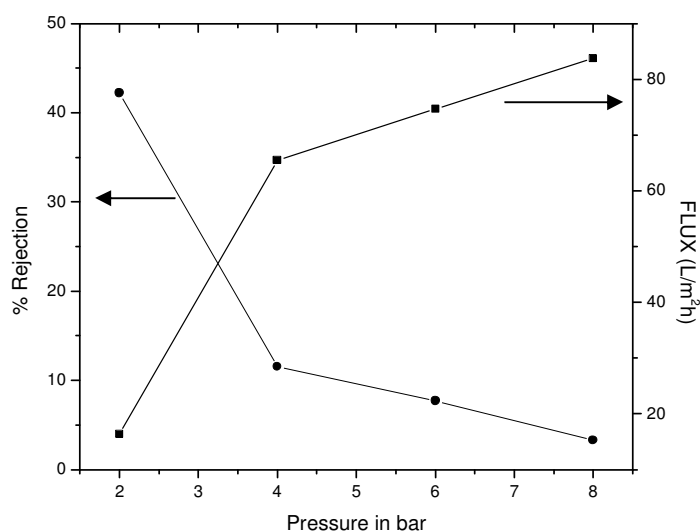
Figure 5.23 Salt rejection and flux of membrane

5.2.3 Conclusions

The prepared polysulfone microporous membrane was converted into nanoporous membrane by depositing aluminium metal. The physical vapor deposition method changed the hydrophobicity of the polysulfone membrane which was evident from the change in the contact angle from 66.84 ° to 89.49 °. This was confirmed by SEM images, AFM study and also by the DSC measurements. Aluminium coated membrane possessed higher T_g value, indicating the elevated thermal stability of the treated membrane. Moreover there is a significant increase in the selectivity of the salt ions. This is one of the best methods for the preparation of nanofiltration membranes and surface modification. Further research in this area may lead to revolution in membrane surface. modification.

5.3 ION BEAM MODIFICATION OF POLYSULFONE/ N-PHTHALOYL CHITOSAN MEMBRANE PERFORMANCE

Ion beam irradiation has long been recognized as an effective method for the synthesis and modification of diverse materials, including polymers (Davenas et al. 1989 and Xu et al. 1995). Ion beam irradiation involves bombardment of a substance with energetic ions. When the ions penetrate through the surface of a membrane, they eliminate the tall peaks and deep valleys resulting in an overall reduction in surface roughness (Xu et al. 1995). As the ions penetrate the membrane, they lose energy to their surroundings (membrane structure) by two main processes: interacting with target nuclei (nuclear stopping) and interacting with target electrons (electronic stopping) (Xu & Coleman 1997). Nuclear stopping energy losses arise from collisions between energetic particles and target nuclei. Atomic displacement occurs when the colliding ion imparts energy greater than certain displacement threshold energy. If the energy is not great enough for displacement, the energy dissipates as atomic vibrations known as phonons (Schwabel 2008). Electronic stopping energy losses arise from electromagnetic interaction between the positively charged ions and the target electrons. Excitation and ionization are two common forms of electronic energy loss. Excitation is the process in which an electron jumps to a higher energy level, while in ionization, an orbital electron is ejected from the atom.

The intensive energy deposition in polymers can lead to the following:

1. Formation of volatile molecules and free radicals which leave defects in the polymer matrix
2. Creation of additional cross-linking between polymer chains
3. Formation of new chemical bonds and
4. Chemical reactions with chemical atmosphere such as oxidation (Lee 1999).

These four events in turn lead to membrane microstructure alterations. Studies examining the effects of ion beam irradiation on water separation membranes are significantly fewer since this application is recent. These studies investigated effects of

ion beam irradiation on the performance of commercial nanofiltration membranes. Specifically, these studies focused on monovalent cations, divalent cations, dissolved organic carbon (DOC) and bacteria.

Membrane performance was evaluated by measuring permeability, selectivity and fouling. Irradiation of sulfonated polysulfone membrane revealed similar removal characteristics for all raw water components with the exception of DOC that had its removal significantly higher in comparison with unmodified membrane. There was an insignificant decrease in membrane flux, while the resistance to fouling was improved. Irradiation of a polyamide membrane caused slight reduction in selectivity for monovalent cations with slight improvement for divalent cations and dissolved organic carbon. While selectivity slightly increased, the increase in membrane permeability suggested that a shift of permeability/selectivity membrane-characteristic curve occurred due to irradiation (Xu & Coleman 1997, Good et al. 2002).

Liu et al. (2007) prepared Poly(vinylidene fluoride) (PVDF) membrane, pre-irradiated by electron beam and then poly(ethylene glycol) methyl ether methacrylate (PEGMA) was grafted onto the membrane surface in the aqueous solution (Figure 5.24). The degree of grafting was significantly influenced by the pH value of the reaction solution. The surface and bulk hydrophilicity were evaluated on the basis of static water contact angle, dynamic water contact angle and the dynamic adsorption process. Furthermore, relative high permeation fluxes of pure water and protein solution were obtained. All these results demonstrate that both hydrophilicity and fouling resistance of the PVDF membrane can be improved by the immobilization of hydrophilic comb-like polymer brushes on the membrane surface.
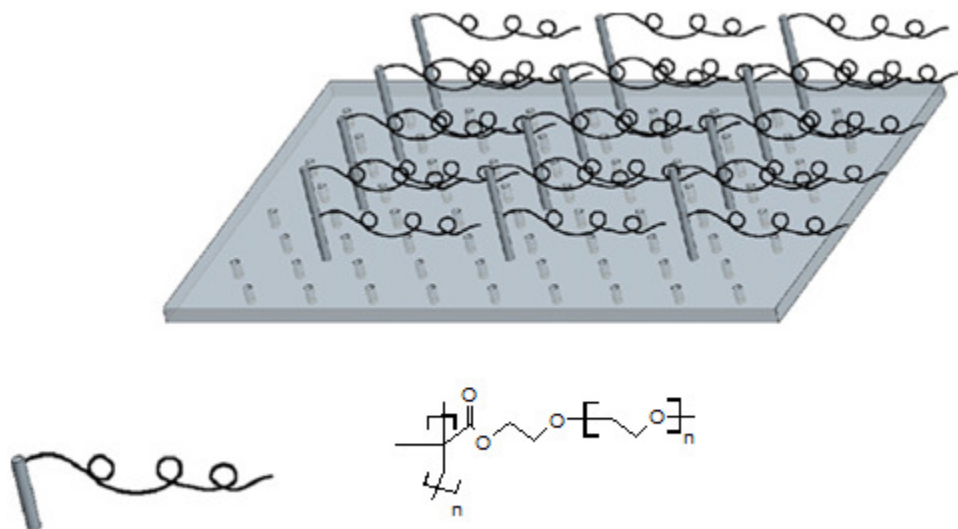
Figure 5.24 Grafting of PEGMA on PVDF membrane

(Source: Liu et al. 2007)

Ishikawa et al. (2007) proposed a novel technique of low-energy N_2 neutral beam (NB) (<10 eV) irradiation and investigated it as a means of controlling the surface nitridation of self-assembled monolayers (SAMs). This low-energy process without UV photons was able to nitride the surfaces of terphenyl SAMs. Furthermore, by varying the on/off period of irradiation, a pulse-time modulated NB process could be used to control the atomic ratio of nitrogen in terphenyl molecules. Time-of-flight secondary ion mass spectra revealed that hydrogen in the terphenyl group was substituted by a -NH_2 group because of irradiation by N_2 beam (Figure 5.25). The data suggested that the low-energy NB technique caused less damage to modified surfaces than the conventional plasma process. Therefore, it is a potential damage-free process for modifying the surfaces of soft organic materials and films.
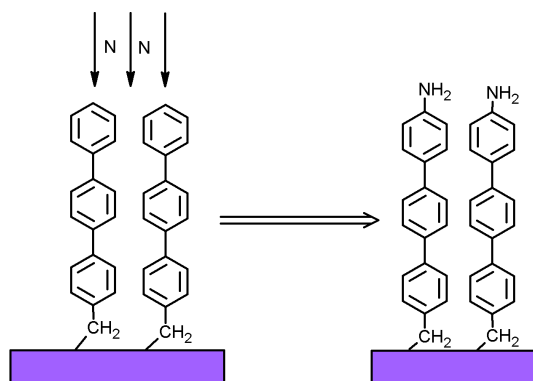
Figure 5.25 Schematic representation of formation of amine group by nitrogen irradiation (Source: Ishikawa et al. 2007)

Linggawati et al. (2012) studied effect of electron beam on Nylon-66 membrane. Nylon-66 contains functional groups which form hydrogen bonds with inorganic silica networks and allow the creation of hybrid membranes. As a typical semicrystalline polymer, nylon-66 can be cross-linked through electron beam (EB) irradiation to form nanofiltration membranes. The effect of aminopropyltriethoxylsilane (APTEOS) and EB irradiation on the physical and separation properties of nylon-66 membranes were studied. Nylon-66 membrane with 10 wt % of APTEOS irradiated at 70 kGy exhibited satisfactory permeability, excellent removal of neutral solutes and improved rejection of divalent ions as a result of improved membrane pore size and ratio of membrane thickness to porosity.

Hegde et al. (2010) reported synthesis and desalination performance of Ar^+ and N^+ irradiated polysulfone based new NF membrane. Polysulfone and poly(1,4- phenyl-ether-ether sulfone) membrane surface was irradiated by cold plasma and their properties were studied. N^+ irradiated membranes showed better performance than Ar^+ irradiated membrane because, they showed relatively larger dielectric properties indicating greater void volume.

Wanichapichart et al. (2012) studied chain scission and anti fungal effect of electron beam on cellulose membrane. Two types of bacterial cellulose (BC) membranes were produced under a modified medium using sucrose as a carbon source, with and

without coconut juice supplement. After being irradiated with electron beams under oxygen limited and ambient condition, water contact angle of the irradiated membrane increased from 30° to 40°. Irradiation under oxygen ambient condition showed higher contact angle. In comparison with the control membranes, irradiated membrane showed smaller water flux indicating a reduction of membrane pore area.

In light of these observations, it was decided to study the effect of N^+ beam on membranes. PSf:NCS blend membranes were prepared and irradiated with N^+ with an aim to improve the membrane performance.

5.3.1 Experimental

5.3.1.1 Preparation of blend membranes

Membranes were prepared by phase inversion method. PSf (Sigma Aldrich, 35000 Da) and the prepared NCS with percent composition of 95:05 were dissolved in NMP (N-methylpyrrolidone) at 60°C for 24 hrs to get clear homogenous solution. The obtained viscous solution was filtered by G4 sand filter before casting. The membrane was made by casting the solution on a glass plate. The thickness of the wet membrane was maintained at 0.2 mm. It was then evaporated at 25±1°C for 30 seconds and immersed in a coagulation water bath for 30 min. Demixing of solvent in coagulation bath resulted in separation of the membrane. The membrane was washed with distilled water and stored in distilled water for further characterization.

5.3.1.2 Ion beam irradiation

The membranes were dried at room temperature for 24 hrs and were used for ion beam bombardment. Figure 5.26 shows schematic representation of ion beam irradiation cell. The procedure was followed as described in manuscript of Wanichapichart and Yu (2007) (Wanichapichart et al. 2012). Square sample of the membranes of a size of about 5×5 cm^2 were bombarded with nitrogen ion (mixed 20 % N^+ and 8 % N^{2+}) accelerated by 60 kV to several doses, ranging from $1.5\text{-}14 \times 10^{14}$ ions/cm^2 in vacuum with a pressure of 10^{-14} Pa. The range of nitrogen ion at given energies (60 keV and 100 keV) was estimated

using the profile code and found to be between 300 and 500 nm. The sputtering at the given doses was negligible and hence the implanted ions were stopped within the thickness of the membrane.
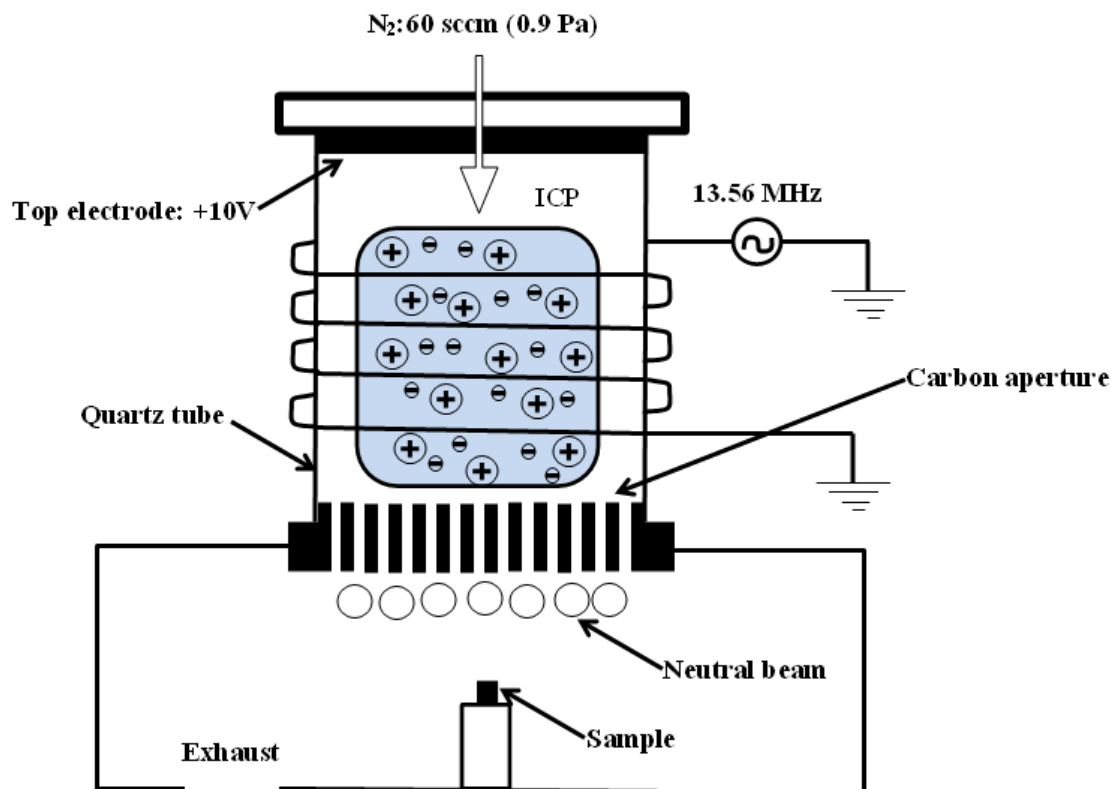
Figure 5.26 Schematic representation of ion beam irradiation unit

5.3.2 Results and discussion

The membrane surface morphology and roughness were investigated. AFM images in Figure 5.27 (**a-f**) shows the membrane surface morphology. In all the surface images, the pores were noticeable. After ion bombardment, the surface generally becomes rough. The N^+ ion irradiated membrane using 100 keV showed more roughness than others. The membrane surface roughness was increased with increasing ion fluence, however surface roughness normally decreased with increasing ion energy. But in this case, the increase of the ion energy increased the surface roughness. This change is more obvious in ion bombardment. It is known that the sputtering yield depends on both ion species and target material. From the results, it was seen that the membrane surface morphological change

was more influenced by ion energy and also nitrogen ion. The result implies that the ion-bombardment roughened surface creating more surface area and making it more active.
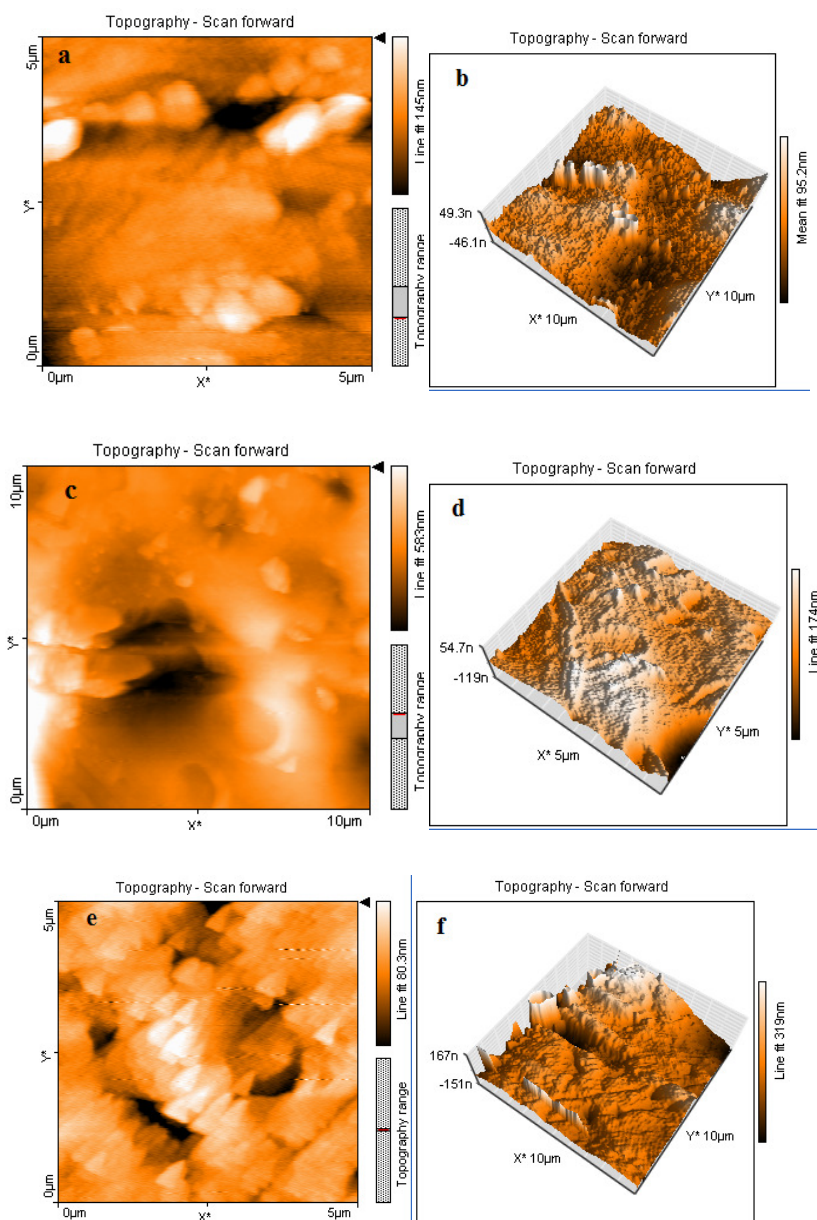
Figure 5.27 AFM images (**a**) surface of the PSf:NCS 95:05 membrane (**b**) 3D of PSf:CS 95:05 membrane (**c**) surface of N^+ ion irradiated membrane using 60keV (**d**) 3D of N^+ ion irradiated membrane using 60 keV (**e**)Surface of N^+ ion irradiated membrane using 100 keV (**f**) 3D of N^+ ion irradiated membrane using 100 keV.

Pure water permeability was obtained by measuring the flux for pure water against operating pressure. As shown in Figure 5.28, the flux increases linearly with the operating pressure. The membrane irradiated with higher energy of 100 keV showed lowest water flux and hydraulic permeability coefficient. The hydraulic permeability coefficient of the membrane has been shown in Table 5.3. It can be explained that the membrane pore size decreased by increase in the surface roughness thereby leading to large surface area. To confirm the surface area, dielectric constant of the membranes were studied.

Table 5.3 Hydraulic permeability coefficient of membranes

Membrane	L_p in (m.S^{-1}.Pa^{-1})
PSf:CS 95:05	8.47×10^{-12}
N$^+$ 100 keV	7.47×10^{-12}
N$^+$ 60 keV	9.91×10^{-12}

Figure 5.29 represents the dielectric spectra which are independent of the frequencies between $0\text{-}3 \times 10^6$ Hz. Among the three membranes, low energy irradiated (60 keV) membrane possesses the smallest dielectric constant. The membrane which was bombarded with higher energy (100 keV) possessed the greatest value. The highest dielectric constant represented larger area of the membrane and this was verified by the smallest water flux shown in Figure 5.28.

As reported before, porous PSf:NCS 95:05 membrane possessed weak cationic charges. Further implementation of N$^+$ ions using high energy beams strengthened the surface charges or changed its surface property. To verify this hypothesis, filtration of NaCl solution was done using all three membranes. Figure 5.30 (**a**), (**b**) and (**c**) showed the salt rejection of the PSf:CS 95:05, N$^+$ 100 keV and N$^+$ 60 keV respectively.

The salt rejection of the N$^+$ beam irradiated with 100 keV showed same rejection as PSf:NCS 95:05 membrane at 200 kPa pressure but permeate flux of NaCl solution was more in the N$^+$ beam irradiated membrane. Increase of pressure, decreases the rejection
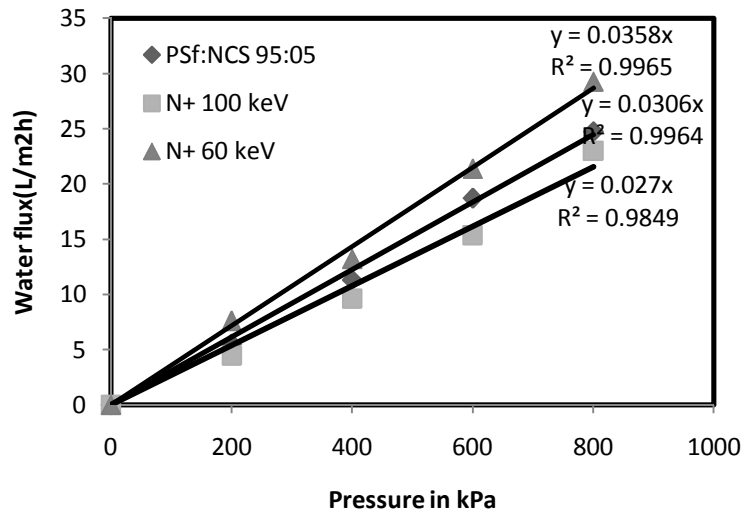
Figure 5.28 Water flux of membranes before salt rejection
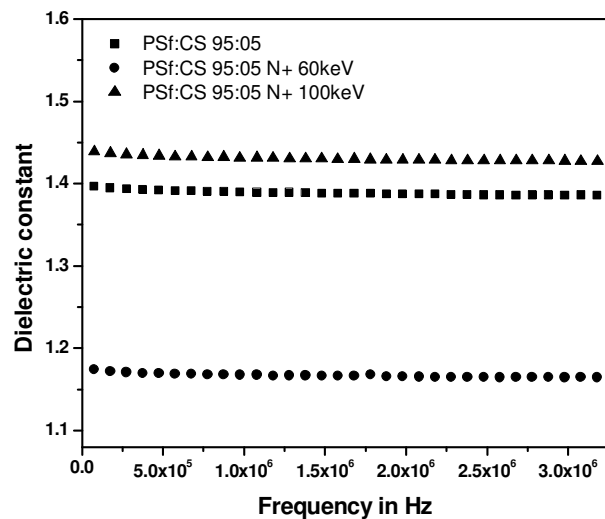
Figure 5.29 Dielectric constant of membranes before rejection

and increased the permeate flux. This effect was attributed to shortening of the polymer chain, as similar effect was observed in Polyethylene terphthalate (PET) membrane (Drabik et al. 2007). 60 keV irradiated membrane showed low rejection than the other two membranes.
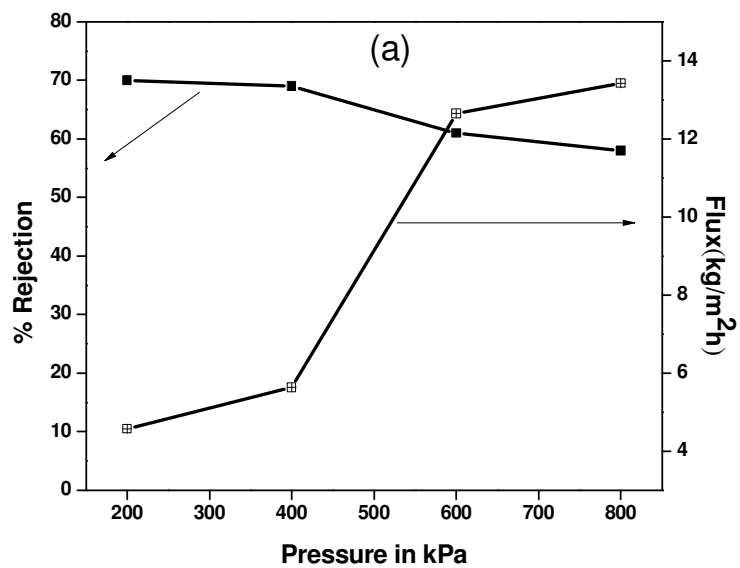
Figure 5.30(**a**) Salt rejection and flux of PSf:CS 95:05 membrane
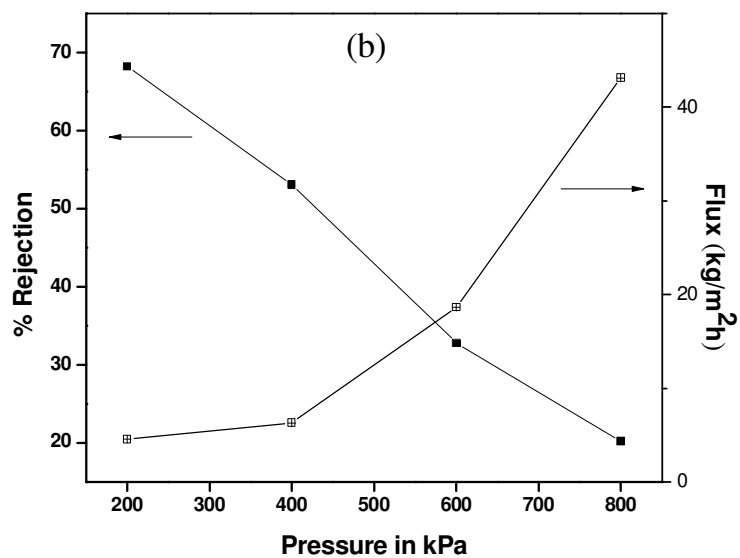
Figure 5.30(**b**) Salt rejection and flux of N$^+$ 100 keV membrane
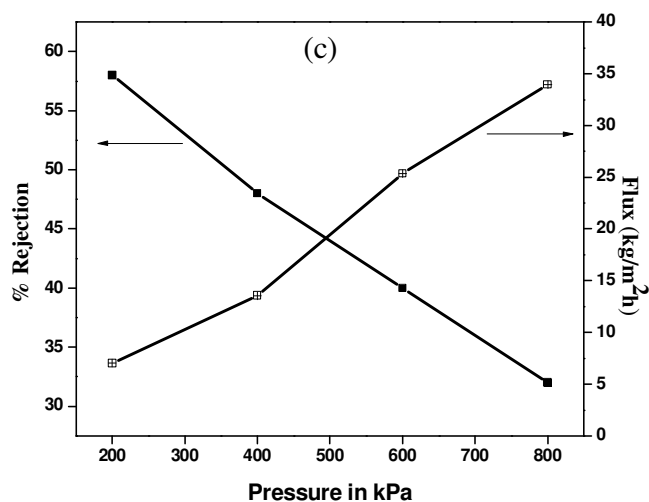
Figure 5.30(**c**) Salt rejection and flux of N$^+$ 60 keV membrane
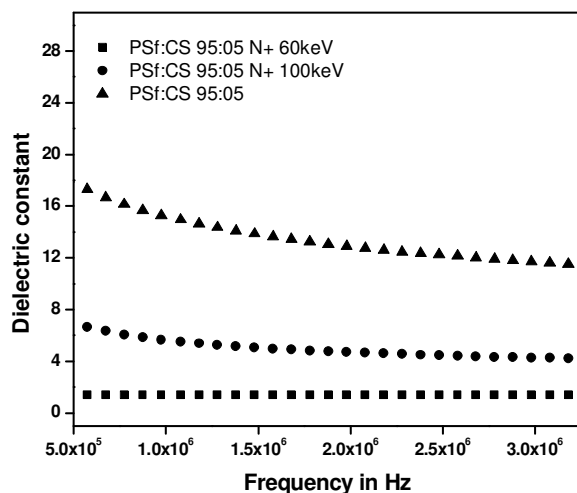
Figure 5.31 Dielectric constant of membranes after rejection

The beam irradiated membranes showed decrease in salt rejection with increase in permeate flux with respect to increase in pressure which was due to increase in pore size. To confirm the increase in the pore size of the membrane, the membrane which was used for salt rejection was reused for the study of water flux and dielectric constant.
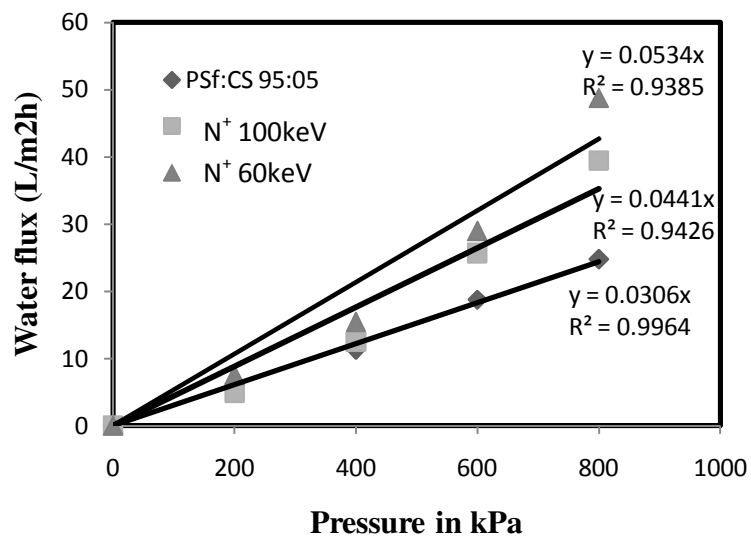
Figure 5.32 Water flux of membranes after salt rejection

Figure 5.31 and Figure 5.32 shows dielectric constant and water flux of the used membrane respectively. Water flux increases and dielectric constant decreases as compared to the unused membrane. Increasing flux indicated increase in the pore size and decrease in the dielectric constant indicated smaller surface area. This is because initially the ions shorten the polymer chain and later they get deposited on surface to block the pores. When the pressure is increased the ions pass into the pores thereby increasing the pore size.

5.3.3 Conclusions

Nitrogen beam of 60 keV and 100 keV could modify Polysulfone:N-Phthaloyl chitosan 95:05 membrane surfaces. Surface roughness was measured by AFM and roughness was more in 100 keV beam irradiated membrane. Beam irradiation leads to higher hydrophilicity in terms of water flux. At lower pressure increase in rejection and decrease in flux was observed however that trend reversed with increase in pressure. The lower energy beams of N^+ ions acted as a scissors in the membranes leading to increase in water permeation and decrease in salt rejection.

Abstract: This provides the summary of the work presented in the thesis along with the conclusions and scope for further development in the field of membrane filtration.

6.1 SUMMARY AND CONCLUSIONS

Present work emphasize on the synthesis of novel polymers and polymer modification. These polymers are being used for the membrane preparation. Also this work focuses on surface modification of the membrane in order to increase its performance. The following polymers were prepared and blend with polysulfone for the preparation of membranes.
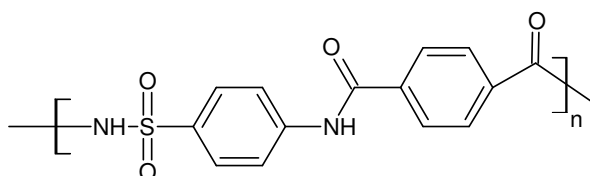
Polysulphonylaminobenzamide (PSAB)
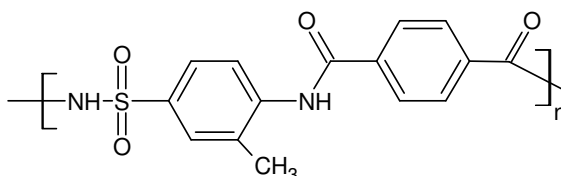
Methylated polysulphonylaminobenzamide (mPSAB)
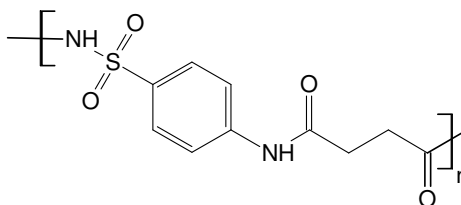
Poly[(4-aminophenyl)sulfonyl]butanediamide (PASB)
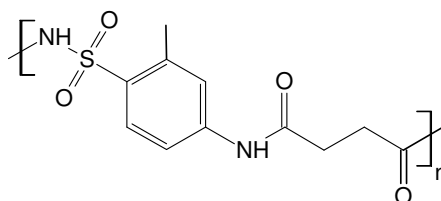
Methylated Poly[(4-aminopheonyl)sulfonyl]butanediamide (mPASB)

Figure 6.1 Structures of novel polymers

Initially Polysulphonylaminobenzamide:Polysulfone membranes showed Molecular weight cut off of 1000 Da. Enhanced hydrophilicity was confirmed by water uptake and contact angle measurement. Highest water uptake was observed in acidic and basic pH as compare to neutral water. This was attributed to unstability of amide and sulfonamide bond in extreme acidic and basic pH which led to more porosity or increased pore size. Membranes performed excellently for the desalination of salt water. The salt rejection of the membrane was enhanced in an effective manner. The decreasing trend was noticed for salt rejection in acidic and basic pH. Also, decrease in rejection was observed with dilution of feed sample.

Poly[(4-aminophenyl)sulfonyl]butanediamide:Polysulfone membranes were hydrophilic and showed good resistance towards high pressure and pH. The hydrophilicity was confirmed by water uptake and contact angle. Membranes were found to be stable at different pH values and showed 1000 Da Molecular weight cut off. No changes were observed in water uptake in acidic and basic pH. Membranes have performed appreciably for desalination. The membrane methylated Poly[(4-aminophenyl)sulfonyl] butanediamide:Polysulfone 90:10 showed 74 % of rejection and Poly[(4-aminophenyl)sulfonyl]butanediamide:Polysulfone 60:40 showed 40 % rejection of NaCl solution. A steady rejection trend was witnessed at all pressures. From our current study, it was very clear that the pore size of the membranes played vital role in the performance of the membrane.

Next chapter emphasis on the modification of chitosan and preparation of polypropylene support membrane. Chitosan is a biomaterial which is environmentally safe. It is hydrophilic in nature and is extensively used for water purification. However, its use is limited because of its inability to get dissolved in organic solvents. Hence, N-Phthaloyl chitosan was prepared from Chitosan to improve its solubility in organic solvent so that it can be easily blend with some other polymers like polysulfone. Initially, N-Phthaloyl chitosan membranes were prepared to study the properties but the prepared membranes were not mechanically strong. In order to increase the mechanical strength of

N-Phthaloyl chitosan, polypropylene supported N-Phthaloyl chitosan membrane was prepared and also the properties were compared with the polypropylene supported Chitosan membrane. Even though the hydrophilicity of the N-Phthaloyl chitosan membrane was quite good, its performance was less effective. With this basic knowledge of modified Chitosan, it was decided to prepare N-phthaloylchitosan and polysulfone blend membranes to increase the performance of the membrane.
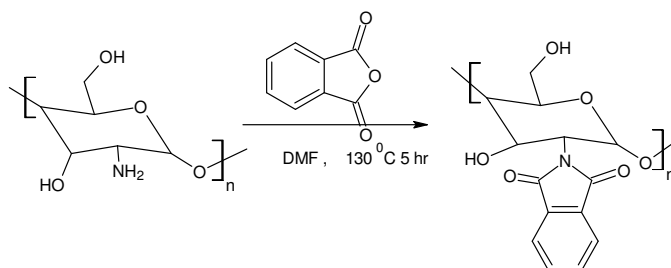
Figure 6.2 Preparation of N-Phthaloyl chitosan

Blend membranes performed in the range of nano to ultra-filtration with respect to concentration of N-Phthaloyl chitosan. The increase in N-Phthaloyl chitosan content made membrane more and more hydrophilic in nature, leading to better water swelling and enlargement in pore size. In addition, the membrane swelling property was observed to be pH dependent. The smallest swelling occurred at pH 3 and was maximized to 65 % at pH 5. Polysulfone:N-Phthaloyl chitosan 95:05 and 90:10 membranes were categorized as nanofiltration membranes with 95 % of $MgSO_4$ rejection, 78 % of Na_2SO_4 rejection and 75 % of NaCl rejection. The Polysulfone:N-Phthaloyl chitosan 85:15 and 80:20 were classified as ultra-filtration membranes with much smaller rejection for the above salts.

To create the negative charge on the membrane surface, sulfonated polysulfone was used as a blend material. Sulfonation of polysulfone was done by using chlorosulfonic acid as sulfonating agent. The degree of sulfonation and ion exchange capacity was determined by titration method. Further charge confirmation was done by diffusion potential study using self-constructed cell.
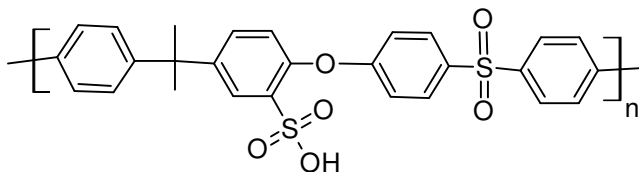
Figure 6.3 Sulfonated polysulfone

Membrane diffusion potential and Ion exchange capacity of the membrane confirmed that the prepared membrane had negative surface charge. Hydrophilicity and membrane charge was greatly affected by sulfonation of polysulfone and increased with the sulfonate polysulfone concentration. Hydrophilicity of the membrane was studied by water swelling test and contact angle measurement. Membrane with 60:40 (sulfonated polysulfone:N-Phthaloyl chitosan) composition showed 1000 Da of molecular weight cutoff. It was observed that, increase in the concentration of sulfonatedPolysulfone decreases the molecular weight cutoff. Using these experimental data, it was concluded that the concentration of sulfonated polysulfone affected the performance of the membrane.

There are three main areas of interest when it comes to improving membrane performance: the synthesis process, the application process and post-synthesis modification (surface modification). Improvement by Synthesis process involves the techniques, methods and materials of manufacturing processes to produce high performance membrane. The application process involves the specific operating parameters for a membrane system. These include selecting the feed solution characteristics, operating pressure and cleaning intervals to allow the system to operate at maximum efficiency. Post-synthesis modification (surface modification) involves modifying the membrane after completion of the synthesis of polymers.

In present work, three different type of post-synthesis modification was done namely chemical modification, vapor phase deposition and N^+ beam irradiation.

In chemical modification, Polysulfone and Poly isobutylene-alt-maleic anhydride blend membrane were prepared and treated with alkali solution to break anhydride group

into acid groups. These acid groups created negative charge on the membrane surface. The surface charge was confirmed by ion exchange capacity measurement. This increased the hydrophilicity as well as selectivity of the membranes.
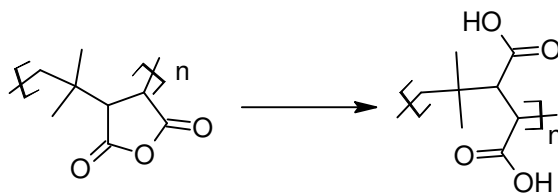
Figure 6.4 Hydrolysis of Poly isobutylene-alt-maleic anhydride

Membranes before alkali treatment showed less salt rejection and flux. However, alkali treatment resulted in hydrolysis of the anhydride group into acid groups which imparted charge onto the membranes surface. Among the tested salt solutions, Na_2SO_4 showed maximum salt rejection due to the charge interaction. Hydrolysis of anhydride groups by alkaline treatment is an interesting method for increasing the flux and salt rejection of NF membranes.

In vapor phase deposition, the microfiltration membrane was converted into nanofiltration membrane by depositing the Aluminum metal on to membrane surface. Due to metal deposition micro pores were blocked, as a result of which the effective pore size was reduced. This is a novel method which is applicable to reduce the membrane pore size. There was significant increase in salt rejection. This is one of the best methods for preparation of nanofiltration membranes via surface modification.

The N^+ beam irradiation is another process for post-synthesis modification technique. Polysulfone and N-phthaloyl chitosan membrane was used for N^+ beam irradiation. The effects of ion beam irradiation on surface morphology, selectivity and productivity was studied. Beam irradiation leads to higher hydrophilicity which was witnessed by water flux study. The lower energy beam of N^+ ions however, acted as a scissor in the membranes leading to an increase in water permeation and decrease in salt rejection.

6.2 SCOPE FOR THE FUTURE WORK

The increasing demand of more and more cost effective and compact materials has led to a tremendous growth of membrane industry. Synthesis of novel polymer, polymer grafting and surface modification phenomenon such as those studied in the present work, are opening pathways for efficient fictionalization of membranes. The art of membrane technology encompassing synthesis of novel polymers, blending with commercially available polymers and surface modification of membrane is rapidly being taken up as research challenge by many membrane scientists around the globe. As per the requirement, preparation of membranes using novel polymers and their surface modification with exciting novel properties and functionalities can be explored. Keeping these factors in view, the scope of present work can be extended to following experiments.

1. To study phase inversion process using phase diagrams.
2. To study bio-fouling of the membranes.
3. Preparation of mixed matrix or composite membranes for synergistic combination of different functions using different (polymeric and inorganic) materials.
4. Insertion of nanoparticales to improve membrane property.
5. To study the rejection of heavy metal ions.
6. Some of the prepared charged membranes can also be extended for fuel cell applications.

REFERENCES

Aerts, P., Greenberg, A. R., Leysen, R., Krantz, W. B., Reinsch, V. E. and Jacobs, P. A. (2001). "The influence of filler concentration on the compaction and filtration properties of Zirfon®- composite ultrafiltration membranes." *Separation and Purification Tech.,* 22-23, 663-669.

Amiji, M. (1995). "Permeability and blood compatibility properties of chitosanpoly (ethylene oxide) blend membranes for hemodialysis." *Biomaterials*, 16, 593–599.

Amini, M., Homayoonfal, M., Arami, M. and Akbari, A. (2009). "Modification and characterization of prepared polysulfone ultrafiltration membranes via photografted polymerization: Effect of different additives." *Desalination and Water Treatment*, 9, 43-48.

Ang, A.K.S. (2000). "Low-temperature graft copolymerization of 1-vinyl imidazole on polyimide films with simultaneous lamination to copper foils—effect of crosslinking Agents." *Polymer*, 41, 489–498.

Anita, S., Chan, W., Micheal, W. and Cecile, M-J. (2009). "Self-assemble of alternating copolymers and the role of hydrophobic interactions; charecterisation by molecular modeling." *Molecular Simulations. 1*, 1-9.

Arthanareeswaran, G. and Starov, V.M. (2011). "Effect of solvents on performance of polyethersulfone ultrafiltration membranes: Investigation of metal ion separations." *Desalination*, 267, 57–63.

Bargeman, G., Vollenbroek, J.M., Straatsma, J., Schroën, C.G.P.H. and Boom, R.M. (2005). "Nanofiltration of multi-component feeds. Interactions between neutral and charged components and their effect on retention." *J. Membr. Sci.*, 247, 11–20.

Bargeman, G., Vollenbroek, J.M., Straatsma, J., Schroën, C.G.P.H. and Boom, R.M. (2005). "Nanofiltration of multi-component feeds. Interactions between neutral and charged components and their effect on retention." *J. Membr. Sci.*, 247, 11–20.

Bartels, C., Mark, W., Warren, C. and Jeff, C. (2008). "New generation of low fouling nanofiltration membranes." *Desalination*, 221, 158-167.

Baruah, K., Hazarika, S., Borthakur, S. and Dutta, N. (2012). "Preparation and Characterization of Polysulfone–Cyclodextrin Composite Nanofiltration Membrane: Solvent Effect." *J. Appl. Polym. Sci.*, 125, 3888–3898.

Basri, H., Ismail, A.F. and Aziz, M. (2011). "Polyethersulfone (PES)–silver composite UF membrane: Effect of silver loading and PVP molecular weight on membrane morphology and antibacterial activity." *Desalination*, 273, 72–80.

Baszkin, A., Nishino, M. and Ter-Minassian-Saraga, L. (1976). "Solid—liquid adhesion of oxidized polyethylene films: Effect of temperature." *J. Colloid Interface Sci.*, 54, 317-328.

Baszkin, A., Nishino, M. and Ter-Minassian-Saraga, L. (1977). "Solid-liquid adhesion of oxidized polyethylene films. Effect of temperature on polar forces." *J. Colloid Interface Sci.*, 59, 516-524.

Belfer, S. (2001). "Effect of surface modification in preventing fouling of commercial SWRO membranes at the Eilat seawater desalination pilot plant." *Desalination*, 139, 169–176.

Blais, P., Carlsson, D. J., Csullog G. W. and Wiles, D. M. (1974). "The chromic acid etching of polyolefin surfaces, and adhesive bonding." *J. Colloid Interface Sci.*, 47, 636-649.

Bottino, A., Capannelli, G. and Comite, A. (2002). "Preparation and characterization of novel porous PVDF-ZrO$_2$ composite membranes." *Desalination*, 146, 35-40.

Bottino, A., Capannelli, G., D'Asti,V. and Piaggio P. (2001). "Preparation and properties of novel organic–inorganic porous membranes." *Separation and Purification Tech.*, 22-23, 269-275.

Bouranene, S., Szymczyk, A., Fievet, P. and Vidonne, A. (2007). "Influence of inorganic electrolytes on the retention of polyethyleneglycol by a nanofiltration ceramic membrane." *J. Membr. Sci.*, 290, 216–221.

Boussu, K., Vandecasteele, C. and Van der Bruggen, B. (2006). "Study of the characteristics and the performance of self-made nanoporous polyethersulfone membranes." *Polymer*, 47, 3464–3476.

Bryjak, M., Gancarz, I., Poźniak, G. and Tylus, W. (2002). "Modification of polysulfone membranes 4. Ammonia plasma treatment." *Eur. Poly. J.*, 38, 717-726.

Bryjak, M., Poźniak, G., Gancarz, I. and Tylus, W. (2004). "Microwave plasma in preparation of new membranes." *Desalination*, 163, 231-238.

Castro, A. U.S. patent 4,247,498, 1981.

Chahroudi, D. (1991). "Transparent Glass Barrier Coatings for Flexible Film Packaging." 34th Annual Technical Conference Proceedings of the Society of Vacuum Coaters 130.

Chaing, Y., Hsub, Y., Ruaan, R., Chuang, C. and Tung, K. (2009). "Nanofiltration membranes synthesized from hyperbranched polyethyleneimine." *J. Membr. Sci.*, 326, 19-26.

Chao, H.S. and Elsey, D.R. Process for preparing sulfonated poly(arylether)resins. US patent number 4,625,000; 1986.

Chen, M., Chiao, T. and Tseng, T. (1996). "Preparation of sulfonated polysulfone/polysulfone and aminated polysulfone/polysulfone blend membranes." *J. Appl. Poly. Sci.*, 61, 1205–1209.

Chennamsetty, R., Escobar, I. and Xu, X. (2006). "Polymer evolution of a sulfonated polysulfone membrane as a function of ion beam irradiation fluence." *J. Membr. Sci.*, 280, 253-260.

Dai, Q. W., Xu, Z. K. and Wu J. (2004). "A Novel Approach for the Surface Modification of Polymeric Membrane with Phospholipid Polymer" *Chinese Chem. Lett*., 15, 993-996.

Davenas, J., Xu, X.L., Boiteux G. and Sage, D. (1989). "Relation between structure and electronic properties of ion irradiation polymers." *Ncl. Instr. Meths. In Phys. Res*., 8–9, 754–763.

Deng, B., Yang, X., Xie, L., Li, J., Hou, Z., Yao, S., Liang, G., Sheng, K. and Huang, Q. (2009). "Microfiltration membranes with pH dependent property prepared from poly(methacrylic acid) grafted polyethersulfone powder." *J. Membr. Sci*., 330, 363–368.

Drabik, M., Dworkie, K., Tanczyk, R., Wasik, S. and Zuk J. (2007). "Surface modification of PET membrane by ion implementation." *Vacuum*, 81, 1348-1351.

Drioli, E. and Giorno, L. (2009). "Membrane operations." Wiley-VCH Verlag Gmbh & Co. KGaA.

Escoda, A., Fievet, P., Lakard, S., Szymczyk, A. and Deon, S. (2010). "Influence of salts on the rejection of polyethyleneglycol by an NF organic membrane: pore swelling and salting-out effects." *J. Membr. Sci*., 347, 174–182.

Fan, L., Nguyen, T., Roddick, F. and Harris, J. (2008). "Low-presure membrane filtration of secondary effluent in waste water: pre-treatment for fouling reduction." *J. Membr. Sci*., 320, 135-142.

Fievet, P., Labbez, C., Szymczyk, A., Vidonne, A., Foissy, A. and Pagetti, J. (2002). "Electrolyte transport through amphoteric nanofiltration membranes." *Chem. Engn. Sci*., 57, 2921-2931.

Fischer, D. and Eysel, H. H. (1994). "Analysis of polyethylene surface sulfonation." *J. Appl. Polym. Sci*., 52, 545-548.

Florian, E., Modesti, M. and Ulbricht, M. (2007). "Preparation and characterization of novel solvent-resistant nanofiltration composite membranes based on crosslinked polyurethanes." *Ind. Chem. Eng. Res.*, 46, 4891-4899.

Freger, V., Arnot, T. C. and Howell, J. A. (2000). "Separation of concentrated organic/inorganic salt mixtures by nanofiltration." *J. Membr. Sci.*, 178, 185–193.

Friedrich, J., Kühn, G., Mix, R. and Unger, W. (2004). "Formation of Plasma Polymer Layers with Functional Groups of Different Type and Density at Polymer Surfaces and their Interaction with Al Atoms." *Plasma Processes and Polymers*, 1, 28–50,

Gagon, D. R. and McCarthy T. J. (1984). " Polymer surface reconstruction by diffusion of organic functional groups from and to the surface." *J. Appl. Polym. Sci.*, 29, 4335-4340.

George Soney, C. and Sabu, T. (2001). "Transport phenomena through polymeric systems." *Prog. Polym. Sci.*, 26, 985-1017.

Ghosh, A. K., Ramachandhran, V., Hanra, M. S. and Misra, B. M. (2000). "Synthesis, Characterization and performance of Nitrated Polysulfone Membranes." *J. Macromolecular Sci. Part A.*, 37, 591-608.

Gong, X., Dai, L., Griesser, H. J. and W.H. Mau, (2000). "Surface immobilization of poly(ethylene oxide): Structure and properties." *J. Poly. Sci. Part B: Poly. Phy.*, 38 2323–2332.

Good, K., Escobar, I. C., Xu, X. L., Coleman M. R. and Ponting, M. (2002). "Effects of ion beam irradiation on the transport properties and fouling control of commercial membranes." *Desalination*, 146, 259–264.

Greene, G. and Tannenbaum, R. (2004). "Adsorption of polyelectrolyte multilayers on plasma modified porous polyethylene." *Appl. Surf. Sci.*, 233, 336–342.

Guan, R., Zou, H., Lu, D., Gong, C. and Liu, Y. (2005). "Polyethersulfone sulfonated bychlorosulfonic acid and its membrane characteristics." *Eur. Polym. J*., 41, 1554-1560.

Han, K., Yu, B. Y. and Kwak, S. (2012). "Hyperbranched poly(amidoamine)/polysulfone composite membranes for Cd (II) removal from water." *J. Membr. Sci.*, 396, 83–91.

Hass, G., Schroeder, H. H., and Turner, A. F. (1956). "Mirror Coatings for Low Visible and High Infrared Reflectance." *Applied Optics*, 46, 31-35.

Hegde, C., Isloor, A., Padaki. M., Wanichapichart, P. and Liangdeng, Y. (2011). "Synthesis and Desalination Performance Of, Ar^+ -N^+Irradiated Polysulfone Based New NF Membrane." *Desalination*, 265, 153-158.

Henry, S. M., El-Sayed, M. E. H., Pirie Christopher, M., Hoffman Allan, S. and Stayton Patrick, S. (2006). "pH-Responsive poly(styrene-altmaleic anhydride) alkylamide copolymers for intracellular drug delivery." *Biomacromolecules*, 7, 2407–2414.

Herber, S., Olthuis, W. and Bergveld, P. (2003). "A swelling hydrogel-based PCO2 sensor." *Sensors and Actuators B-chemical*, 91, 378-382.

Hester, J. F., Banerjee, P. and Mayes, A. M. (1999). "Preparation of protein-resistant surfaces on poly(vinylidene fluoride) membranes via surface segregation." *Macromolecules*, 32, 1643–1650.

Higuchi, A. and Nakagawa, T. (1990). "Surface modified polysulfone hollow fibers. III. Fibers having a hydroxide group." *J. Appl. Polym. Sci*., 41, 1973-1979.

Higuchi, A., Iwata, N. and Nakagawa, T. (1990). "Surface-modified polysulfone hollow fibers. II. Fibers having $CH_2CH_2CH_2SO_3-$ segments and immersed in HCl solution." *J. Appl. Polym. Sci*., 40, 709-717.

Higuchi, A., Iwata, N., Tsubaki, M. and Nakagawa, T. (1988). "Surface-modified polysulfone hollow fibers." *J. Appl. Polym. Sci*., 36, 1753-1767.

Higuchi, A., Koga, H. and Nakagawa, T. (1992). "Surface-modified polysulfone hollow fibers. IV. Chloromethylated fibers and their derivatives." *J. Appl. Polym. Sci.*, 46, 449-457.

Higuchi, A., Mishima, S. and Nakagawa, T. (1991). "Separation of proteins by surface modified polysulfone membranes." *J. Membr. Sci.*, 57, 175-185.

Hilal, N. (2003). "Photochemical modification of membrane surfaces for (bio) fouling reduction: a nano-scale study using AFM." *Desalination*, 158, 65–72.

Holmes-Farley, S.R., Reamey, R. H., Nuzzo, R., McCarthy T. J. and Whitesides, G. M. (1987). "Reconstruction of the interface of oxidatively functionalized polyethylene and derivatives on heating." Langmuir, 3, 799-815.

Hu, Z., Yin, Y., Okamoto, K., Moriyama, Y. and Morikava, A. (2009). "Synthesis of characterization of sulfonated polyimides derived from 2.2'-bis(4-sulfophenyl)-4,4'oxydianiline as polymer electrolyte membranes for fuel cell applications." *J. Membr. Sci.*, 329, 146-152.

Ishikawa, Y., Okumura, K., Ishida, T. and Samukawa, S. (2009). "Controllable modification of self-assembled monolayer surface by using N_2 neutral beam process." *J. Appl. Phys.,* 105, 094320-094326.

Cadotte, J. E. (1977). "Reverse osmosis." U S patent 4 039 440.

Jaleh, B., Parvin, P., Wanichapichart, P., Pourakbar Saffar, A. and Reyhani, A. (2010). "Induced super hydrophilicity due to surface modification of polypropylene membrane treated by O_2 plasma." *Appl. Surface Sci.*, 257, 1655–1659.

Jansen, J. C., Macchione, M. and Drioli, E. (2005). "High flux asymmetric gas separation membranes of modified poly(ether ether ketone) prepared by the dry phase inversion technique." *J. Membr. Sci.*, 255, 167-180.

Jayaraj, M. K., Draeseke, A. D., Tate J. and Sleight, A. W. (2001). "p-Type transparent thin films of CuY1−xCaxO$_2$." *Thin solid films*, 397, 244-248.

Jeon, M., Yoo, S. and Kim. C. (2008). "Performance of a negatively charged nanofiltration membranes prepared from mixtures of various dimethacrylate and methacrylic acid." *J. Membr. Sci.*, 313, 242-249.

Jia, Z. and Tian C. (2009). "Quantitative determination of polyethylene glycol with modified Dragendorff reagent method." *Desalination*, 247, 423–429.

Jin, L., Shi, W., Yu, S., Yi, X., Sun, N., Ma, C. and Liu,Y. (2012). "Preparation and characterization of a novel PA-SiO$_2$ nano filtration membrane for raw water treatment." *Desalination*, 298, 34-41.

Kaminska, K., Brown, T., Beydaghyan, G., Robbie, K., (2003). "Vacuum Evaporated Porous Silicon Photonic Interference Filters." *Applied Optics.* 42, 4212-4219.

Kato, K., Uchida, E., Kang, E. T., Uyama, Y. and Ikada, Y. (2003). "Polymer surface with graft chains." *Prog. Polym. Sci.*, 28, 209–259.

Khayet, M., Feng, C. Y., Khulbe. K. C. and Matsuura. T. (2002). "Preparation and characterization of polyvinylidene fluoride hollow fiber membranes for ultrafiltration." *Polymer*, 43, 3879-3890.

Kim, M. (1991). "Water flux and protein adsorption of a hollow fiber modified with hydroxyl groups." *J. Membr. Sci.*, 56, 289–302.

Kim, S. Y., Cho, S. M., Lee, Y. M. and Kim S. J. (2000). "Thermo- and pH responsive behaviors of graft copolymer and blend based on Chitosan and N-isopropylacrylamide." *J. Appl. Polym. Sci.*, 78, 1381-1391.

Labbez, C., Fievet, P., Szymczyk, A., Vidonne, A., Foissy, A. and Pagetti, J. (2002). "Analysis of the salt retention of a titania membrane using the "DSPM" model: effect of pH, salt concentration and nature." *J. Membr. Sci.*, 208, 315–329.

Lee, E. H. (1999). "Ion-beam modification of polymeric materials: Fundamental principles and applications." *Ncl. Instr. Meths. in Phys. Res. B.*, 151, 29–41.

Lee, K. Y., Park, W. H. and Ha, W. S. (1997). "Polyelectrolyte complexes of sodium alginate with chitosan or its derivatives for microcapsules." *J. Appl. Polym. Sci.*, 63, 425-432.

Lee, Y. M. (1993). "Modified chitosan membranes for pervaporation." *Desalination*, 90, 277-290.

Li, X., Feyter, S. and Vankelecom, I. (2008). "Polysulfone/sulfonated poly(ether ether ketone) blend membranes: morphology study and application in the filtration of alcohol based feeds." *J. Membr. Sci.*, 324, 67-75.

Lin, D., Chang, C., Huang, F. and Cheng, L. (2003). "Effect of salt additive on the formation of microporous poly(vinylidene fluoride) membranes by phase inversion from $LiClO_4$/Water/DMF/PVDF system." *Polymer*, 44, 413-422.

Linggawatia, A., Mohammada, A. W. and Leob, C. P. (2012). "Effects of APTEOS content and electron beam irradiation on physical and separation properties of hybrid nylon-66 membranes." *Materials Chemistry and Physics*, 133, 110– 117.

Liu. F., Moghareh Abed, M. R. and Li, K. (2011). "Preparation and characterization of poly(vinylidene fluoride) (PVDF) based ultrafiltration membranes using nano γ-Al_2O_3" *J. Membr. Sci.*, 366, 97-103.

Lloyd, D. R., Kinzer, K. E. and Tseng, H. S. (1990). " Microporous membrane formation via thermally induced phase separation. I. Solid-liquid phase separation." *J. Membr. Sci.*, 52, 239-261.

Lu, X., Bian, X. and Shi, L. (2002). "Preparation and characterization of NF composite membrane." *J. Memb. Sci*., 210, 3-11.

Mahendran, R., Malaisamy, R. and Mohan, D. (2004). "Cellulose acetate and polyethersulfone blend UF membranes. Part I. preparation and characterization." *Polym. Adv. Technol*., 15, 149-157.

Mahendran, R., Malaisamy, R. and Mohan, D. (2004). "Preparation, characterization and effect of annealing on performance of cellulose acetate/sulfonated Polysulfone and cellulose acetate/epoxy resin blend ultrafiltration membranes." *Eur. Poly. J*., 40, 623–630.

Malardier-Jugroot, C., van de Ven, T. G. M., Cosgrove, T., Richardson, R. M. and Whitehead, M. A. (2005). "Novel self-assembly of amphiphilic copolymers into nanotubes: Characterization by small angle neutron scattering." *Langmuir*. 21, 10179–10187.

Manttari, M., Pihlajamaki, A. and Nystrom, M. (2006). "Effect of pH on hydrophilicity and charge and their effect on the filtration efficiency of NF membranes at different pH." *J. Memb. Sci*., 280 311–320.

MeCoy, B. J. (1995). "Membrane Sieving of a Continuous Polydisperse Mixture Through Distributed Pores." *Separ, Sci, Technol*., 30, 487-493.

Meihong, L., Sanchuan, Y., Yong, Z. and Congile. G. (2008). "Study on the thin-film composite nanofiltration membrane for the removal of sulfate from concentrated salt aqueous: preparation and performance." *J Membr. Sci*., 310, 289-295.

Miao, J., Chen, G., Gao, C., Lin, C., Wang, D. and Sun, M. (2006). "Preparation and characterization of N,O-carboxymethyl Chitosan (NOCC)/polysulfone (PS) composite nanofiltration membranes." *J. Membr. Sci*., 280, 478–484.

Minko, S. (2008). "Grafting on solid surfaces: "grafting to" and "grafting from" methods, in: S. Manfred (Ed.), Polymer Surfaces and Interfaces: Characterization,

Modification and Applications." E-Publishing, Springerlink.com, Berlin/Heidelberg, 215–234.

Morgan, P. W. and Kwolek, S. L. (1996). "Interfacial polymerization II. Fundamentals of polymer formation and liquid interfaces." *J. Polym. Sci. A.*, 34, 531–559.

Mu, T., Cong, Y., Wang, W. and Zhang, B. (2012). "Preparation and characterization of novel chitosan composite nanofiltration membrane containing mesogenic units." *Desalination*, 298, 67–74.

Mulder, M. (1996). "Basic principles of membrane technology." Kluwer Academic Publishers, The Netherlands.

Musale, D. A. and Kulkarni, S. S. (1996). "Fouling reduction in poly(acrylonitrile-co-acrylamide) ultrafiltration membranes." *J. Membr. Sci.*, 111, 49-56.

Nair, S. V., Sreekala, M. S., Unnikrishnan, G., Johnson, T., Thomas, S. and Groeninckx, G. (2000). "The role of crosslinking and crystallisation on the transport characteristics of ethylene–propylene rubber membranes." *J. Membr. Sci.*, 177, 1-7.

NamHan, K., Yu, B. Y. and Kwak, S. Y. (2012). "Hyperbranched poly(amidoamine)/polysulfone composite membranes for Cd (II) removal from water." *J. Membr. Sci.*, 396 83– 91.

Nataly, V., Moris, E. and Raphael S. (2008). "Membranes in desalination and water treatment." *MRS Bulletin*, 33, 16-20.

Nilsson, M., Tragardh, G. and Ostergren, K. (2008). "The influence of pH, salt and temperature on nanofiltration performance." *J. Membr. Sci.*, 312, 97-106.

Nowak, K. M. (1989). "Synthesis and properties of polysulfone membranes." *Desalination*, 71, 83-95.

Ohya, Y., Marushashi, S., Shizuno, K., Mano, S., Murata, J. and Ouchi. T. (1999). "Graft polymerization of styrene on Chitosan and the characteristics of the polymer." *J. Macromolecular Sci-Part-A.*, 36, 339-353.

Palacio, L., Calvo, J. I., Prádanos, P., Hernandez, A., Vaisanen, P. and Nystrom, M. (1999). "Contact angles and external protein adsorption onto UF membranes." *J. Membr. Sci.*, 152, 189-201.

Petersen, R. J. (1993). "Composite reverse osmosis and nanofiltration membranes." *J. Membr. Sci.*, 83, 81-150.

Pinnau, I. and Koros, W. J. (1991). "Structures and gas separation properties of asymmetric polysulfone membranes made by dry, wet, and dry/wet phase inversion." *J. Appl. Polym. Sci.,* 43, 1491–1502.

Qin, J., Oo, M. and Kekre, K. (2007). "Nanofiltration for recovering waste water from a specific dyeing facility." *J. Membr. Sci.*, 56, 199-203.

Ranaa, D., Matsuura, T., Narbaitzb, R. M. and Feng, C. (2005). "Development and characterization of novel hydrophilic surface modifying macromolecule for polymeric membranes." *J. Membr. Sci.*, 249, 103–112.

Reiners, G., Beck, U. and Jehn, H. A. (1994). "Decorative optical coatings." *Thin Solid Films,* 253, 33-40.

Reuvers, A. J. and Smolders C. A. (1987). "Formation of membranes by means of immersion precipitation: Part II. The mechanism of formation of membranes prepared from the system cellulose acetate-acetone-water." *J. Membr. Sci.*, 34, 67-86.

Rickerby, D. S., Bull, S. J., Robertson, T. and Hendry, A., (1990). "The role of titanium in the abrasive wear resistance of physically vapor-deposited TiN." *Surf. and coat. Tech.*, 41, 63-74.

Risbud, M., Hardikar, A., Bhat, S. and Bhonde, R. (2000). "pH-sensitive freeze-dried chitosan-polyvinyl pyrrolidone hydrogels as controlled release system for antibiotic delivery." *J. Controlled Release*., 68, 23-30.

Roberts, G. A. F. (1992). "Chitin Chemistry." The Macmillan Press Ltd., London,UK.

Schwabel, F. (2008). "Advanced Quantum Mechanics." 4th ed., Springer, 253.

Sebistien, M., Hammes, F., Tarber, J., Salhi, E., Gunten, U. and Pronk, W. (2007). "Permeability of low molecular weight organics through nanofiltration membranes." *Water Res*., 41, 3968-3976.

Song, Z., Zhi, W., Xin, W., Boran, Z., Jixiao, W., Shangbao, Y. and Shichang, W. (2011). "Performance improvement of polysulfone ultrafiltration membrane using PANIEB as both pore forming agent and hydrophilic modifier." *J. Membr. Sci*., 385– 386, 251– 262.

Stropnik, C. and Kaiser, V. (2002). "Polymeric membranes preparation by wet phase separation: mechanisms and elementary processes." Desalination, 145, 1-3.

Taurozzi, J. S., Arul, H., Bosak, V. Z., Burban, A. F., Voice, T. C., Bruening, M. L. and Tarabara, V. V. (2008). "Effect of filler incorporation route on the properties of polysulfone-silver nanocomposite membranes of different porosities." *J. Membr. Sci.,* 325, 58-68.

Tian, Y., He, C., Tao, Y., Cui, S., Ai, J. and Li. (2006). "Fabrication of polyethyleneimine and poly(styrene-alt-maleic anhydride) nanotubes through covalent bond." *J. Nanosci. Nanotech.,* 7, 2072–2076.

Udayashankar, N. K., Rajasekaran. S. and Nayak, J. (2008). "Oxidation and corrosion resistance of $TiAl_3$ coatings." *T. Indian I. Metals*, 61, 231-233.

Ulbricht. M. (2006). "Advanced functional polymer membranes". *Polymer*, 47, 2217-2262.

Van de Witte, P., Dijkstra, P. J., Van den Berg, J. W. A. and Feijen, J. (1996). "Phase separation processes in polymer solutions in relation to membrane formation." *J. Membr. Sci.*, 117, 1-31.

Vetere, A., Donati, I., Campa, C., Semeraro, S., Gamini, A. and Paoletti, S. (2002). "Synthesis and characterization of a novel glycopolymer with protective activity toward human anti-{alpha}-Gal antibodies." *Glycobiology.* 4, 283–290.

Vourch, M., Balannec, B., Chaufer, B. and Dorange, G. (2005). "Nanofiltration and reverse osmosis of model process waters from the dairy industry to produce water for reuse." *Desalination*, 172, 245-256.

Wang, T., Wang, Y. Q., Su, Y. L. and Jiang, Z. Y. (2006). "Antifouling ultrafiltration membrane composed of polyethersulfone and sulfobetaine copolymer." *J. Membr. Sci.*, 280, 343–350.

Wang, X., Wang, W. and Wang, D. (2002). "Experimental investigation on separation performance of nanofiltration membranes for inorganic electrolyte solutions." *Desalination*, 145, 115-122.

Wang, X., Yumin, D., Fan, L., Liu, H. and Hu, Y. (2005). "Chitosan- metal complexes as antimicrobial agent: synthesis, characterization and Structure-activity study." *Polym. Bull.*, 55, 105-113.

Wanichapichart, P., and Yu, L. D. (2007). "Chitosan membrane filtering characteristics modification by N-ion beams." *Surf. Coat. Tech.*, 201, 8165-8169.

Wanichapichart, P., Taweepreeda, W., Nawae, S., Choomgan. P. and Yasenchak, D. (2012). "Chain scission and antifungal effect of electronbeam on cellulose membrane." *Radiation Physics and Chemistry*, 81, 949–953.

Wara, N. M., Francis, L. F. and Velamakanni, B. V. (1995) "Addition of alumina to cellulose acetate membranes" *J. Membr. Sci.,* 104, 43-49.

Wijmans, J. G. and Baker, R. W. (1995). "The solution-diffusion model: a review." *J. Membr. Sci*., 107 (1-2), 1-21.

Wittmann, E., Cote, P., Medici, C., Leech, J. and Turner, A.G. (1998). "Treatment of a hard boreholewater containing low levels of pesticide by nanofiltration." *Desalination*, 119 (1–3), 347–35.

Wu, K. X. and Li, M. N. (1999). "The immune regulation of carboxymethyl polysaccharides." *Chin. Chem. Bull*., 9, 54-57.

Wu, X. M., Wang, L. L., Wang, Y., Gu, J. S. and Yu, H. Y. (2012). "Surface modification of polypropylene macroporous membrane by marrying RAFT polymerization with click chemistry." *J. Membr. Sci*., DOI: http://dx.doi.org/10.1016/j.memsci.2012.06.033

Xie, R., Chu, L., Chen, W., Xiao, W., Wang, H. and Qu, J. (2005). "Characterization of microstructure of poly(N-isopropylacrylamide)-grafted polycarbonate track-etched membranes prepared by plasma-graft pore-filling polymerization." *J. Membr. Sci*., 258, 157-166.

Xu X. L. and Coleman, M. R. (1997). "Atomic force microscopy images of ion-implanted 6FDA- pMDA polyimide films." *J. Appl. Polym. Sci*., 66, 459–469.

Xu, X., and Coleman, M. R. (1999). "Preliminary investigation of gas transport mechanism in a H^+ irradiated polyamide-ceramic composite membrane." *Ncl. Instr. Meths. in Phys. Res. B*., 152, 325–334.

Xu, X. L., Dolveck, J. Y., Boiteux, G., Escoubes, M., Monchanin, M., Dupin J. P. and Davenas, J. (1995). "A new approach to microporous materials — application of ion beam technology to polyimide membranes." *Mat. Res. Soc. Symp. Proc*., 354, 351–356.

Xu, X. L., Dolveck, J. Y., Boiteux, G., Escoubes, M., Monchanin, M., Dupin J. P. and Davenas, J. (1995). "Ion beam irradiation effect on gas permeatin properties of polyimid films." *J. Appl. Polym. Sci*., 55, 99–107.

Xu, Y. Z. and Lebrun, R. E. (1999). "Comparison of nanofiltration properties of two membranes using electrolyte and nonelectrolyte." *Desalination*, 122, 95–106.

Yamaguchi, T., Nakao, S. and Kimura, S. (1991). "Plasma-graft filling polymerization: preparation of a new type of pervaporation membrane for organic liquid mixtures" *Macromolecules*, 21, 5522–5527.

Yan, C., Zhang, S., Yang, D. and Jain, X. (2007). "Prepared and characterized to the chloromethylated/Quaternized poly(phthlazinone ether sulfone ketone) (CMPPESK/QAPPESK) for positively charged nanofiltration membranes." *J. Appl. Polym. Sci.*, 107, 1809-1816.

Yan, L., Li, Y. S., Xaing, C. B. and Xainda. S. (2006). "Effect of nano-sized Al2O3-particals addition on PVDF ultrafiltration membrane performance." *J. Membr. Sci.*, 276, 162-167.

Yang, T. and Zall, R.R. (1984). "Chitosan membrane for reverse osmosis application." *J. Food Sci.*, 49, 91-93.

Yoshimaga, K., Kondo, K. and Kondo, A. (1997) "Capabilities of polymermodified monodisperse colloidal silica particles as biomaterial carrier Colloid." *Polym. Sci.,* 275, 220–226.

Young-Nam, K. and James, L. (2006). "Hypochlorite degradation of crosslinked polyamide membranes changes in chemical/morphological properties." *J. Membr. Sci.*, 283, 21-26.

Yu, S., Liu, X., Liu, J., Wu, D., Liu, M. and Gao., C. (2011). "Surface modification of thin-film composite polyamide reverse osmosis membranes with thermo-responsive polymer (TRP) for improved fouling resistance and cleaning efficiency." *Separation and Purification Tech.*, 76, 283-291.

Yu, S., Lü, Z., Chen, Z., Liu, X., Liu, M. and Gao, C. (2011). "Surface modification of thin-film composite polyamide reverse osmosis membranes by coating N-

isopropylacrylamide-co-acrylic acid copolymers for improved membrane properties." *J. Membr. Sci.*, 371, 293-306.

Yuana, N., Tsaia, R., Hob, M., Wanga, D., Laic, J. and Hsieha, H. (2008). "Fabrication and characterization of chondroitin sulfate-modified chitosan membranes for biomedical applications." *Desalination*, 234, 166–174.

Zhang, C., Ping, Q., Zhang, H. and Shen, J. (2003) "Synthesis and characterization of water-soluble O-succinyl-chitosan" *Euro. Poly. J.,* 39 1629–1634.

Zhang, Z. H., An, Q. F., Liu, T., Zhou, Y., Qian, J. W. and Gao, C. J. (2012). "Fabrication and characterization of novel SiO_2-PAMPS/PSF hybrid ultrafiltration membrane with high water flux." *Desalination*, 297, 59-71.

Zhao, Z. P., Wang, Z. and Wang, S. C. (2003). "Formation, charged characteristic and BSA adsorption behavior of carboxymethyl Chitosan/PES composite MF membrane." *J. Membr. Sci*., 217, 151-158.

Zheng, H. and Du, Y. M. (2002). "Structure and antibacterial activity of cellulose carboxymethylation chitosan blend films." *Polym. Mater. Sci. Eng. (Chin.)*., 18, 124-127.